1978

Geology And The Genesis Of Gold-silver Base Metal Sulphide-bearing Veins, At Mahd Ad Dahab Kingdom Of Saudi Arabia

Hashim Darweesh Hakim

GEOLOGY AND THE GENESIS OF GOLD-SILVER BASE METAL SULPHIDE-BEARING VEINS, AT MAHD AD DAHAB KINGDOM OF SAUDI ARABIA

by

Hashim Darweesh M. Hakim

Department of Geology

Submitted in partial fulfillment
of the requirements for the degree of
Doctor of Philosophy

Faculty of Graduate Studies
The University of Western Ontario
London, Ontario
August, 1978

Frontispiece. Looking south to Jabal Mahd AD Dahab from next ridge north. Middle left on skyline outcrop of older granodiorite, centre, Mahd AD Dahab mountain with conical hill of porphyritic rhyolite with old workings, behind it appears one of the major northeast trending fractures occupied with an andesite dike. Old pits appear at the base of the mountain in upper rhyolite tuff and chert. Barren quartz veins trending north are at far right. Mill and dump from recent mining operation are east and north of the porphyritic rhyolite body.

ABSTRACT

Gold occurs at Mahd AD Dahab in the Precambrian Arabian Shield mainly as microscopic inclusions and veinlets of electrum and less commonly as gold tellurides within and between grains of quartz, chlorite, chalcopyrite, galena and sphalerite. These mainly occur together with pyrite, hematite, argentite and tellurides of silver, bismuth and lead in bands at the margins of quartz veins which traverse 1.2 km of a steeply dipping layered sequence of andesite, fragmental rocks, and a lenticular body of porphyritic rhyolite. Veins terminate against chert at the top of the layered sequence. Gold and base metal-bearing veins are most abundant in and immediately adjacent to the rhyolite body and less frequent and barren away from that body. Wall rocks and veins have small FeO/Fe_2O_3 and wall rocks adjacent to quartz veins and vein selvages are characterized by propylitic, phyllic and potassic alteration mineral assemblages. Veins and wall rocks are cut by andesite dikes which appear to feed overlying flows.

The interpretation is that during a break in the stages of island arc type volcanism rocks cooled by convection of sea water. The sea water percolated downward over a broad area, became a reduced, hot, brine-like fluid capable of leaching silica and metals from rocks at depth and returned

to surface in a focused discharge area about the porphyritic rhyolite, the local heat source at Mahd AD Dahab. Near surface, the ascending fluid mixed with cold, oxygenated water resulting in precipitation of silica and metal as veins in fractures and as chert on the sea floor. The next extrusion of lava began with emplacement of andesite dikes which cut the veins. The veins of Mahd AD Dahab are hence interpreted as a stratabound type of mineralization, an integral part of volcanism that deposited the middle and the upper parts of the Proterozoic Halaban Group during the Hijaz Tectonic Cycle.

ACKNOWLEDGEMENTS

I am very grateful to the Institute of Applied Geology in general and to Dr. A. Alshanti in particular for giving me the chance to carry on this task and for the financial support, without it this work would have not been possible. I would like also to thank Sheikh A.Z. Yamani for giving me the opportunity to do this work through the Institute of Applied Geology.

My thesis supervisor, Professor R.W. Hodder, is gratefully acknowledged for his help, orientation, discussions during the field work and writing of the thesis.

Dr. Kerrich is also thanked for his guidance during the laboratory work and Professor Fyfe is thanked for his in the field and for the discussion during research work.

Thanks are also due to the late Dr. H. Hunter for his guidance during the analytical work, Mr. T. LaTour for various discussions, Mr. J. Forth for thin, polished and probe sections preparation and Mr. R.L. Barnett for microprobe analyses. Mr. A. Bagdady and Mr. R. Roberts of the U.S.G.S. in Jiddah are also thanked for their help at the beginning of this work.

TABLE OF CONTENTS

LIST OF PHOTOGRAPHIC PLATES

LIST OF TABLES

LIST OF FIGURES

CHAPTER 1

INTRODUCTION

1.1. General Statement

The Mahd AD Dahab gold mine is on the west side of the Arabian Precambrian Shield within the Southern Hijaz Quadrangle bounded by longitudes 38° and 42° East and latitudes 20° to 24° North (Fig. 1). Mahd AD Dahab has had by far the largest production of any gold mine in the Arabian Shield as evidenced by some 400,000 tons of dump left by ancient miners and an estimated production from 1939 until 1954 of 765,768 fine ounces of gold and 1,002,029 ounces of silver (Goldsmith, 1971). It is not presently producing but is being reinvestigated.

Gold occurs principally as electrum at Mahd AD Dahab with base metal sulphide minerals in quartz veins and stockworks traversing andesite, agglomerate, rhyolite tuff, lithic crystal tuff and porphyritic rhyolite. These rocks are well exposed in a mountain 2.5 km by 1.2 km which rises 1238 m above sea level and 800 m above the surrounding plain.

Copper has also been recovered in the general area by ancient miners at Umm AD Damar, 38 km north east of Mahd AD Dahab and Jabal Sayid, 40 km to the north. Umm AD

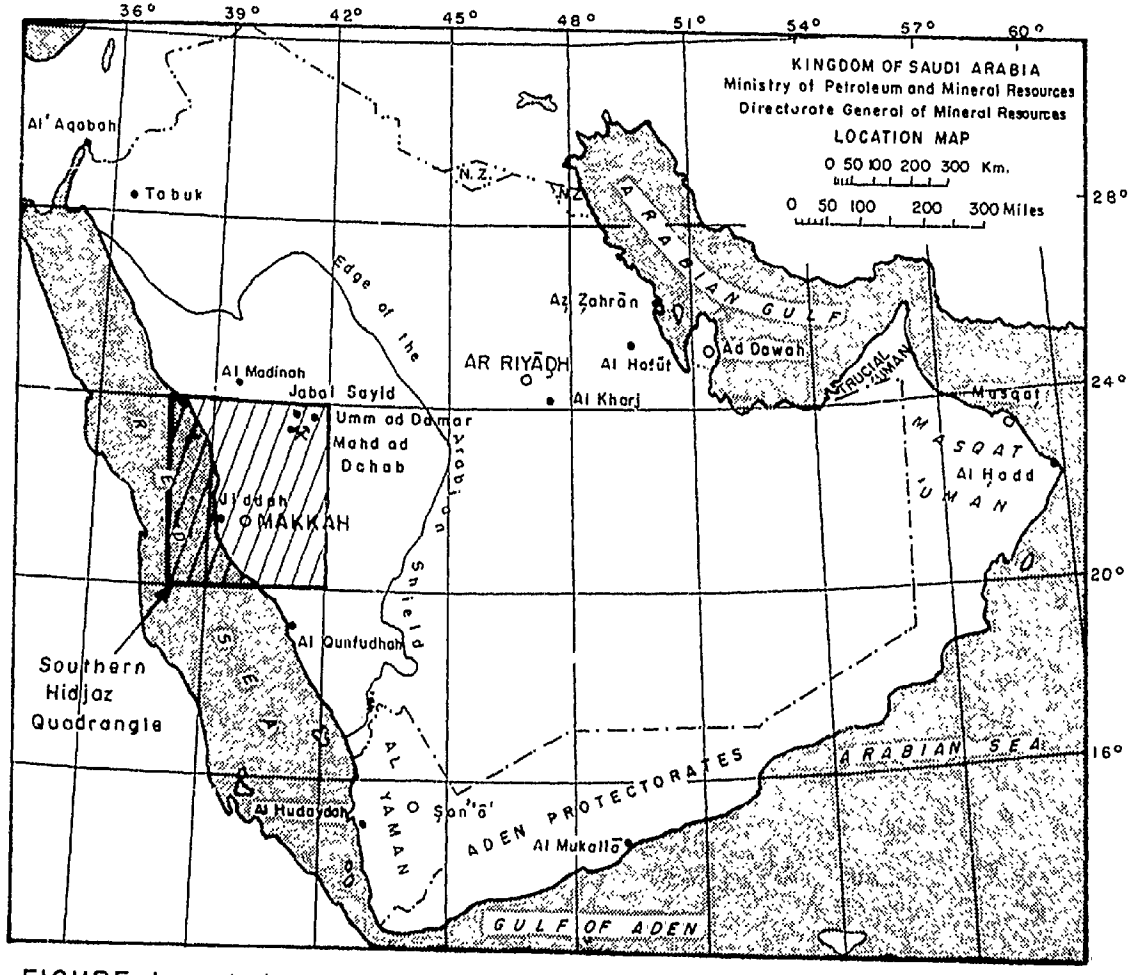

FIGURE 1. Index map of the ARABIAN PENINSULA, outline of the PRECAMBRIAN SHIELD and location of MAHD AD DAHAB

Damar has 108,800 tons of slag (Goldsmith, 1971) most of which probably came from smelting copper ore mined throughout the area. Exploration for copper is in progress at Jabal Sayid. There are several other old metallic prospects (Brown et al., 1962) particularly in the north and in the southeast corner of the Southern Hijaz Quadrangle (Fig. 2). Non-metallic prospects and mines are predominant in the west and the northeast part of the quadrangle (Fig. 3). All of these mines and prospects are within Precambrian volcanic rocks intruded by Precambrian granitic plutons.

1.2. Location and Access

Mahd AD Dahab is 60 Km fromthe north border of the Southern Hijaz Quadrangle (Fig. 4). The only town in the area is Madh AD Dahab, or Al Mahd, with a population of 20,000. Al Madinah, which is 200 km northwest of Al Mahd is the nearest large city and supply centre. There are no wells for drinking water at Al Mahd in spite of a search by drilling between 1939 and 1954 when the mine was in operation. Water for the mine was brought by pipeline from the village of Sufainah, 60 km to the southwest at the edge of Tertiary and Quaternary basalts. Inhabitants of Al Mahd now have water delivered by truck from Sufainah.

The area can be easily reached from Jiddah by road in 8 hours. The road from Jiddah to Al Taif and for 30 km farther east is paved. The rest is a desert dirt road. The area can also be reached from Al Madinah, by 3 hours

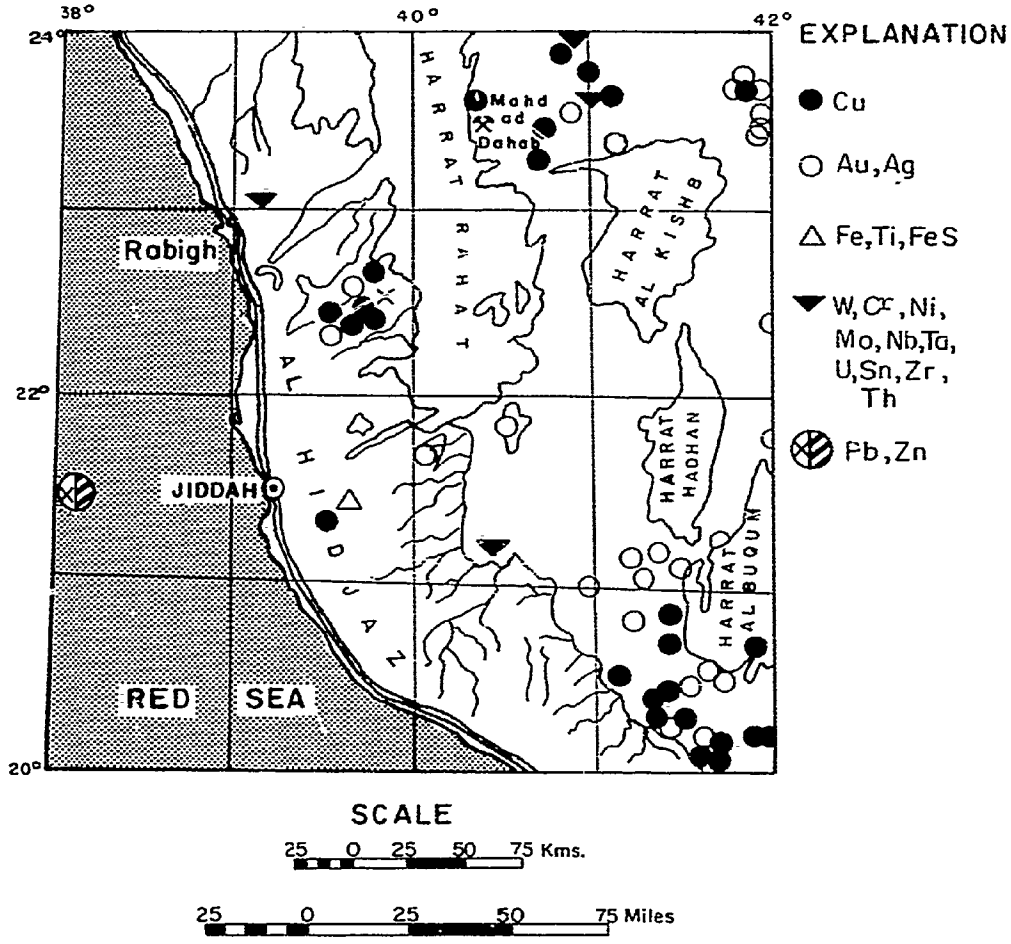

FIGURE 2. METALLIC MINERAL LOCALITY MAP OF THE SOUTHERN HIJAZ QUADRANGLE

Compiled by H. van Daalhoff (1974)

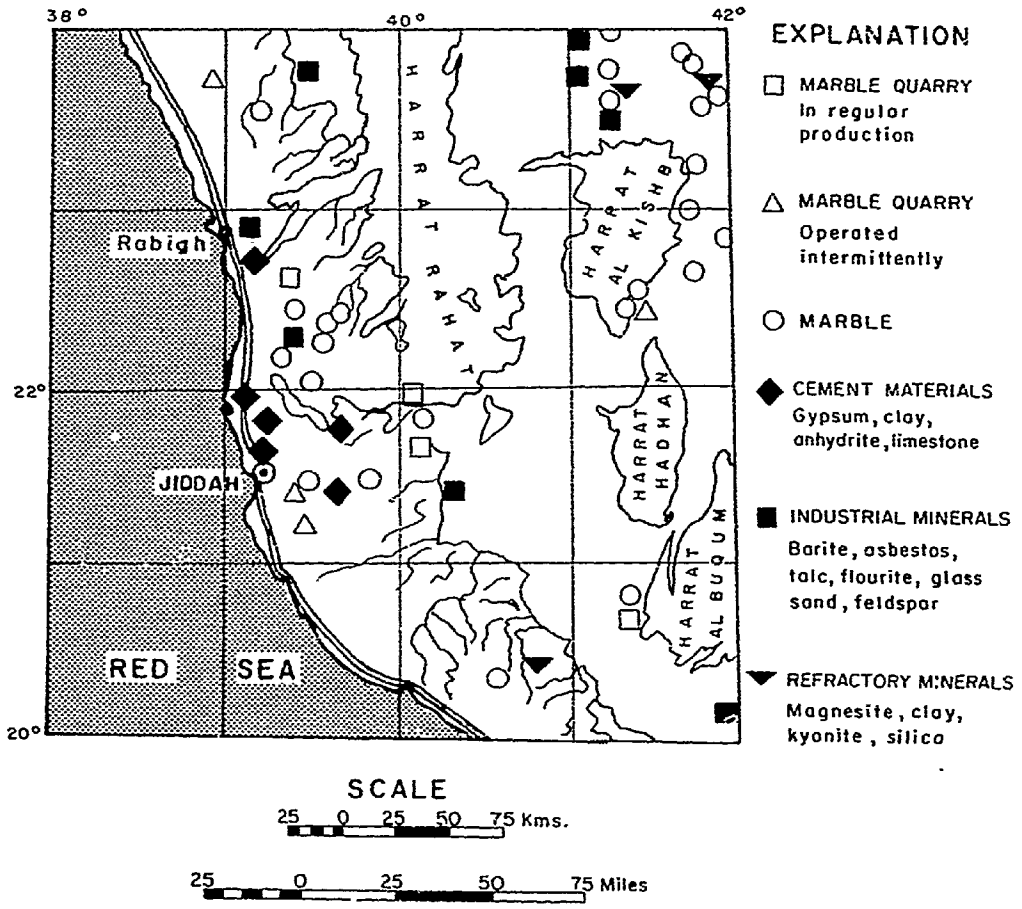

FIGURE 3. NON-METALLIC MINERAL LOCALITY MAP OF THE SOUTHERN HIJAZ QUADRANGLE

Compiled by H. van Daalhoff (1974)

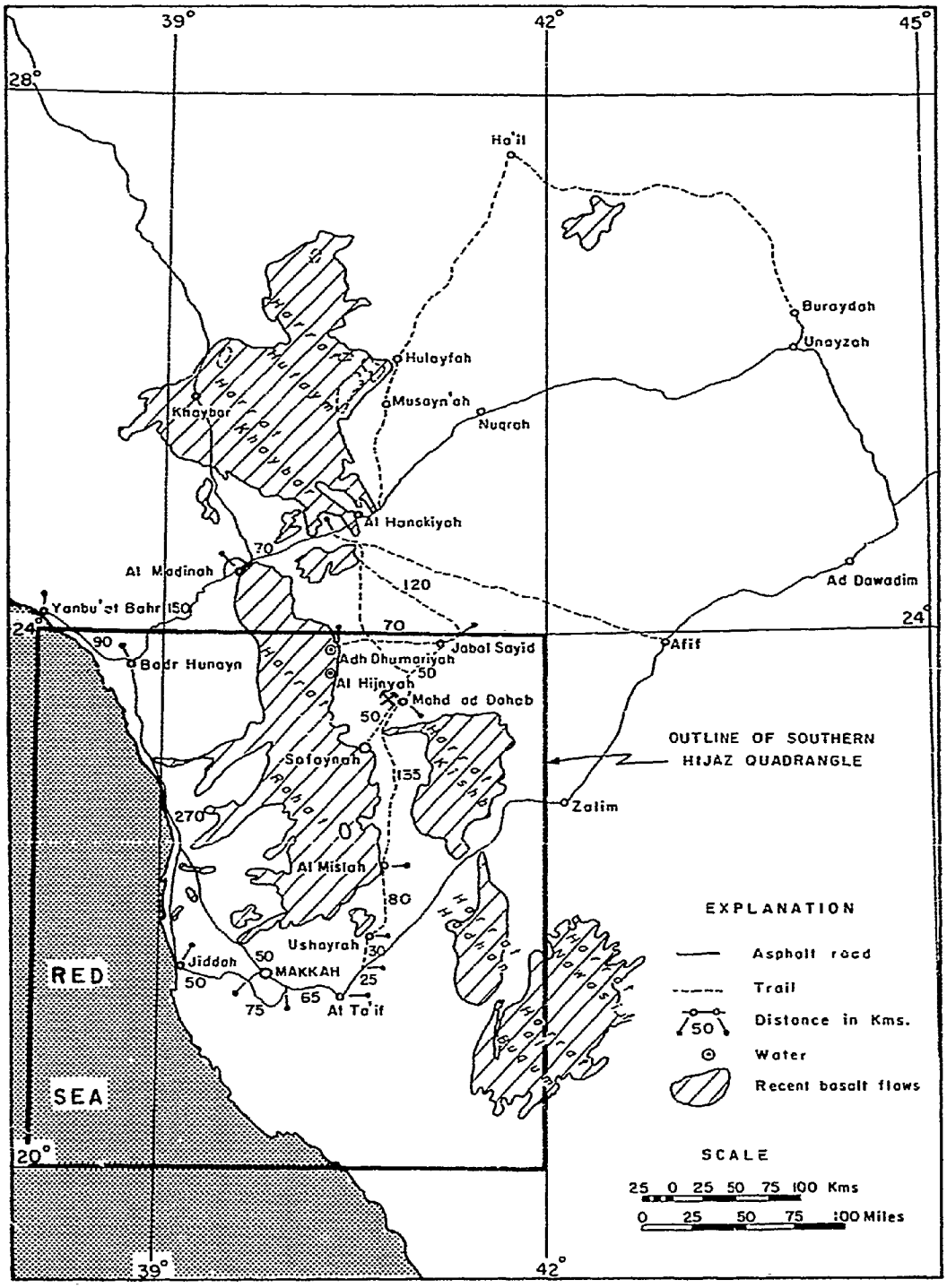

FIGURE 4. GENERAL LOCATION AND ACCESS

driving over 200 km of desert trail. There is a dirt air strip for light aircraft at Mahd AD Dahab.

1.3. Previous Work and Purpose of Current Study

In the early 1930's geologists of the Arabian Mining Syndicate visited the Mahd AD Dahab area and subsequently published brief reports on the area (Dirom, 1946, 1947; Playter, 1953). In 1961 MacLean, a geologist of the Directorate General of Mineral Resources, defined and named the fragmental rocks, which are distinctive to the area, as the Mahd AD Dahab Series and in 1962 Brown et al. of the USGS mapped the regional geology of the Southern Hijaz Quadrangle at 1:500,000. Theobald Jr. (1965a) of the USGS did detailed mapping and geochemical sampling near the Mahd AD Dahab mine. Davis et al. (1965) did shallow geophysical exploration on the west side of Jabal Al Mahd. Goldsmith and Kouther (1971) of the USGS and the Directorate General of Mineral Resources, mapped the regional geology at 1:100,000 for an area of about 2750 km^2 between Jabal Hadb AD Diaheen and Umm AD Damar in the north and Madh AD Dahab in the south. Ten holes were drilled by the Arabain Drilling Company for the Directorate General of Mineral Resources in 1973 and 1974. Core from these holes was logged by geologists of the USGS in Jiddah.

In 1975, Robert et al. of the USGS prepared a geologic map of 1:2,500 of Jabal Mahd AD Dahab accompanied by a descriptive report. This has served as a base for the

current study which began in 1976 designed to describe and contrast barren and metal-bearing quartz veins and their wall-rock and, to interpret the sequence of events that produced the stratigraphic section of Jabal Al Mahd and ultimately the transportation and deposition of silica and associated metals in veins. Field work included detailed sketch maps at 1:100 prepared by tape and compass of some old workings, and documentation of the nature of quartz veins and their relationship to rock types and in particular to the upper rhyolite tuff, chert, porphyritic rhyolite and, andesite dikes. Petrographic and chemical analyses were made of the different rock units, and metalliferous and barren quartz veins at the laboratories of the University of Western Ontario.

CHAPTER 2

REGIONAL GEOLOGY

2.1. General Statement

The Southern Hijaz Quadrangle is underlain mainly by metavolcanic and metasedimentary rocks of late Proterozoic age (Fig. 5). Metavolcanic rocks cover larger areas than metasedimentary rocks (Brown et al., 1962) and are folded, faulted, regionally metamorphosed to greenschist facies, and intruded by igneous bodies that range in composition from gabbro to granite. Granitic plutons are concentrated mostly in the north and northeast and dioritic plutons are most common in south and southeast parts of the quadrangle. Both layered rocks and intrusions are oldest in the south part of the quadrangle and youngest in the north (Brown et al., 1962).

Olivine basalt flows of Tertiary and Quaternary age cover vast areas mostly in the north half of the quadrangle. Some of these outpourings, such as Harrat Rahat, extend more than 500 km from north to south and have a width in excess of 50 km. The coastal plain or Tihamah, extends along the west edge of the quadrangle with a width of 2 to 5 km and is Tertiary sandstone, shale and gypsum covered by alluvium and windblown material of Quaternary to Recent age (Goldsmith, 1971).

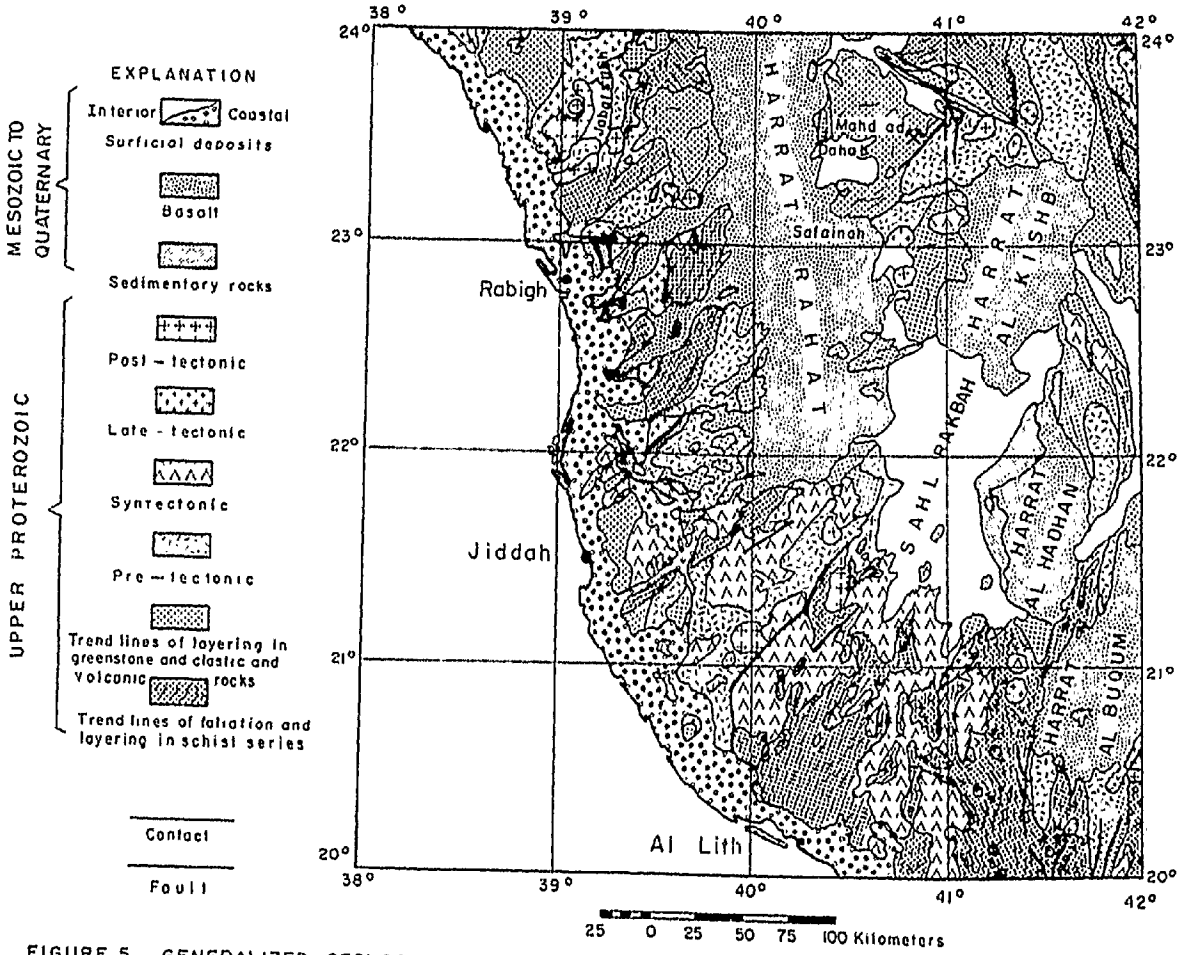

FIGURE 5. GENERALIZED GEOLOGIC MAP OF SOUTHERN HIJAZ QUADRANGLE, KINGDOM OF SAUDI ARABIA

Modified from Goldsmith (1971) ; Terminology after Goldsmith (1971) and Brown (1972).

2.2. Layered Rocks

Metavolcanic and metasedimentary rocks have been unitized by Brown et al. (1962) (Table 1) from oldest to youngest as follows:

2.2.1. Wadi Lith Series

These rocks are dominant in the southwest part of the quadrangle and are defined by Brown et al. (1962) as a complex of metadiorite, metagabbro, amphibolite, gneissic granite, minor slate and quartzite which is commonly foliated. The regional metamorphism is retrograde from amphibolite to greenschist facies.

2.2.2. Amphibolite Schist

This is local in distribution in the southwest part of the quadrangle and is believed derived largely from both mafic and felsic volcanic rocks as it includes foliated amphibolite and sericite schist as well as minor gray, pink and tan marble and, quartzite. It is commonly intruded by granite (Brown et al., 1962) and is in greenschist to amphibolite facies of regional metamorphism.

2.2.3. Sericite and Chlorite Schist

This unit is dominant in the south and the west parts of the quadrangle. It is mostly quartzite, metaarkose, quartzitic schist and marble. Greenschist facies metamorphism prevails.

Table 1. Correlation of layered rock units of Brown et al. (1962), Goldsmith (1971) and Schmidt et al. (1973)

Brown et al. (1962)	Goldsmith (1971)	Schmidt et al. (1973)
Rhyolite, trachyte and phonolite plugs		
Shammar rhyolite	Clastic Sedimentary and Volcanic rocks	Shammar Group
Fatima and Abla Formations		
Murdama Formation		Murdama Group
Halaban Andesite		Halaban Group
Andesite, Diabase, Slate Greenstone Conglomerate and rhyolite and porphyritic Andesite	Greenstone	Jiddah Formation
Chlorite Schist		Baha Group
Sericite and Chlorite Schist		Baish Group
		Hali Group
Amphibolite Schist	Schist Series	Khamis Mushyat gneiss
Wadi Lith Series		

2.2.4. Chlorite Schist

This is more prevalent than the Sericite and Chlorite Schist and its major occurrences are at the southeast and the northwest corners of the quadrangle. It is mostly derived from mafic and felsic volcanic rocks with interbedded sandstone and shale by metamorphism to greenschist facies.

2.2.5. Andesite, Diabase, Slate, Greenstone, Conglomerate, Rhyolite and Porphyritic Andesite

This is common in the north and west parts of the Southern Hijaz Quadrangle with a few occurrences at the southeast corner. It is mostly intruded by granite and cut by dike swarms of rhyolite and diabase. Rocks are in the greenschist facies.

2.2.6. Halaban Andesite

This is very common in the northeast and east parts of the quadrangle and is of particular importance because most of the significant metal occurrences such as Mahd AD Dahab are within it. Brown et al. (1962) describe Halaban Andesite as fine-grained andesite and felsite with subordinate dacite trachyte, rhyolite breccia, agglomerate interbedded phyllite, quartzite, and marble. The metamorphism is greenschist facies. On the geologic map of the Arabian Peninsula (USGS, ARAM Co. 1963) the name Halaban Formation was used for the same lithostratigraphic unit. The term

Halaban Group was applied by Schmidt et al. (1973) who proposed a three-fold division of the Halaban Group:

2.2.6.1. Lower Halaban

This is predominantly clastic unit of thick conglomerate, sandstone and siltstone of largely andesitic derivation. Detailed geologic mapping by B.R.G.M. at Jabal Sayid (Alabouvette, 1973) adds a fourth subdivision at the base of the Lower Halaban consisting of serpentine, dolomite, limestone, andesite and basalt with splitic mineralogy. Aguttes and Duhamel (1971) and Alabouvette (1973) describe this as an ophiolite suite, but this designation is contentious as the rock can also be thought of as simply an ultramafic to mafic basal assemblage in a differentiated accumulation.

2.2.6.2. Middle Halaban

This is green massive andesite, agglomerate, volcanic breccia, tuff and locally thick basaltic flows. This division includes the rocks at Mahd AD Dahab.

2.2.6.3. Upper Halaban

This is green to buff rhyolite and trachyte flows plus felsic pyroclastic rocks.

2.2.7. Murdama Formation

Brown et al. (1962) were the first to define this unit and the nomenclature has been used by Goldsmith (1971). Schmidt et al. (1973) introduced the term Murdama Group. It is unconformable upon Upper Halaban, is most prominant at the northeast corner of the quadrangle, and is mostly massive bedded sandstone, siltstone, shale, slate and argillite. The lowest part of the unit is a thick, massive conglomerate. It is metamorphosed to lower greenschist facies.

2.2.8. Abla and Fatima Formations

The Abla formation was mapped by Brown et al. (1962) only at one location in the southeast corner of the quadrangle where it is sandstone, wacke, conglomerate, red sandstone, limestone, arkose and purple shale. The Fatima Formation is mapped at two localities in the north part of the quadrangle (Brown et al., 1962) and is mainly arkose, red and purple shale, siltstone, tuffaceous wacke, basal conglomerate, sandstone and thin limestone. The rocks are gently folded, faulted and cut by a sill of Shammar Rhyolite with andesite and rhyolite dikes (Brown et al., 1962). These rocks are virtually unmetamorphosed.

2.2.9. Shammar Rhyolite

This unit is mapped only in the north part of the Southern Hijaz Quadrangle (Brown et al., 1962) as unconformably overlying the Halaban Group and Fatima Formation.

It is agglomerate and tuff associated with rhyolite flows, dacite and andesite (Brown et al., 1962) associated with the Najd Fault System, which is the youngest tectonic episode recognized in the Arabian Shield. These rocks are not metamorphosed.

2.2.10. Rhyolite, Trachyte and Phonolite Plugs

These rocks are very limited in distribution. Their major occurrence is in the northeast corner of the quadrangle (Brown et al., 1962).

More recently Goldsmith (1971) regrouped the Precambrian rocks of the Southern Hijaz Quadrangle into three main units, (Table 1).

The Schist Series

This is mostly in the south and locally in the northwest corner of the quadrangle and includes the Al Lith Series, the Chlorite and Sericite Schist and the Chlorite Schist of Brown et al. (1962). In the north and northeast the Schist Series is unconformably overlain by less metamorphosed clastic rocks. The Schist Series has rocks in both the amphibolite and greenschist facies. Kyanite is present at one locality (Goldsmith, 1971).

Greenstone

This is well exposed in the central part of the Southern Hijaz Quadrangle but has limited distribution in the south. It is andesite, rhyolite, diabase, slate and conglomerate, and is equivalent to part of the Halaban

Andesite of Brown et al. (1962). It has also been called the Jiddah Greenstone (USGS Aramco map of the Arabian Peninsula, 1963). It is metamorphosed to greenschist facies.

Clastic Sedimentary and Volcanic Rocks

These outcrop mostly in the north and northeast parts of the quadrangle. They are rhyolite, trachyte and phonolite plugs plus the felsic pyroclastic rocks of Halaban Andesite and the three main layered units, the Murdama Formation, the Fatima and Abla Formations, and, the Shammar Rhyolite of Brown et al. (1962). The latter is the youngest Precambrian rock exposed in the Shield.

Most recently Schmidt et al. (1973) have again regrouped the Precambrian section into a compromise of the terminology introduced by Brown et al. (1962) and Goldsmith (1971) (Table 1). Schmidt's et al. terminology is used in this thesis.

2.3. Major Plutons

Brown's geologic map, 1:500,000 of the Southern Hijaz Quadrangle, has five major types and ages of plutonic rocks based mainly on Rb/Sr isotopic age determinations.

2.3.1. Diorite and Granodiorite of Uncertain Age

This also includes minor quartz diorite, commonly foliated, and widely distributed throughout the quadrangle but particularly apparent in the west and northeast. Although their absolute age is uncertain these rocks are, on the basis of texture and field relationships,

believed to be more than 1000 m.y. old.

2.3.2. Granite and Granite Gneiss 1000 m.y. Old

These are broadly distributed, gray in colour and contain many inclusions and zenoliths. They tend to weather into pits and caves.

2.3.3. Quartz Diorite 850 m.y. Old

This rock has very limited distribution and is only mapped in the south part as one main pluton with four smaller bodies scattered around it.

2.3.4. Granite 700 to 750 m.y. Old

This occurs as semi-circular to elongate plutons which have a long dimension of up to 50 km in the northeast corner of the quadrangle. In the southwest, granite plutons of this age are poorly exposed. It is gray to pink calc-alkaline rock cut by numerous rhyolite and andesite dikes of varied trend. At some localities they form low hills. It differs from the above mentioned granite and granite gneiss in that it is younger and contains pegmatite and quartz veins but does not have zenoliths or inclusions.

2.3.5. Red or Pink Granite ± 535 m.y. Old

This has wide distribution in the north half of the quadrangle but is very minor in the south. It occurs generally as circular plugs, stocks and ring dikes. Its composition is alkaline to peralkaline and contains fluorite,

riebeckite and aegerine as accessory minerals. It is massive, medium to coarse grained and rich in K-feldspars. It is the youngest intrusion.

In 1971, Goldsmith grouped these plutonic rocks into two age divisions: 1,000 m.y. old to 700 and,700 to 535 m.y. old. The former group is gray to greenish gray hornblende diorite, and light gray granodiorite to quartz monzonite. These rocks are gneissic, plagioclase is partly saussitized, and the mafic minerals are partly converted to epidote and chlorite. According to their mineralogy, metamorphic grade, and geographic distribution, this group of plutonic rocks includes four of the five types of plutonic rocks of Brown et al. (1962). Such rocks are found in the west central part of the quadrangle and extend to the east and south of Mahd AD Dahab. They outcrop extensively in the scarp mountains north of Jiddah (Goldsmith, 1971).

Goldsmith's younger group of plutonic rocks, 700 to 535 m.y. old are gray, medium grained, and commonly contain biotite and also some hornblende. They also include the orange, pink to gray, medium to coarse-grained granitic masses. They are found locally in the Al Baha region in the south and are common in the Al-Taif region and east of Mahd AD Dahab.

In 1972, Brown on his tectonic map of the Arabian Peninsula reclassified plutonic rocks of the Arabian Shield into four groups of which all are represented in the

Southern Hijaz Quadrangle (Fig. 5). This grouping is based on structure and texture as well as a general trend from older calc-alkaline to younger peralkaline types. The first three groups were named according to whether they were emplaced prior, synchronous with, or at the end of the Hijaz Tectonic Cycle. The fourth group is post-Najd orogeny (Brown, 1972). Greenwood et al. (1976) used the name Hijaz Tectonic Cycle to indicate both orogenies and divided this tectonic cycle into four main events which were given local names (Table 2). The intrusions are grouped relative to these events as follows:

Pre-tectonic granitoid rocks 1000 m.y. old. These are exposed along the west edge of the quandrangle and are granodiorite and quartz diorite.

Syntectonic granitic rocks of 800 to 650 m.y. old. These are quite common in the south central part of the quadrangle and in the northeast corner. They are gneissic.

Late-tectonic calc-alkaline granitic rocks 650 to 600 m.y. old. These are absent in the south half of the quadrangle and have limited distribution in the northeast. They are calc-alkaline and massive.

Post-tectonic plutons 600 to 490 m.y. old are small plutons, not more than 10 km in diameter and occur at many localities in the Southern Hijaz Quadrangle. They are alkaline or peralkaline and are commonly characterized by either riebeckite or aegirite (Brown, 1972).

Table 2. Orogenic events and plutonic rocks according to Brown's tectonic map (1972) and Greenwood et al. (1976).

Brown (1972)		Greenwood et al. (1976)		
Plutonic Rocks		Orogenic Events		Plutonic Rocks
Najd Orogeny	Post-Tectonic 600-490 m.y.	Hijaz Tectonic Cycle	Bishah Orogeny	Granite and Quartz monzonite 570-550 m.y.
			Yafikh Orogeny	Quartz monzonite 650-600 m.y.
Hijaz Orogeny	Late-Tectonic 600-650 m.y.		Rannyah Orogeny	Injection gneiss 785 m.y.
	Syntectonic 800-650 m.y.			Second Dioritic Series 800 m.y.
	Pretectonic 1000 m.y.		Aqiq Orogeny	First Dioritic Series 960 m.y.

In 1973, Greenwood and Brown produced a two-fold petrographic and chemical classifications of the plutonic rocks as follows:

An older calcic series of diorite to trondjhemite composition. These belong to a calcic differentiation series which is dominant in the west and southwest parts of the Southern Hijaz Quadrangle. Dioritic batholiths are along major north trending linear features.

A younger calc-alkaline series of granodiorite and granite. These are large irregular stocks, small batholiths, and circular plugs. They are common at the northeast corner of the Southern Hijaz Quadrangle.

This classification and the precceding three are compared in Table 3 to the most recent terminology of Greenwood et al. (1976) in which plutonic rocks in the south part of the Arabian Shield are placed in five categories based mainly on the calcic to calc-alkaline to alkaline affinities of these plutonic rocks.

First dioritic series 960 m.y. old. These are gabbroic to quartz dioritic batholiths of mantle derivation.

Second dioritic series 800 m.y. old. These are gabbroic to trondjhemitic batholiths. The abundance of trondjhemite appears to be a distinctive feature of the second dioritic series otherwise they are quite similar to the first dioritic series. The first and the second dioritic series have calcic affinities which makes them resemble the older calc-alkaline

Table 3. Correlation of the plutonic rocks in the Southern Hidjaz Quadrangle Brown *et al.* (1962), Goldsmith (1971), Brown's tectonic map (1972), Greenwood and Brown (1973) and Greenwood *et al.* (1976).

	Brown *et al* (1962)	Goldsmith (1971)	Brown (1972)	Greenwood and Brown (1973)	Greenwood *et al* (1976)
5.	Granitic alkaline to peralkaline 535 m.y.	younger plutonic rocks 750-700-535 m.y.	post tectonic or peralkaline 600-490 m.y.	Granitic plutons granodiorite and granite	Granite and monzonite 570-550 m.y.
4.	Granite calc-calkaline 700-750 m.y.		Late tectonic calc-alkaline granitic rocks 600-650 m.y.		Quartz monzonite 650-600 m.y.
3.	Quartz diorite 820 m.y.		Syntectonic mostly dioritic and quartz diorite 800-650 m.y.		Injection gneiss 785 m.y.
2.	Granite and granite gneiss 1000 ± m.y.	older plutonic rocks 100-750-700 m.y.	pretectonic granitoid rocks include granodiorite and quartz diorite and granite and the granite gneiss 1000 m.y.	Diorite batholiths diorite to trondhjemitic	Second dioritic abundant trondhjemite series 800 m.y.
1.	Diorite and granodiorite 1000 m.y. or older				First dioritic series 960 m.y.

series of Greenwood and Brown's classification (1973).

Injection gneiss 785 m.y. old. This is gneissic quartz diorite to quartz monzonite in the form of complex domal structures with a compositional trend from early calcic to late calc-alkaline rocks.

Quartz monzonite 650-600 m.y. These range from gabbro to granite in composition and have calc-alkaline compositional trends similar to Greenwood and Brown's classification (1973).

Granite and quartz monzonite, 570-550 m.y. old. These are the youngest granite plutons.

2.4. Dikes

According to the 1:500,000 geologic map (Brown et al., 1962) dikes cut through all rock units of the Southern Hijaz Quadrangle except the Shammer Group. There are three major types of dikes: Felsic or mostly rhyolite dikes, diabase dikes and, andesite dikes. Only andesite dikes were mapped at Mahd AD Dahab where they cut all rock units on the mountain. North of Mahd AD Dahab, dikes of a pink porphyritic rhyolite with phenocrysts of quartz and white feldspars (Aguttes and Duhamel, 1971) and light gray microdiorite containing biotite and amphibolite with large plagioclase phenocrysts have been mapped. They are latest as they cut through the youngest granite (Alabouvette, 1973).

2,5. Structure

2.5.1. Folds

Large open folds trend and plunge north as described by Brown et al. (1962) primarily from collection of attitudes of lineations. The Schist Series in the southeast part of the Southern Hijaz Quadrangle appears to form a large fold structure that may be a synclinorium (Goldsmith, 1971). Nebert (1965a, b) also recorded north trending fold axes plus smaller recumbent folds with axes paralleling those of the larger folds at Jabal Samran northwest of the Quadrangle. At Jabal Sayid and Jabal Al Mahd the regional structure is a monocline in which beds strike west and dip 50 to 80° north (Alabouvett, 1973).

2.5.2. Faults

Brown et al. (1962) mapped three different fault trends in the quadrangle. In the southeast, north trending faults, some traced for more than 60 km and attributed to the Hijaz Tectonic Cycle, are dominant and traverse rocks of Khamis Mushyat, Hali, Baish and Baha Groups (Schmidt et al., 1973). Plutonic rocks which are traversed and displaced by this type of fault are pre-tectonic, syntectonic and probably late-tectonic (Brown, 1972).

Northeast trending faults are dominant in the Scarp Mountains from Al-Lith in the southwest to Jabal Subh in the northwest. Rocks that these faults traverse are similar to those traversed by the north trending faults as well

as nearly all the plutonic rocks including some post-tectonic granite.

Northwest striking faults are quite common at Jabal Sayid, Umm AD Damar and northeast of the Mahd AD Dahab area. These faults represent the southwest extention of the Najd Fault System and truncate older north trending structures attributed to the Hijaz Tectonic Cycle. All the layered rocks and plutonic rocks of the northeast corner of the quadrangle, including the youngest plutonic rocks of 535 m.y. age, are cut and displaced by these faults.

2.6. Summation

The Southern Hijaz Quadrangle is characterized by a thick sequence of Proterozoic metavolcanic and metasedimentary rocks mostly in the greenschist facies of regional metamorphism which have been grouped by many geologists but which can be summarized from base to top as basement gneiss conformably to slightly unconformably overlain by mafic and ultramafic flows and shallow intrusions, clastic sedimentary rocks, andesite and pyroclastic rocks of intermediate to felsic composition, rhyolite, trachyte, an angular unconformity beneath coarse conglomerate, followed by shale and sandstone, another angular unconformably and, ultimately rhyolite flows and felsic pyroclastic rocks.

Plutonic rocks of comparable age and composition to volcanic members of this layered sequence intrude volcanic and sedimentary rocks and are an assemblage similar

to that described for eugeosyncline or island arc compressional tectonic settings of differentiated submarine volcanic rock, clastic and chemical sedimentary rocks and attendant intrusions described from the literature from Archaean (Goodwin and Riddler, 1970) to the Recent (Dickinson, 1970). It has been suggested that this volcanisn and plutonism is related to subduction beneath a volcanic arc and continental closure (Garson and Shalaby, 1974; Marzouki and Fyfe, 1977, and Marzouki, 1977). The rocks are succeeded by clastic sedimentary and volcanic rocks extruded subaerially during the final stage of volcanism, the tensional Najd Fault System. The Mahd AD Dahab gold mine and other base and precious metal occurrences are within the upper part of the differentiated submarine volcanic section.

CHAPTER 3

GEOLOGY OF THE MAHD AD DAHAB GOLD MINE

3.1. General Statement

The Mahd AD Dahab gold mine is at the north end of the Southern Hijaz Quadrangle in an isolated mountain called Jabal Al Mahd (Plate 1a) which rises 800 m above the desert alluvium and 1238 m above sea level. The mountain consists of a west striking, north dipping volcanic sequence with a base at the south end of 300 m of massive dark green andesite which appears to unconformably overlie granodiorite outcropping 5 km southeast of the mountain. Andesite is overlain successively by 90 to 120 m of agglomerate with angular to subangular fragments of andesite and rhyolite up to 30 cm in diameter. This is overlain by 270 m of lower rhyolite tuff mainly thick bedded, very siliceous and intercalated in its lower part with sandstone and siltstone. One hundred and forty meters of lithic crystal tuff overlie the lower rhyolite tuff and is subangular fragments of various shape up to 35 mm in diameter of rhyolite, andesite, chert and iron oxides embedded in a fine tuffaceous matrix. A fine grained rhyolite tuff is the uppermost unit overlying the lithic crystal tuff and is essentially 2 to 4 mm fragments of rhyolite and andesite in a fine grained ash. The tuff is intercalated with thin bedded chert and siltstone. An

Plate 1

a. View of Jabal Al Mahd looking south, P.R. is the porphyritic rhyolite known as the mine hill. Mill and mine buildings in foreground.

b. The porphyritic rhyolite of the mine hill, looking south into old open stopes on north trending quartz veins and trench and open stope aligned easterly in upper rhyolite tuff and chert.

PLATE 1

a

b

elliptical body of porphyritic rhyolite 350 m long and 260 m wide (Plate 1b) occurs within the upper part of this layered sequence at the northeast corner of Jabal Al Mahd (Fig. 6, 6a).

Quartz viens cut all the layered rocks and the porphyritic rhyolite, are most abundant in the porphyritic rhyolite and the rocks immediately about it, and are less common in the lower rhyolite tuff. Veins stop against and within chert at the very top of the section and the north edge of the mountain (Fig. 7) and, are in turn cut by andesite dikes. Stopes excavated by ancient miners follow quartz veins along strike into the chert where they branch along bedding in the chert. Stopes at the north end of the mountain are therefore T-shaped with the bar of the T in the chert and the stem along the quartz vein.

MacLean (1961) called the layered volcanic and the sedimentary rocks, the Mahd AD Dahab Series. Brown et al. (1962) considered it part of the Halaban Andesite and the Fatima Formation. Goldsmith and Kouther (1971) used the name Mahd AD Dahab Series of MacLean (1961) and they thought the rocks are possibly equivalent to the Murdama and Fatima Formations of Brown et al. (1962). Aguttes and Duhamel (1971) mapped Jabal Al Mahd as Halaban Group. Robert et al. (1975) considered the section as probably belonging to the Murdama Group of Schmidt et al. (1973). In the current thesis the volcanic sequence is considered as middle and upper parts of the Halaban Group of Schmidt et al. (1973), because of its

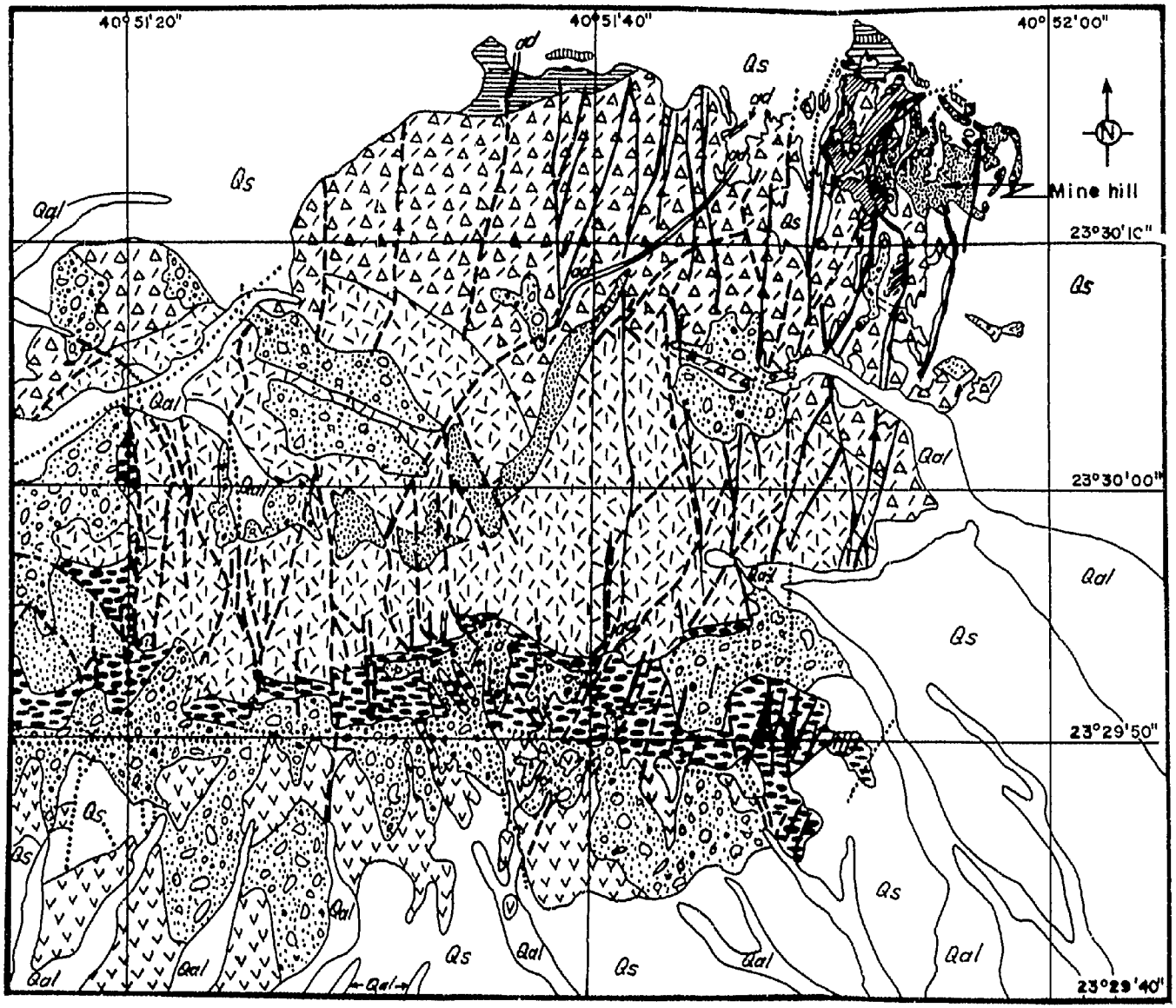

SCALE

100 0 100 200 m.

400 0 400 800 ft.

LEGEND

QUATERNARY

- Qal — Alluvium
- Qs — Older alluvium
- Talus

PRECAMBRIAN

- Qad — Andesite dike
- Porphyritic rhyolite
- Upper rhyolite tuff and chert
- Lithic crystal tuff
- Lower rhyolite tuff
- Agglomerate
- Andesite
- Open pit
- Fault
- Quartz vein
- Silicified zone

FIGURE 6. GEOLOGIC MAP OF JABAL AL-MAHD

Modified from Robert and others (1975)

H.D. HAKIM

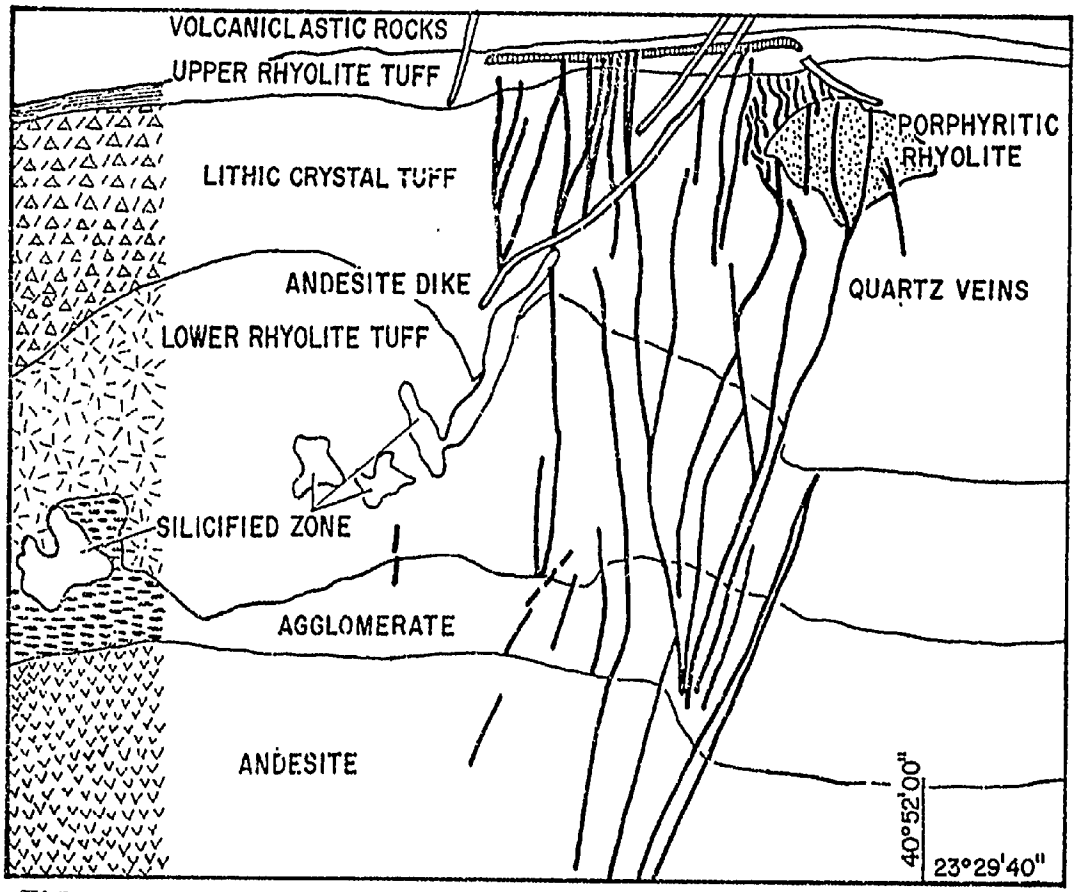

FIG. 6a GENERALIZED GEOLOGIC FEATURES OF JABAL AL-MAHD

SCALE 100 0 100 200 m.
400 0 400 800 ft.

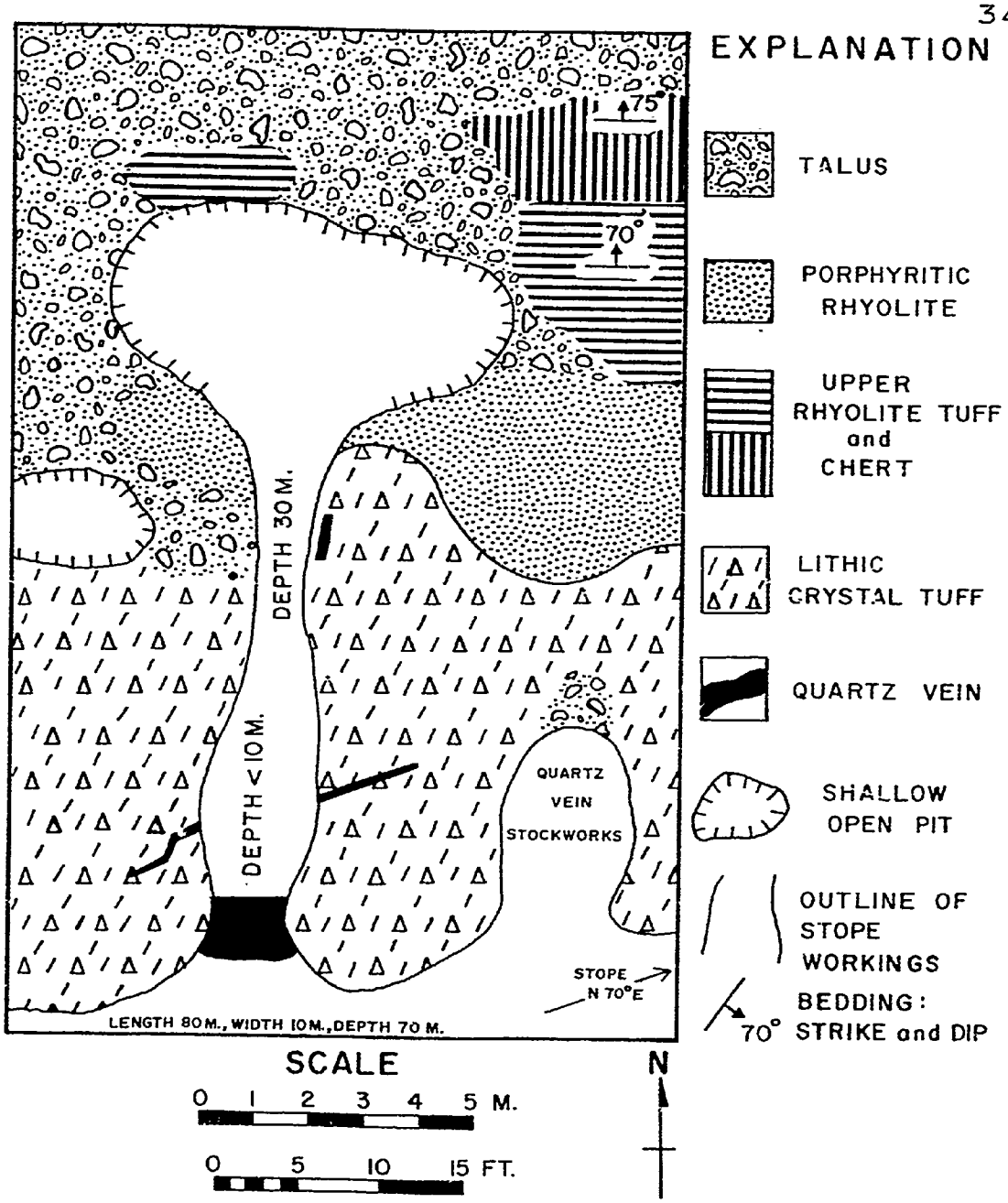

FIGURE 7 PLAN VIEW SKETCH OF SURFACE WORKINGS No 1

Stope trends north along quartz vein, widening at north end to east-west trending pit in Upper Rhyolite Tuff and Chert. Remnants of quartz vein form support pillars in stope.

field relationships and its composition and texture as compared to type sections.

An east striking valley eroded into thin bedded volcanoclastic rocks separates Jabal Mahd AD Dahab from the next outcrop to the north which is essentially a continuation of the north dipping homoclinal succession with andesite at the base overlain by fragmental rocks and topped by massive flow banded rhyolite. These rocks are not traversed by the quartz veins nor by the andesite dikes so distinctive of Jabal Al Mahd.

Veins with the most gold and the most sulphide minerals are most abundant at the north edge of the Jabal and at the top of the section within and about the porphyritic rhyolite body. Barren veins cut through the whole stratigraphic section exposed on Jabal Al Mahd, but are more linear, sharp walled and more dominant in the central part of the mountain.

3.2. Andesite and Dacitic Rocks

Andesite, at the south end of Jabal Al Mahd is the base of MacLean's (1961) Mahd AD Dahab Series and is approximately the middle of the Halaban Andesite as defined by Brown et al. (1962). The exposed thickness of the andesite on the Jabal is 350 m. Its base is covered by alluvium and it is unconformably overlain by agglomerate.

The andesite is dark green to gray, massive with veinlets of chlorite, calcite, and epidote and vesicles

filled with calcite, plus quartz (Plate 2a). Some of the amygdales are mostly filled with chlorite and are lined with small quartz crystals. Magnetite is present as an accessory mineral. The fine-grained matrix is essentially plagiocalse crystals. Phenocrysts are prismatic, euhedral to subhedral and totally occupied by sericite. Ferromagnesium minerals are pseudomorphosed by iron and magnesium-rich chlorite.

The massive andesite grades slightly into a fine-grained dacitic rock. Analyses (Table 4) confirm the assigned field name of andesite and also indicate that the rocks become dacitic with less alumina and more silica in the upper part of the unit than its lower part (Fig. 8). Generally there is no change in TiO_2 content as SiO_2 content changes from 45% to 65% (Fig. 9). No independent Ti minerals such as sphene were identified and no Ti occurs in magnetite. Although there is no definite trend, generally MgO increase as silica decreases (Fig. 10). Where SiO_2 is 63.43%, MgO content is 3.27%. Fe_2O_3:SiO_2 (Fig. 11) has a defined trend where the Fe_2O_3 content decreases with increasing SiO_2. Generally K_2O:SiO_2 has no defined trend (Fig. 12). Compared to analyses of andesites of volcanic arcs such as Tonga-Kermadec (Carmichael et al., 1974) andesite from Mahd AD Dahab has much more K_2O and indeed has the reverse of the usual relative abundances of K_2O and Na_2O. From the above data it is concluded that: a, the magma was originally of basaltic affinity enriched in iron and ferromagnesium minerals; b, continuous crystallization led to the depletion of the magma in ferro-

Table 4. Chemical analyses (major oxides wt.%) of andesite and dacitic rocks from Mahd AD Dahab.

Sample No.	502	602	2202	2502	155	1707	18	24	2508
SiO_2	55.41	62.01	63.43	64.76	63.09	45.81	53.95	46.44	48.61
TiO_2	1.25	1.06	1.04	.20	.97	1.26	1.08	1.35	1.04
Al_2O_3	16.31	13.52	13.19	12.87	11.59	16.52	15.19	17.83	17.97
Fe_2O_3	7.29	8.02	7.20	4.84	9.34	12.67	10.60	11.45	10.14
MnO	.54	.34	.20	.29	.26	.28	.20	.38	.27
MgO	7.82	3.84	3.27	11.30	3.14	5.25	5.20	7.28	7.15
CaO	1.83	1.63	1.10	.00	5.32	6.26	3.23	6.00	5.74
Na_2O	.95	1.81	3.85	2.74	2.64	1.44	1.84	2.22	2.02
K_2O	4.87	4.50	2.56	1.14	.06	3.25	3.53	2.21	2.32
P_2O_5	.49	.42	.25	.02	.18	.26	.24	.24	.18
Total	95.93	97.41	96.08	97.92	96.78	92.80	95.43	95.15	95.25
				Norms (CIPW)					
Q	15.83	33.37	22.64	26.23	.00	29.48	10.69	0.00	13.07
or	29.92	27.23	15.74	6.86	20.60	.37	21.85	13.70	14.67
ab	8.36	15.68	33.90	23.62	12.18	23.09	16.31	19.70	0.00
an	3.05	5.50	4.00	.13	30.84	20.26	15.21	29.59	29.23
co	8.73	3.79	2.79	7.31	.00	.00	3.17	1.52	5.83
ca	.00	.00	-	.05	.00	.00	.00	-	.00
hy	27.30	17.41	15.10	32.97	19.22	16.17	-	10.40	30.96
mt	3.13	3.92	3.12	2.70	4.02	3.42	26.35	3.80	3.66
il	2.47	2.06	2.06	.39	2.35	1.90	3.68	2.69	2.11
ap	1.21	1.02	.62	.05	.56	.44	.60	.60	.46

THE UNIVERSITY OF WESTERN ONTARIO - FACULTY OF GRADUATE STUDIES

C E R T I F I C A T E O F E X A M I N A T I O N

Chief Advisor

Advisory Committe

Examining Board

The thesis by

Hashim Darweesh M. Hakim

entitled

Geology and the Genesis of Gold-Silver
Base Metal Sulphide-Bearing Veins
at Mahd AD Dahab
Kingdom of Saudi Arabia

is accepted in
partial fulfillment of the
requirements of the degree of
Doctor of Philosophy

Date September 18/78

Chairman of Examining Board

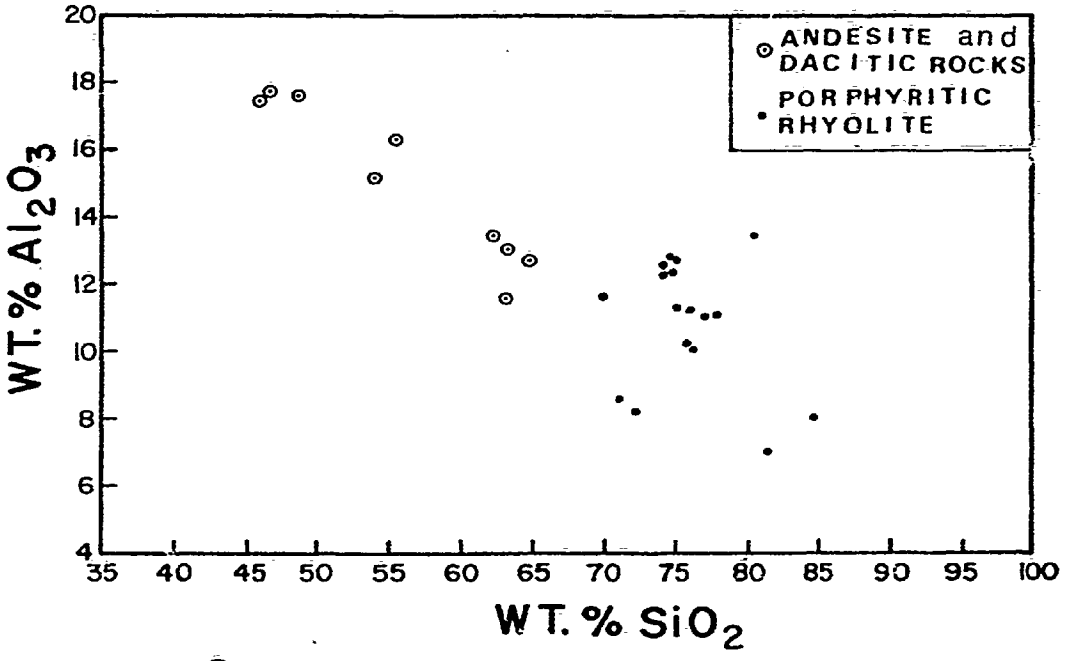

FIGURE 8 - Al_2O_3 versus SiO_2 for Andesite and Dacitic Rocks and for Porphyritic Rhyolite

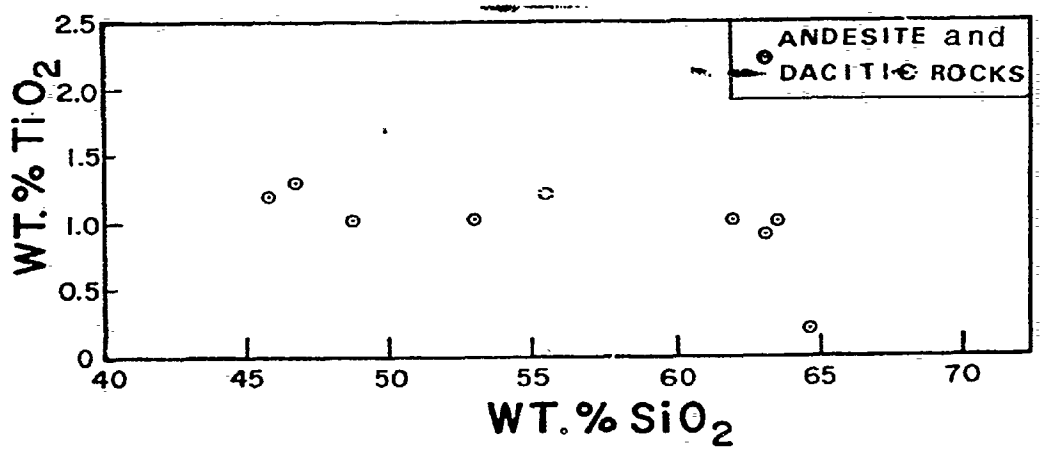

FIGURE 9 - TiO_2 versus SiO_2 for Andesite and Dacitic Rocks

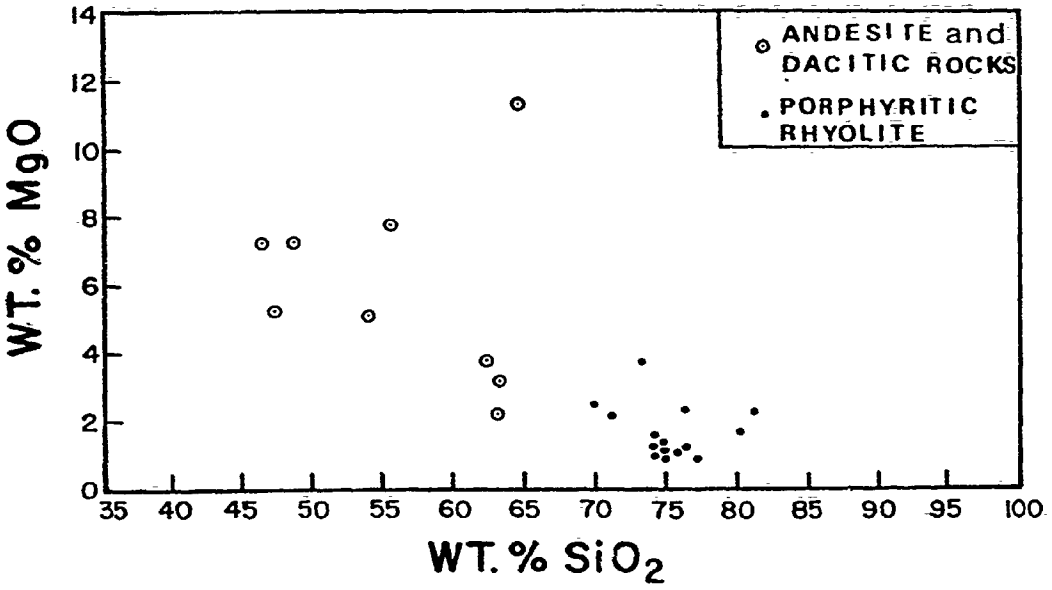

FIGURE 10- MgO versus SiO_2 for Andesite and Dacitic Rocks and for Porphyritic Rhyolite

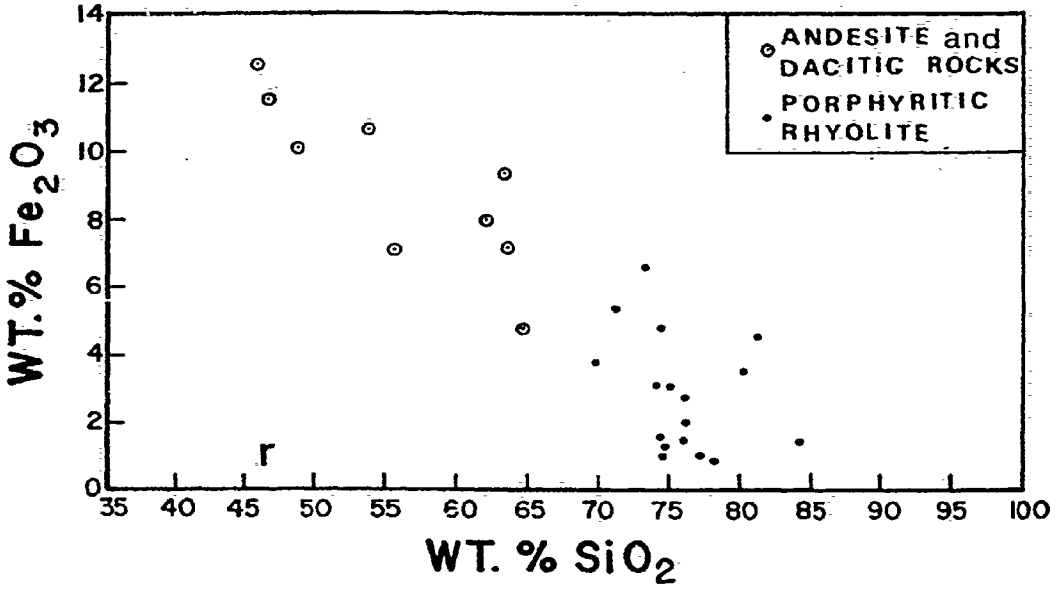

FIGURE 11 - Fe_2O_3 versus SiO_2 for Andesite and Dacitic Rocks and for Porphyritic Rhyolite

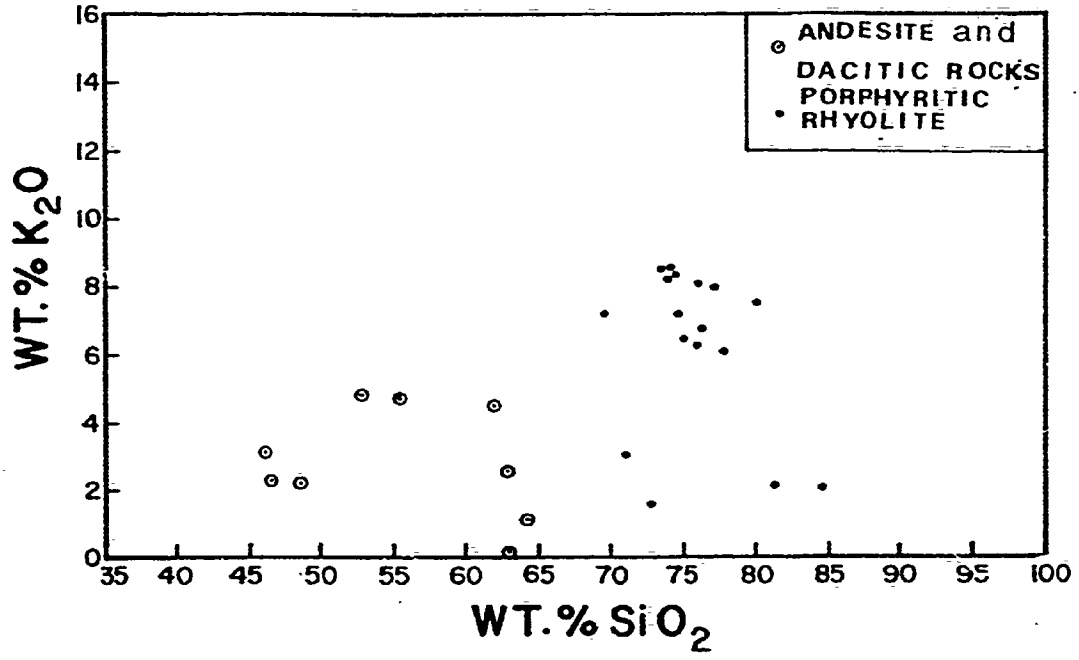

FIGURE 12 - K_2O versus SiO_2 for Andesite and Dacitic Rocks and for Porphyritic Rhyolite

Plate 2

a. Thin section. Amygdales in andesite filled with chlorite, calcite, quartz and epidote. Quartz grains are also along the amygdales walls.

b. Polished slab. Lower rhyolite tuff cut by three generation of quartz.

c. Polished slab. Drill core sample from the lithic crystal tuff, consists of andesite, rhyolite and ferrogenous chert. White patches are calcite.

d. Polished slab. Lithic crystal tuff consists of fragments of andesite, rhyolite, ferrogenous chert, quartz crystal fragments and black chlorite in a very fine matrix. The white irregularly shaped patch in the upper half of the picture is limonite surrounded by black chlorite.

e. Thin section. Large aggregate of polegonal quartz crystals. The quartz is mostly surrounded by calcite and contains some calcite inclusions.

f. Thin section. Lithic crystal tuff. Orthoclase crystal partly occupied by sericite which occurs also along thin fractures and crystal edges. Quartz crystals (white) on the orthoclase grain, The matrix is sericite and some pieces of quartz crystals.

PLATE 2

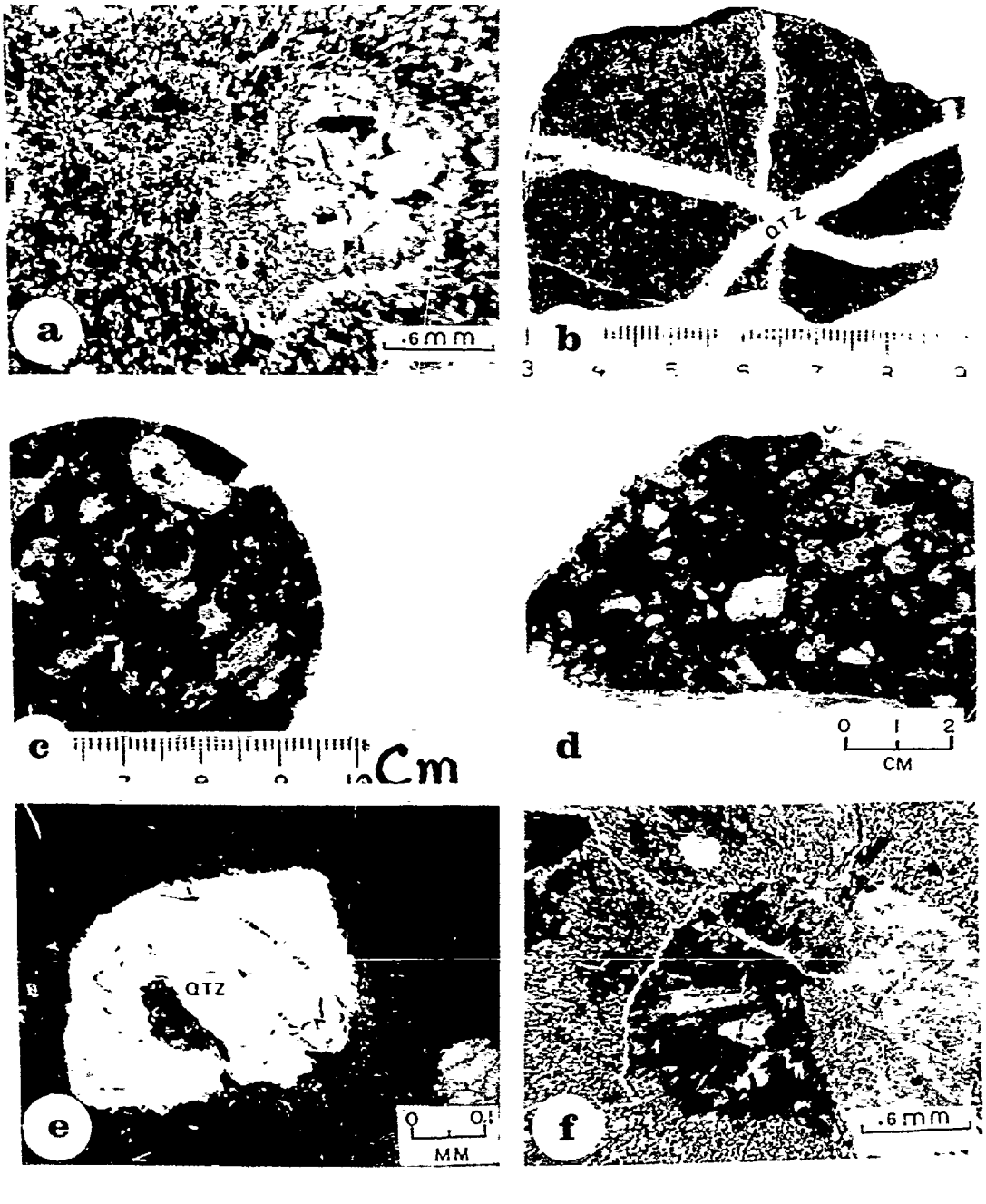

minerals and the SiO_2 content in the rocks increased; c, Ti being an immobile element, remained in constant abundance through continuous crystallization; d, these rocks have been greatly affected by a metasomatism which depleted the Na_2O content and enriched the K_2O content. This is observed through the volcanic section at Mahd AD Dahab. Because dacitic rocks constitute an extremely small proportion of the andesite-dacite rocks, this rock suite is referred to in the text and on the map and some figures as andesite.

3.3. Agglomerate

Agglomerate crops out on the south side of the Jabal Al Mahd and unconformably overlies the andesite. Goldsmith and Kouther (1971) mapped this unit as a basal conglomerate, but the presence of the fragments with great angularity in most instances and the tuffaceous matrix are evidence for it being considered as agglomerate. Robert et al. (1975) mapped the contact with the underlying andesite as a normal fault that strikes east. However, the present study interprets this as a depositional contact.

The agglomerate is dark brown to red in colour on weathered surface. It consists of angular rhyolite and andesite fragments up to 35 cm in diameter set in a very fine tuffaceous matrix. Andesite fragments have plagioclase laths and some fresh pyroxene but most ferromagnesium minerals are pseudomorphed by chlorite. Rhyolite fragments which are more common, consist of quartz, orthoclase and sericite. Isolated crystals of orthoclase in the matrix are mostly covered with sericite and calcite.

Both sulphide-bearing and barren quartz veins cut across the agglomerate and for most veins it is the wall rock of their southern extention. Fewer veins continue into andesite below the agglomerate (Fig. 6a).

3.4. Lower Rhyolite Tuff

Lower rhyolite tuff is the central and highest part of Jabal Al Mahd, standing out as a resistant cliff. Thickness is variable from less than 100 m on the west side to a maximum of 180 m to 200 m in the centre of Jabal Al Mahd. Contact with the underlying agglomerate is gradational over 10 m. The rock is essentially a very fine-grained siliceous ashfall, laminated, with some intraformational sedimentary facies. In its lower part the tuff is in thin laminations, 1 mm thick, and the laminations are intercalated with 3 mm thick subparallel stringers of pyrite, chalcopyrite and quartz. It becomes a thick bed of fine-grained sandstone intercalated with less abundant lapilli tuff and some iron oxides in the middle and grades mainly to lapilli tuff with some shale and cherty beds at its top. Cherty beds are cryptocrystalline, dense layers. There are also 2 mm thick crystalline quartz stringers parallel to bedding.

On its weathered surface the tuff is tan to dark brown in colour. In fresh samples it is olive gray to light yellow. The rock consists generally of quartz phenocrysts with corroded edges, broken surfaces and less than 3% equidiamentional euhedral to subhedral, zoned orthoclase

phenocrysts in a very fine matrix. Few orthoclase phenocrysts retain carlsbad twinning and are generally obscured by sericite and chlorite that occupy the central part of the crystals. Matrix to phenocrysts is 75 to 80%. Pyrite is up to 5% of the whole rock as an accessory mineral and is mostly pseudomorphosed by hematite.

Sulphide-bearing veins are less dominant in this unit than the underlying and overlying rock units. In the central part of Jabal Al Mahd, the lower rhyolite tuff has a zone 100 by 30 m of randomly distributed quartz veins of three generations (Plate 2b) from less than a mm to a few mm thick extending northnortheast from the lower rhyolite tuff to the overlying lithic crystal tuff.

3.5. Lithic Crystal Tuff

This forms the north part of Jabal Al Mahd with thickness varying from 110 to 130 m and is conformable with the lower rhyolite tuff. It was mapped by Goldsmith and Kouther (1971) as an agglomerate and in 1975, Robert et al. applied the name upper agglomerate. Layers strike east following the general trend in the area, are mostly vertical but sometimes dip 60 to 70^{o}N. Colour is quite variable depending upon the type of fragments and the cementing matrix and ranges from dark red on weathered surfaces to olive gray on fresh surfaces. Size of the fragments is from a few mm to 3 cm (Plate 2c, d) and they are rhyolite, andesite, red, gray

and green chert, iron oxide, glass shards, crystals of quartz, andesine, orthoclase and pieces of crystals in a fine-grained matrix of chlorite, epidote, calcite, sericite and quartz. In some rhyolite fragments the central part is black in colour and has a relict glassy nature. Fragments account for 50% of the rock. Quartz crystals are euhedral to subhedral mostly cracked and the crystal edges are rounded (Plate 2e). Most orthoclase crystals are clouded with sericite but some still retain carlsbad twinning (Plate 2f). There are a few sodic plagioclase crystals and crystal pieces in which lamellar twinning is still visible.

Calcite occurs as patches and veinlets. Epidote is found as crystal aggregates and veinlets. Fine-grained disseminated pyrite is up to 5% of the groundmass. Plagioclase sites in the matrix and in the fragments are partly occupied by sericite. Quartz occurs either as veinlets in the fragments and the groundmass or as semi-rounded medium grains arranged around each fragment. The rock fragments and the K-feldspar crystal fragments which are totally occupied by sericite (Plate 3a) are also cut by calcite. In andesite fragments, chlorite, calcite and epidote are the main secondary minerals and calcite can account for up to 20% of the rock either as patches or veinlets cutting each other and displaced by veinlets or sulphide minerals (Plate 3b). There is a greater abundance of quartz veinlets in fragments than in groundmass so that the addition

Plate 3

a. Thin section. Lithic crystal tuff, medium-grained andesite fragment (white) occupied by sericite and chlorite against fine-grained rhyolite fragment (gray). The black crystal between the two fragments is glass with quartz grains along its edges. Crossed nicols.

b. Thin section. Lithic crystal tuff. Very fine-grained rhyolite fragment (dark gray) contains dissiminated pyrite cubes (black and cross-cut by calcite and quartz veins. The quartz vein contains pyrite crystals. Crossed nicols.

c. Thin section. Lithic crystal tuff. Fine-grained rhyolite fragment (dark gray) cut by quartz veins and adjacent to an andesite fragment (whitish). Quartz veining is prior to fragmentation. Crossed nicols.

d. Thin section. Lithic crystal tuff. Perthite phenocrysts in fine matrix of rhyolite fragments. Quartz crystals are cut at the top of the phenocryst and to the left hand side in the andesite fragment. Crossed nicols.

e. Thin bedded rhyolite tuff intercalated with thick bedded chert (white). Thin band of chert is also in the lower part of the picture. Sample location northwest corner of Jabal Al Mahd.

f. Chert (white) intercalated with upper rhyolite tuff (light to dark gray) with soft sediment slumpage.

PLATE 3

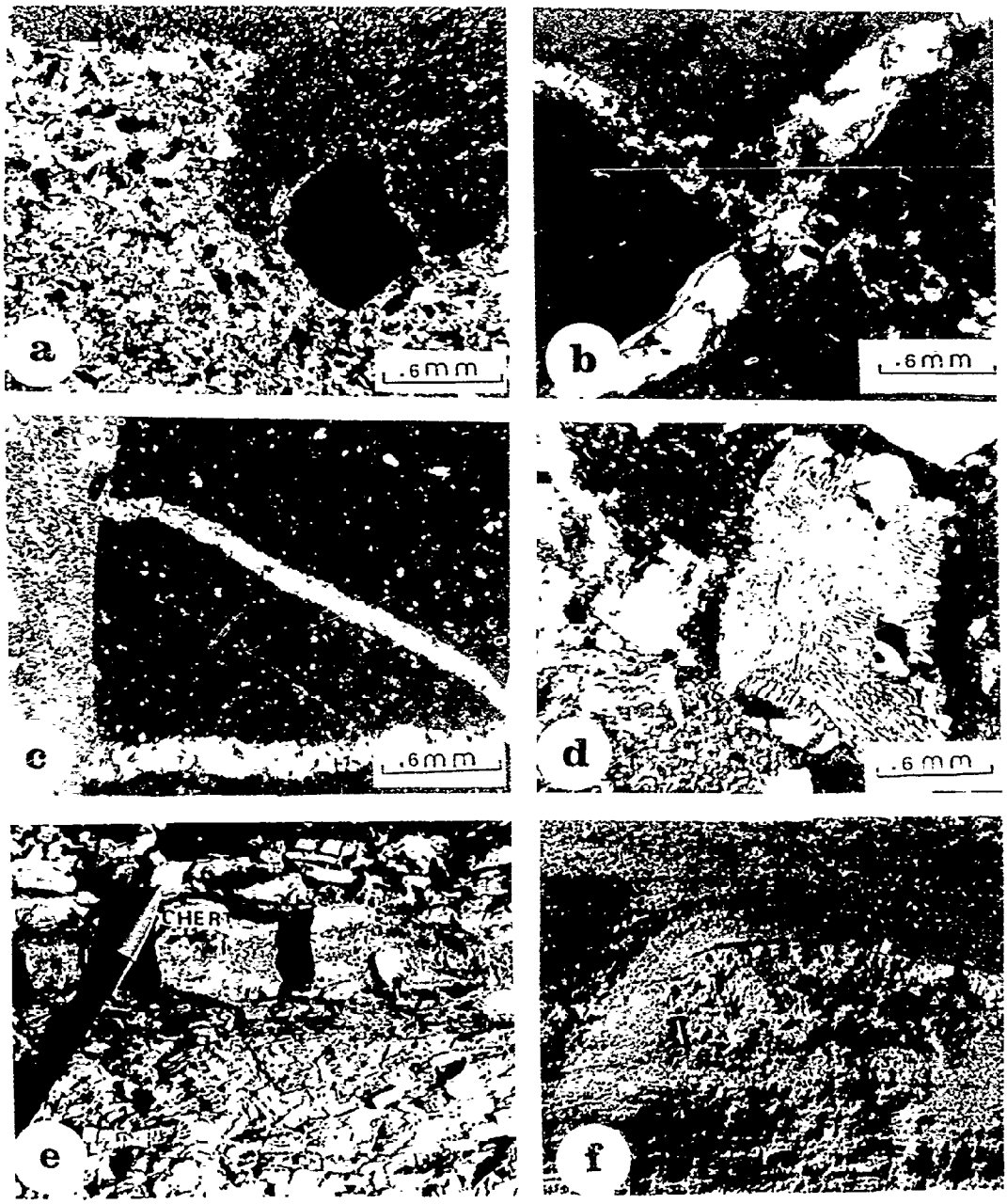

of silica was, partly, prior to fragmentation (Plate 3c). Perthitic intergrowths of feldspars are common (Plate 3d).

3.6. Upper Rhyolite Tuff

The upper rhyolite tuff at the north side of Jabal Al Madh is 200 m thick (Robert et al., 1975) and rests conformably on the lithic crystal tuff. In the Wadi north of the mountain, the tuff is partly covered by alluvium. It is thin bedded (Plate 3e), very fine-grained white to yellow in colour, weathers to red and purple and is fine volcanic ash and crystals of orthoclase, plagiocalse and quartz. It also contains disseminated pyrite grains which oxidize to hematite and make the rocks red. In the fine matrix, there are fragments of rhyolite, andesite and chert. Calcite veinlets crosscut the matrix.

The tuff grades locally into ash intercalated with chert and both tuff and chert have soft sediment slump features (Plate 3f). Intercalated chert bands are from 1 cm to 2.5 cm thick, tan to red in colour, and with some local structures (Plate 4a) not present in the thinly bedded tuff. Both chert and tuff are displaced by small faults (Plate 4b) with a few cm displacement. The chert and the tuff strike east and dip 45° to 50° north, or stand vertical.

3.7. Prophyritic Rhyolite

This rock type is in an elliptical body 350 m by 250 m which crops out on the northeast corner of Jabal Al

Plate 4

a. Development of a z fold on 2 chert bands, each 5 cm thick. This type of folding is a soft sediment deformational feature.

b. Thin bedded upper rhyolite tuff intercalated with thick bedded chert from the northwest corner of Jabal Al Mahd. Small local faults trending northwest displace chert and tuff beds.

c. Thin section. Porphyritic rhyolite . Grayish white euhedral orthoclase phenocryst in a fine-grained matrix of mostly quartz and plagioclase. The phenocryst is partly covered by sericite. Carlsbad twinning is still visible. Crossed nicols.

d. Thin section. Porphyritic rhyolite, dark gray orthoclase phenocryst occupied by quartz and sericite at the centre. The orthocalse phenocryst is surrounded by quartz grain. Crossed nicols.

e. Thin section. Porphyritic rhyolite, pyrite cube weathered to hematite and filled along edges with quartz grains. The crystal is embedded in fine grains of quartz and plagioclase. Crossed nicols.

f. Thin section. Porphyritic rhyolite, pyrite cube weathered to hematite and mostly filled with quartz. Crossed nicols.

PLATE 4

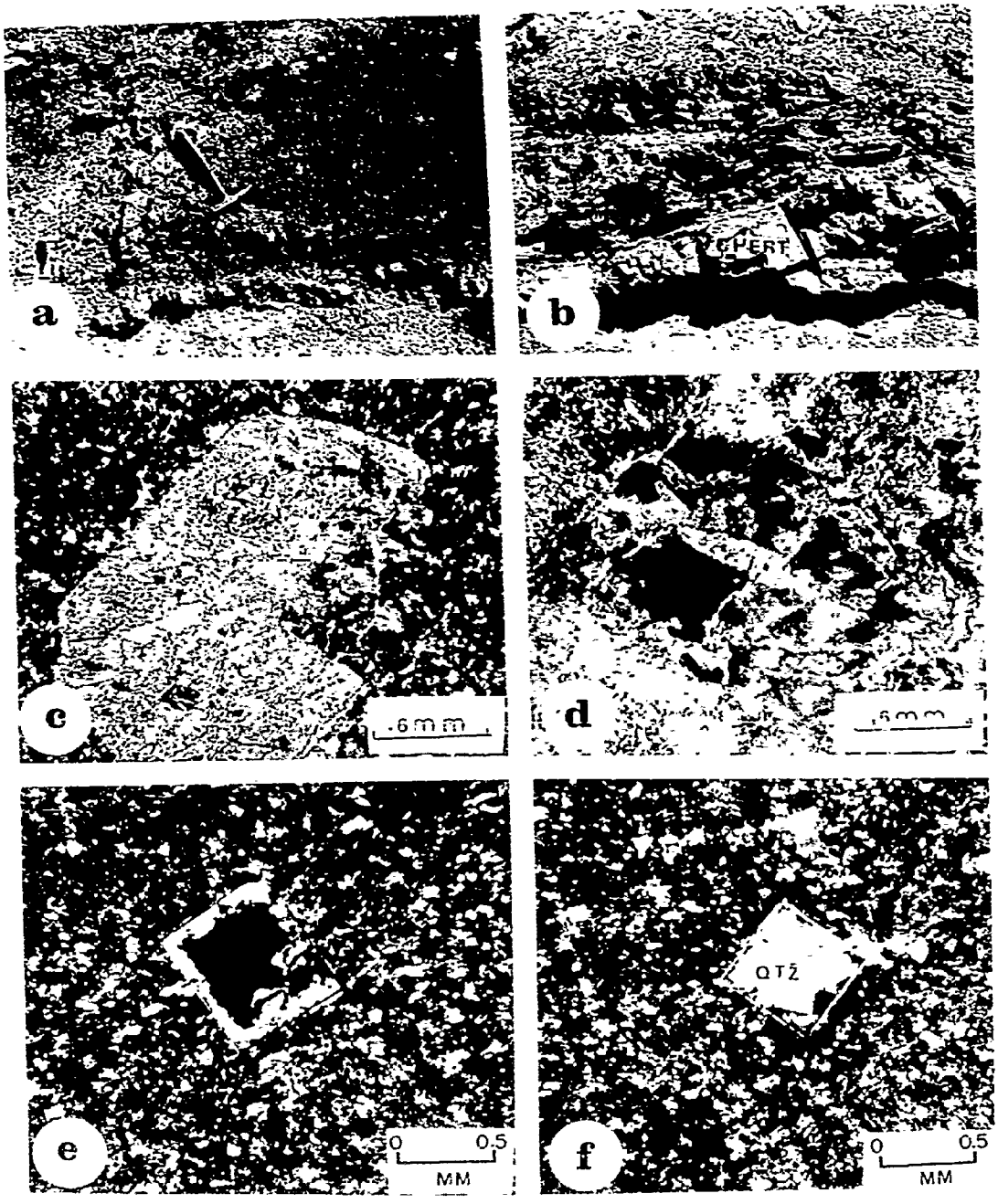

Mahd. Dirom (1947) considered it a volcanic flow overlain unconformably by the rhyolitic lithic crystal tuff. Robert et al. (1975) considered it a plug-like intrusion. Routhier and Delfour (1974) considered it an intrusion against which the lithic crystal tuff is in fault contact. In this current study the porphyritic rhyolite is interpreted as a very shallow intrusion and in part an extrusion in sharp contact with the underlying lithic crystal tuff and the overlying upper tuff.

The rock is black to olive green and weathers light brown. In some instances it is red in colour because of the abundance of hematite. Most hematite does not pseudomorph sulphide or silicate minerals, is not associated with limonite or geothite, and in some instances is completely enveloped in quartz. The hematite is therefore considered as a primary mineral. Euhedral to subhedral phenocrysts of orthoclase (Plate 4c), quartz and plagioclase account for 40 to 45% of the rock and they are set in a fine-grained microcrystalline matrix. Orthoclase phenocrysts are equidimentional some with corroded edges and either partly or totally occupied by sericite (Plate 4d). Sericite forms patches in phenocrysts and along cracks normal to the crystal elongation. Orthoclase phenocrysts may be surrounded with fine quartz grains. Quartz phenocrysts are euhedral and subhedral bipyramidal with corroded edges. Generally, they account for 5% of the phenocrysts, but rarely exceed 10%. Elongated euhedral to subhedral plagiocalse phenocrysts are rare and where they occur

they are oligoclase with extinction angles of less than 15^{o}. Some are occupied by sericite. In fresh phenocrysts lamellar twinning is still preserved particularly at the edges whereas the centre is occupied by sericite and quartz grains. Magnetite amounts to 2% and partly surrounds quartz phenocrysts. Hematite accounts for up to 5% as cubes either partly occupied by quartz grains along the internal edges of the cube (Plate 4e) or totally leaving some hematite as relict along the edges (Plate 4f). The groundmass is essentially very fine quartz grains with thin acicular fibrous plagioclase laths (Ab_{70}-An_{30}) covered by clay minerals, sericite and calcite. Calcite occurs either as patches or thin veinlets. Less commonly chlorite occurs in patches in the groundmass and accounts for 2 to 3% and rarely 15%. One to 2 mm intersecting quartz stringers are randomly distributed throughout the groundmass. The top part of the porphyritic rhyolite is characterized by stockwork quartz stringers. Along its flanks, the rock is siliceous and is cut by 2 to 5 cm thick veinlets of orthoclase that surrounds quartz patches.

The porphyritic rhyolite (Table 5) has less alumina as silica increases (Fig. 8). Average abundances are 11.49% and 74.5 respectively. The MgO and Fe_2O_3 versus silica (Figs. 10 and 11) do not establish a general trend.

Table 5. Chemical analyses (major oxides wt.%) of the porphyritic rhyolite at Mahd AD Dahab.

SiO_2	74.68	74.91	74.05	75.90	77.00	71.06	74.04	74.46
TiO_2	.18	.17	.18	.18	.18	.26	.18	.19
Al_2O_3	12.70	11.26	12.42	11.21	11.09	8.42	12.14	12.73
*Fe_2O_3	1.09	3.15	4.95	2.13	1.07	5.49	3.18	1.68
MnO	.00	.27	.00	.00	.00	.35	.00	.00
MgO	1.21	1.31	1.42	1.13	1.02	2.19	1.21	1.33
CaO	.18	.12	.08	.13	.05	.13	.07	.07
Na_2O	.00	.00	.00	.00	.00	.00	.00	.00
K_2O	8.29	6.42	8.50	8.12	8.04	3.19	8.34	7.23
P_2O_5	.00	.00	.00	.00	.00	.00	.00	.00
Total	98.35	97.66	101.64	98.82	98.48	91.13	99.21	97.74
			Norm (CIPW)					
Q	40.80	48.57	38.62	43.35	44.65	58.31	40.51	45.71
or	49.82	38.87	49.45	48.54	48.26	20.78	49.72	43.74
an	.91	.61	.39	.65	.25	.71	.35	.36
co	3.46	4.19	3.03	2.21	2.33	5.22	3.01	4.89
hy	4.50	4.97	3.48	2.85	4.00	11.86	3.04	3.39
mt	.16	2.47	.00	1.53	.15	2.57	.00	.00
il	.35	.33	.15	.35	.35	.54	.19	.37
hm	.00	.00	4.79	.54	.00	.00	3.10	1.55

*Fe_2O_3 is present predominantly as hematite considered a primary mineral in the porphyritic rhyolite. The only other iron-bearing mineral is chlorite as samples chosen for these analyses were not pyrite-bearing.

The porphyritic rhyolite has a very large K_2O content and minor Na_2O next to the vein areas (Table 5). By comparison to published analyses of rhyolite, the porphyritic rhyolite at Mahd AD Dahab is not normal, principally because of the abundance of K_2O, the depeltion either partly or totally of Na_2O and, the presence of most of the iron as hematite. This suggests addition of K_2O and a drastic removal of Na_2O probably through metasomatism.

Age of Mahd AD Dahab porphyritic rhyolite has not been determined isotopically but Brown (1973) has determined a 696 m.y. age by Rb/Sr whole rock method for a similar appearing rhyolite body 12 km northeast of Mahd AD Dahab.

3.8. Andesite Dikes

These are the only dikes in Jabal Al Mahd. They are up to 2 m wide, strike N45^{o}E and dip 70^{o}E and weather into deep trenches. Their length is variable from a few metres to more than 250 m. They cut through the lower rhyolite tuff, the lithic crystal tuff, the upper rhyolite tuff, the porphyritic rhyolite, the quartz veins and appear to feed overlying flows (Fig. 13). They are green to greenish gray, light gray on weathered surface and composed essentially of plagiocalse laths, chlorite, epidote, calcite, quartz veinlets, quartz grains and up to 3% accessory magnetite. Chlorite occurs as a secondary mineral, after primary ferromagnesium minerals as patches, lining the walls of amygdales or filling the whole amygdales. There are 2 varieties of epidote, one

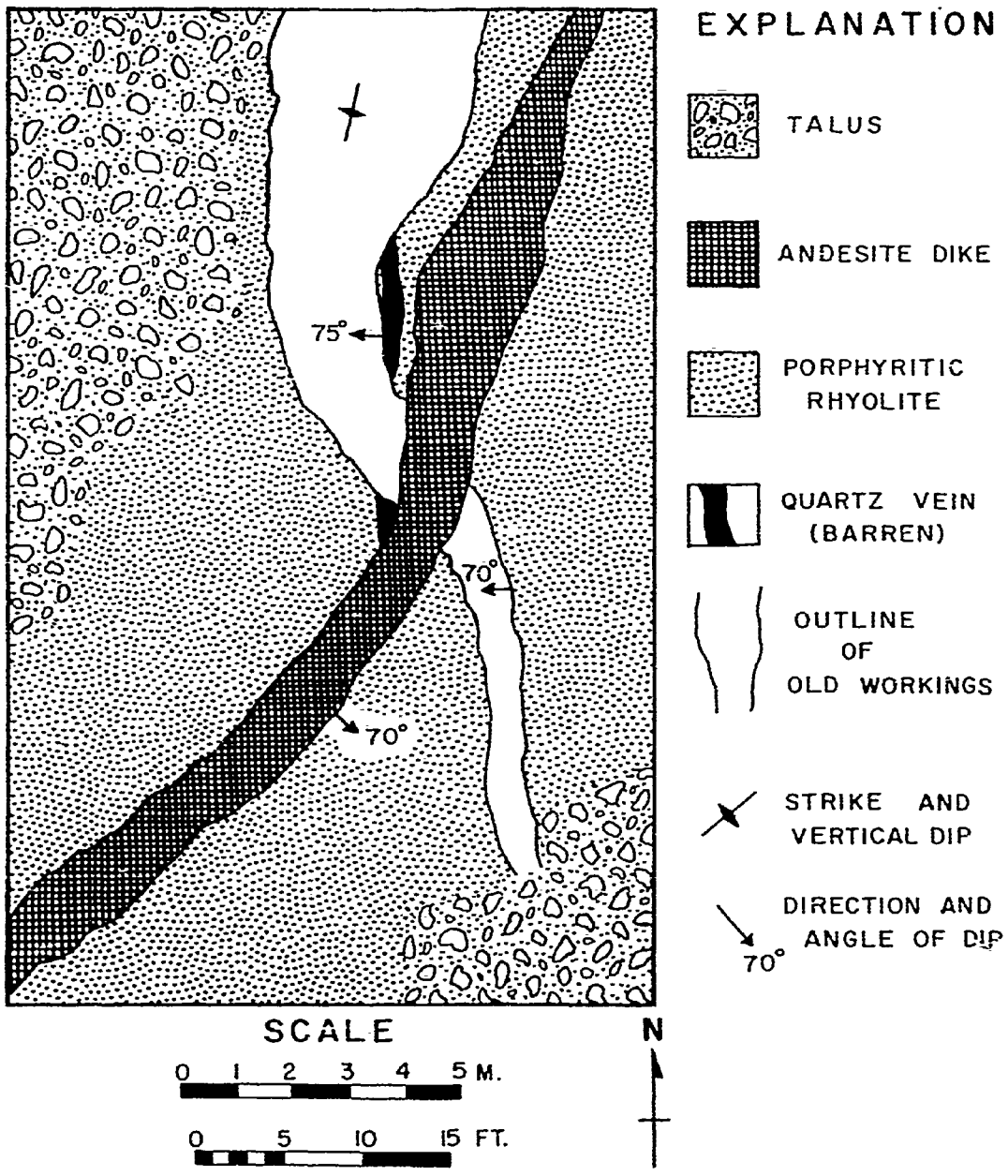

FIGURE 13 PLAN VIEW SKETCH OF SURFACE WORKINGS Nº 2

Old workings occupy site of sulphide-bearing quartz vein cross-cut by northeast-trending Andesite Dike.

is fine grained patchy saussurite coming from the breakdown of the plagioclase and the other is well crystallized acicular epidote filling amygdales. Thin veinlets of calcite are cut by quartz veinlets.

3.9. Granodiorite

The nearest pluton to Mahd AD Dahab is 5 km to the south southeast. It is approximately 7 km long and 2 to 3 km wide and was mapped by Brown et al. (1962) as a gray or pink calc-alkaline granite. In 1971, Goldsmith and Kouther mapped it as quartz monzonite. The current stuy classifies it as a granodiorite. Its age, falling within the similar rocks determined by the Rb/Sr isotopes, is 700 to 750 m.y. (Brown et al., 1962). This age was confirmed lately (Brown et al., 1973) by Rb/Sr age determination on biotite of a similar pluton located 80 km northeast of Mahd AD Dahab. Hence the granodiorite is probably older than the porphyritic rhyolite at Mahd AD Dahab.

The granodiorite is coarse grained, massive, pink with iron tarnishes on weathered surface. It is essentially composed of elongate euhedral plagioclase crystals in the oligoclase-andesine range. Plagioclase is partly covered with zoisite. Microperthite occurs in a few scattered crystals. Subrounded quartz crystals are the second principle rock-forming mineral and have a light brown colour because of clay mineral impurities. Biotite is the only primary ferromagnesium mineral and is mostly altered to green chlorite.

Epidote occurs as small veinlets cutting plagioclase crystals. Magnetite is the only accessory mineral. Myrmekitic texture, which is especially typical in granodiorite (Moorhouse, 1959) is an irregular branching intergrowth between plagiocalse and quartz. It is less common than micrographic texture (Plate 5a, b).

The rock, classified after Streckesin (1967) is in field 4 (Fig. 14) and the granodiorite field. Compared to Nockold s granodiorite (Table 6), it has more SiO_2 (Fig. 15), less K_2O and more Na_2O. Compared with the Al Hada granodiorite (Marzouki, 1977), the Mahd AD Dahab granodiorite has K_2O that ranges from 1.71% to 1.91% and averages to 1.84%, whereas the K_2O in the Al Hada granodiorite ranges from 2.7% to 4.1% with an average of 3.8%. Sodium content ranges from 5.23% to 5.90% and averages to 5.5% in the Mahd AD Dahab granodiorite and the Al Hada granodiorite has lesser amounts of Na_2O that range from 3.7% to 5.7% and the average is 4.88%.

3.10. Structure

Jabal Al Mahd is an east trending north dipping homocline with local variations in dip from moderately steep to vertical. The homocline is cut by fracture systems which are as follows from oldest to youngest:

1. A N40^{O}W striking fracture system which is not common and was only located in 2 places where it contains minor quartz veins which have been mined. These fractures are displaced by dominant N20W to N10E striking fractures.

Table 6. Chemical analyses (major oxides wt.%) of granodiorites at Mahd AD Dahab.

Mahd AD Dahab Granodiorite					Nockolds Granodiorite (1954)		
Sample No.	857	858	859	860	5	6	7
SiO_2	76.50	77.16	76.96	75.10	70.47	68.97	65.50
TiO_2	.22	.22	.22	.22	.30	.45	.61
Al_2O_3	12.43	12.46	12.37	12.32	15.50	15.47	15.65
Fe_2O_3	2.00	2.01	2.01	2.11	2.73	2.17	4.40
MnO	.06	.06	.07	.06	.03	.06	.09
MgO	.49	.47	.48	.42	.65	1.15	1.86
CaO	1.18	.80	1.00	.81	1.91	2.99	4.10
Na_2O	5.23	5.78	5.64	5.90	4.12	3.69	3.84
K_2O	1.91	1.82	1.84	1.71	3.59	3.16	3.01
P_2O_5	.57	.57	.56	.52	.15	.19	.23
Total	100.71	101.39	101.18	99.21	99.45	98.30	99.11
			Norms (CIPW)				
Q	36.91	35.26	35.40	33.59	27.1	26.2	20.0
or	11.21	10.61	10.75	10.19	21.1	18.9	17.8
ab	43.95	48.24	47.17	50.33	34.6	31.4	31.5
an	2.15	.28	1.32	.66	8.6	14.2	16.4
co	.96	.87	.60	.53	1.7	0.7	-
hy	1.21	1.15	1.18	1.05	4.40	5.1	8.4
mt	1.00	.99	1.03	1.34	0.9	1.6	2.3
il	.41	.41	1.41	.42	0.6	0.8	1.2
hm	.85	.84	.82	.65	-	-	-
ap	1.34	1.33	1.31	1.28	0.3	0.4	0.6

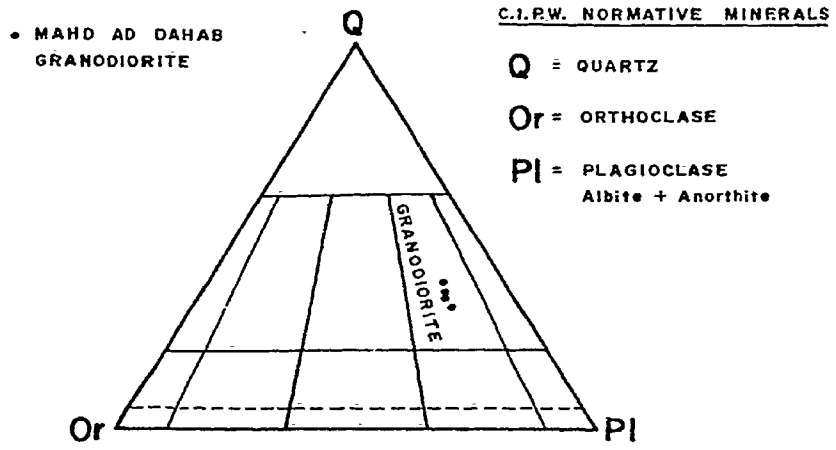

FIGURE 14- Normative Classification of the Plutonic Rocks at Jabal Al Mahd after Streckeisen (1967)

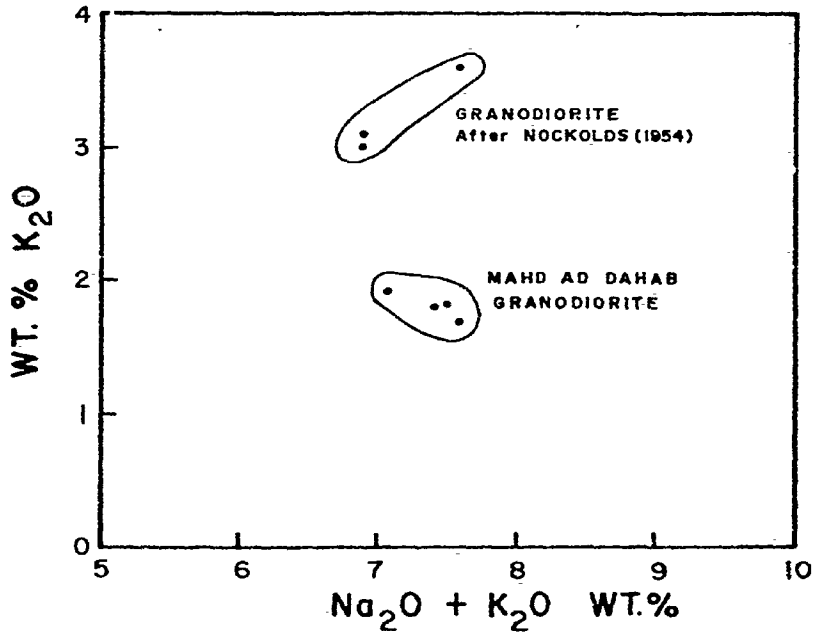

FIGURE 15- K_2O versus $Na_2O + K_2O$ for Granodiorite after Nockolds (1954) and Mahd Ad Dahab Granodiorite (1978)

Plate 5

a. Thin section. Granodiorite with myrmekitic texture resulting from an intergrowth of plagioclase and quartz. The white large phenocryst at the bottom of the picture is a quartz crystal. The white drop-shaped and the irregularly shaped grains are also quartz. Crossed nicols.

b. Thin section. Granodiorite with micrographic texture as intergrowth between quartz and albite. Crossed nicols.

c. N10W trending 2 cm wide quartz vein displaced by a younger N40E trending 1 cm wide quartz vein.

d. A series of north trending quartz veins cut by younger N45E trending quartz veins of which one of them is broken and displaced by a later north trending fracture.

e. A few cm wide north trending quartz vein displaced by N45W trending fault of the Najd Fault System.

PLATE 5

2. The N10W to N20E striking fracture system is recorded in many locations throughout the whole section from the porphyritic rhyolite in the north to the andesite in the south. These fractures are either vertical or steeply dipping west. Barren quartz veins 25 cm wide are broken and displaced by these fractures and those noted below.

3. The N30E to N70E striking fracture system is less common than the N10W to N20E fracture system. It is best represented by the N70E trending and 65 to 70 NW dipping fault located at the northwest corner of the porphyritic rhyolite. Two meter wide quartz veins that were mined by the ancients have the attitude of these fractures and are now represented by workings 70 m deep, 6 to 10 wide and 70 m long.

The N30E to N45 E striking fracutres are long, continuous fractures which contain from 1 to 2 m wide andesite dikes. The fractures mostly dip 75W. They have caused some displacement to most of barren and mineralized quartz veins trending N10W to N20E.

4. The N30W to N75W striking fracture system is vertical to steeply west dipping. This set of fractures has displaced older sets at many localities and with different displacements A one meter wide quartz vein in the N10E trending fracture is displaced horizontally for 9 meters by the younger N75W striking fracture system. A 2 cm wide quartz vein trending N10E is broken by a series of step fractures trending N60W (Plate 5c).

5. The N45W striking fault system is mostly vertical. These faults are long, continuous and cause a few cm to 1 m displacement of N10W to N20E striking quartz veins at the west side of Jabal Al Mahd (Plate 5d, e). This N45W trending fault set belongs to Najd Fault System, the youngest of the tectonisms affecting the Arabian Shield.

The N40°W, N30E to N70E, N10W to N20E, and the N45W striking fracture and fault systems coincide with regional trends throughout the Southern Hijaz Quadrangle. The first four are generally attributed to Hijaz Tectonic Cycle and the fifth to the Najd Fault System.

3.11. Summation

Mapping and analyses of representative samples of the volcanic rock section at Jabal Mahd AD Dahab indicate an increase in the fragmental nature, frequency of intercalated chemical sedimentary rocks, and relative abundance of silica upward in the section from andesite to upper rhyolite tuff. The increase in silica is manifested as increased quartz in the volcanic rocks, thin bands of chert, and quartz veins and stringers which cut the middle and the upper part of the section to end in the overlying chert at the north end of Jabal Mahd AD Dahab. Increase in silica throughout the lower rhyolite tuff, lithic crystal tuff, porphyritic rhyolite and the upper rhyolite tuff is accompanied by tremendous increase in K_2O and a decrease in Na_2O evidenced by late growth of orthoclase and sericite after plagioclase in the rocks and

in selvages of quartz veins.

The quartz veins carrying the base and precious metal minerals which must have been introduced in this phase of siliceous and potassic volcanism are localized as late fracture filling. Volcanic rocks and quartz veins at Jabal Mahd AD Dahab are cut by andesite dikes which appear to feed the next cycle of volcanism.

CHAPTER 4

THE VEINS

4.1. General Statement

Quartz veins traverse the steeply dipping section of andesite, mixed fragmental rocks, rhyolite tuff and the lenticular body of porphyritic rhyolite to end against red banded chert interbedded with thinly bedded fine tuff (Plate 6a, b, Fig.16). There are both metal-bearing quartz veins and barren quartz veins. The metal-bearing veins have pyrite, chalcopyrite, bornite, covellite, chalcocite, neodigenite, galena, sphalerite, electrum, pyrargyrite, hessite, joseite, altaite, calaverite, plus malachite and azurite. They strike N10W to N20E and, N30E to N70E and are essentially vertical. They are most abundant in and adjacent to the porphyritic rhyolite body. Most are exposed as pillars in the old workings and their extent is marked by the long deep stopes (Plate 6c). Barren quartz veins are more abundant west of the porphyritic rhyolite body and their frequency decreases downward through the section. They strike N10E, N30E to N70E and, N30W and dip steeply.

Plate 6

a. Banded upper rhyolite tuff intercalated with chert band trending east. Man is standing in trench parallel to bedding in tuff and chert and pointing with his right hand at a north trending trench contained metal-bearing quartz vein.

b. Barren quartz vein contains some hematite, having sharp contact with the adjacent host rock (dark gray).

c. Looking south to mine hill. The porphyritic rhyolite body with north trending open stopes that contained metal-bearing quartz veins.

PLATE 6

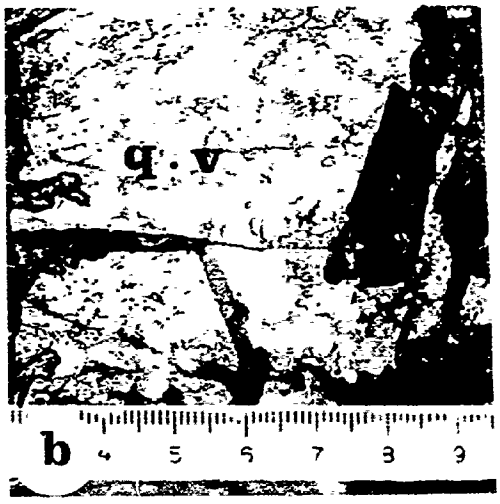

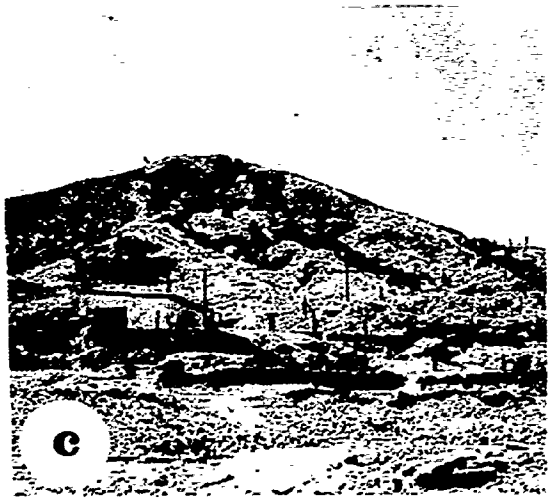

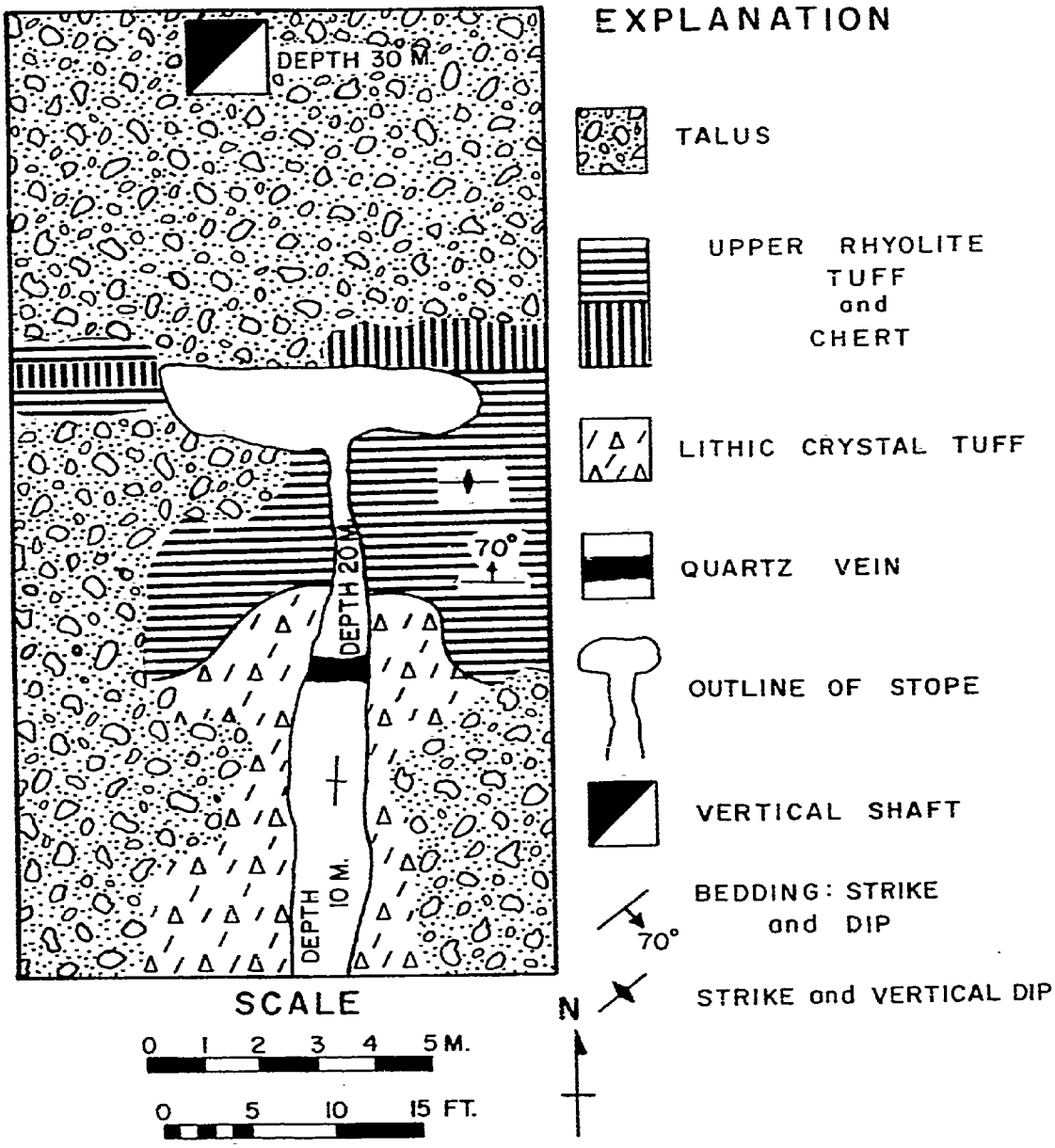

FIGURE 16 PLAN VIEW SKETCH OF SURFACE WORKINGS Nº 3

Stope trends north along quartz vein cross-cutting Lithic Crystal Tuff and branches east and west into Upper Rhyolite Tuff and Chert.

4.2. Metal-Bearing Quartz Veins

Metal-bearing quartz veins have three distinctive morphologies recognized in dump material, unmined pillars and drill core; 1, massive milky quartz veins, 2, crustified milky quartz veins and 3, veins of quartz-cemented breccia of wall-rock fragments. Most known metal-bearing veins have been mined by ancients to depths of 90 m and appear to pinch out at 200 m (Goldsmith and Kouther, 1971). Average width of these veins is 2 m and the strike length is up to 200 m. These veins occur in the northeast, southeast and southwest part of the mountain. All are cut by barren quartz veins striking N30W, N30E to N70E. These in turn are displaced by N30E to N45E trending andesite dikes.

4.2.1. Massive Milky Quartz Veins

These are sharp walled veins of white massive, milky, dense, crystalline fine to medium grained quartz. Euhedral elongate 3 to 35 mm long and up to 8 mm wide quartz crystals point from vein walls toward the centre in comb texture (Plate 7a). Contact with the wall rocks is sharp (Plate 7b). A thin film of chlorite 1 mm thick envelopes quartz crystals (Plate 7c) and near vein margins yellowish patches of calcite are randomly distributed in fine grained quartz (Plate 7d) and as thin selvages 2 to 3 mm along the contact with wall rock. The metallic minerals are dispersed along the edges of the veins. Seven grab samples HH1, HH1A,

Plate 7

a. Polished slab. Quartz vein with comb structure. Prismatic quartz crystals on vein walls pointing toward open cavity at the centre of the vein.

b. Polished slab. Quartz vein with sharp and well defined contact against andesite dike.

c. Polished slab. Massive milky quartz vein. Chlorite (black) occurs at the left hand side with white patches of cryptocrystalline quartz. Two to 3 cm long prismatic quartz crystals coated with a thin film of chlorite, to the right, point toward the centre of the fracture. The central part of the vein is filled with cryptocrystalline quartz. The darker patches are calcite chlorite and ankerite.

d. Polished slab. Same as plate 7c but with zonation in the prismatic quartz crystals.

e. Polished slab. Crustified quartz vein with margins of banded chlorite (black) alternating with chalcopyrite (light gray) and cryptocrystalline quartz (white).

f. Polished slab. Crustified quartz vein. Chlorite (black) at the right side of the slab alternating with cryptocrystalline quartz. The light gray band is a cryptocrystalline quartz with included chlorite. To the left side appears white fine grained quartz with dispersed chlorite.

PLATE 7

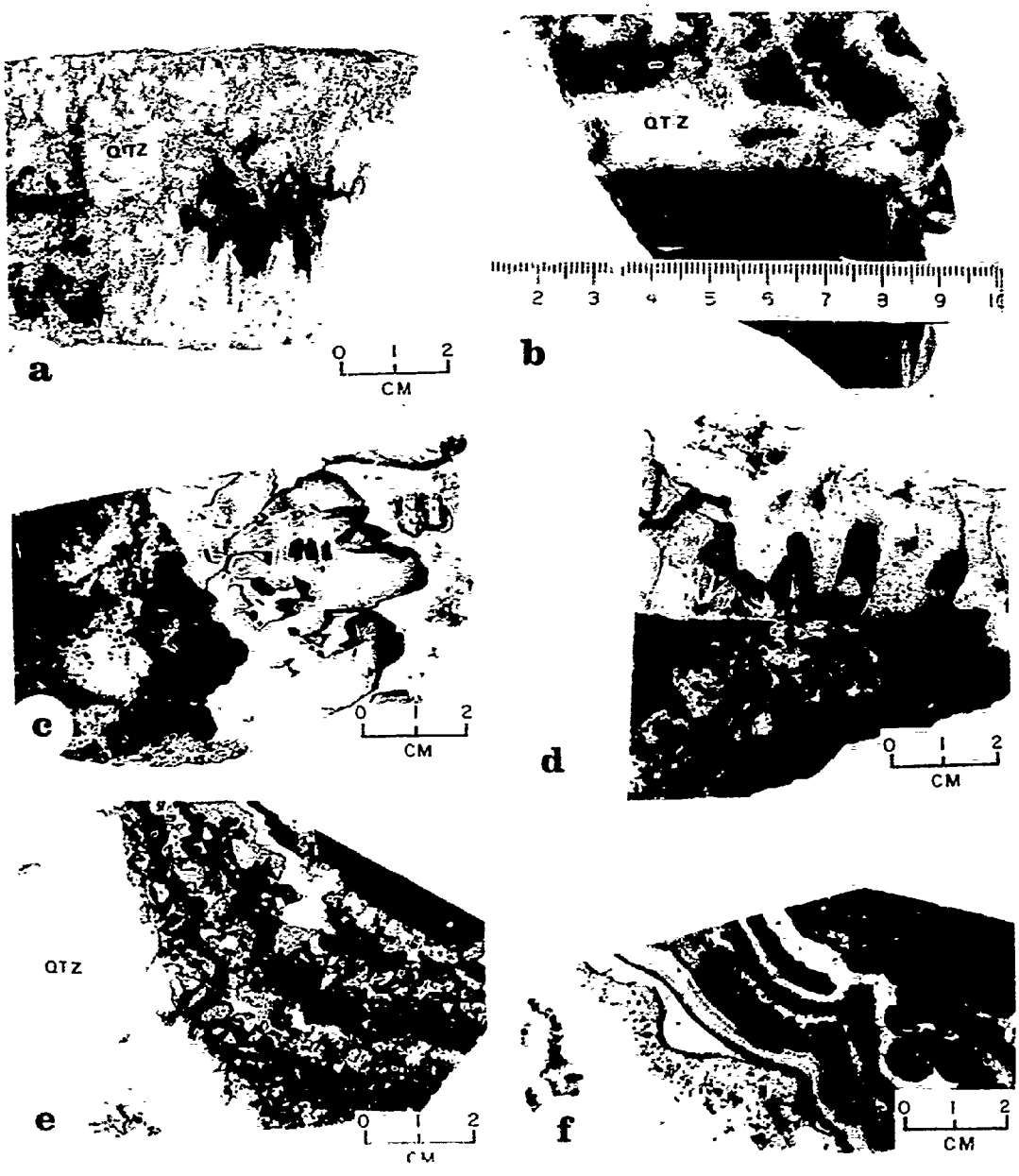

HH24, HH26, HH27, HH33 and HH10H6 (Appendix 6) representing the massive milky quartz veins have 0.01 to 170.9 ppm Au and 1.38 to 128 ppm Ag.

4.2.2. Crustified Milky Quartz Veins

These veins are milky to yellowish dense medium-grained quartz with patches of calcite. They outcrop within the lithic crystal tuff and the agglomerate striking N10W and standing vertical. Their width is from 5 cm to 1 meter. Metallic minerals are in vein selvages as repetitious bands, 2 to 3 cm wide of chalcopyrite, galena, sphalerite and chlorite between bands of cryptocrystalline quartz (Plate 7e, f).

Six grab samples HH10, HH30, HH40, HH45, HH46, and HH3 (Appendix 5) representing this type of metal-bearing veins have 0.98 to 288 ppm Au and 10 to 292 ppm Ag. Gold and silver content is totally coincident with abundance of chalcopyrite and galena. Gold content in the samples rich in chalcopyrite exceeds silver in all instances and galena rich samples have more silver than gold.

Zoned, equidimentional, euhedral, well developed quartz crystals 4 to 9 mm occur about the sulphide minerals (Plate 8a) and black chlorite occurs in 3 forms: as dispersed thin elongated flakes 2 mm long along vein selvages, as thin bands, or enveloping chalcopyrite grains (Plate 8b).

Plate 8

a. Polished slab. Crustified quartz vein with pure, white, six-sided, zoned quartz crystals (QTZ), which also occur at the left hand side of the picture, surrounded by chlorite (black) and galena (GAL) light gray. Chalcopyrite (CPY) in the lower right surrounded with cryptocrystalline quartz (white)

b. Polished slab. Crustified quartz vein. Chalcopyrite (light gray) is the main constituent with banded chlorite black and cryptocrystalline quartz (white). In the upper half chalcopyrite blebs are surrounded by chlorite which in turn surrounds chlorite.

c. Polished slab. Quartz cemented-breccia vein. Rock fragments, black chlorite and disseminated chalcopyrite and galena are cemented together by quartz. The fine dissiminated black grains in the upper left corner are orthoclase grains.

d. Country rock included in quartz.

e. Very sharp walled barren quartz vein.

f. Barren quartz vein crustified with 3 to 4 mm pink orthoclase band (OR) followed by impure quartz band (dark gray) and white pure quartz band. In the vein centre the quartz is spotted with black chlorite.

PLATE 8

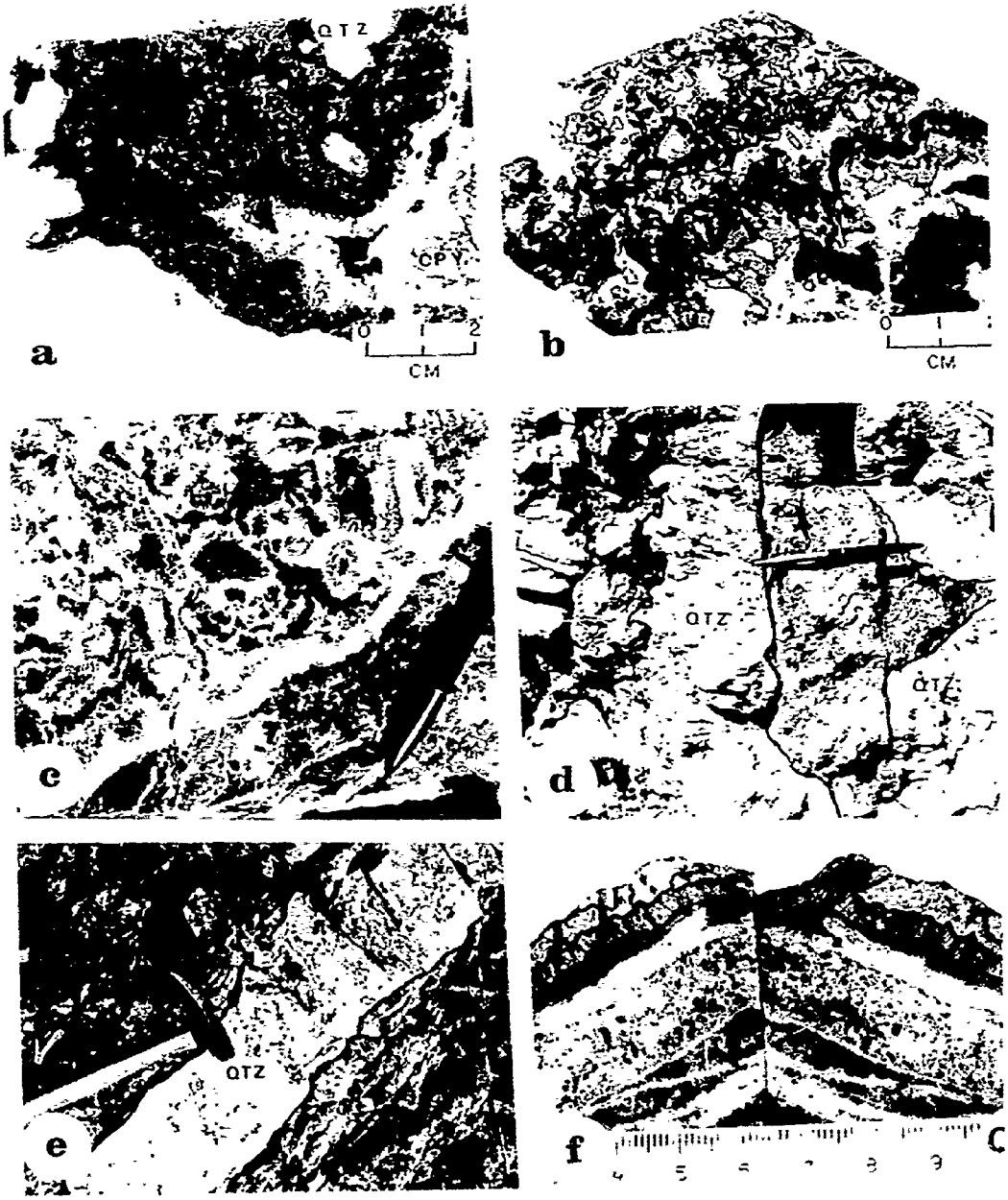

4.2.3. Quartz Cemented-Breccia Veins

This type of vein is by far the least abundant of the metal-bearing veins. It has not been found in place but rather as dump material and consists of fragments of different lithologies, shape and size healed by cross-cutting quartz stringers and veinlets forming a complex network (Plate 8c). Fragments are predominantely red and green chert, angular rhyolite, and well-developed quartz cyrstals. Dispersed K-spar crystals occur in the quartz matrix and also as 2 mm thick veinlets and patches within the sulphide minerals. Cementing quartz makes up to 40% of the rock. Well developed rhombohedral calcite crystals 2 to 3 mm long grow from the walls of vesicles toward the centre although calcite is much less common as a cementing material than quartz. Small patches, 1 to 2 mm in diameter of ankerite are also present.

Sphalerite and galena are the common sulphide phases in these veins. Fine to medium grained galena is up to 2 to 3%. Chalcopyrite constitutes up to 1% by volume in the form of dispersed small grains or aggregates mostly within chlorite.

One grab sample, HHBV, and 1 drill core sample, HH29H7, representing this vein type have less than 1 ppm gold and up to 6.36 ppm silver (Appendix 5).

The metal-bearing and the barren quartz veins at Mahd AD Dahab (Plate 8e, d) were dated 690 ± 35 m.y. by the

Rb/Sr method (Routhier and Delfour, 1974) using the pink orthoclase which occurs either as elongated crystals or thin layers along vein selvages (Plate 8f).

4.3. Metallic Minerals

4.3.1. Pyrite

Pyrite is the only iron sulphide mineral known in Mahd AD Dahab. Pyrite is by far the most common sulphide mineral and it occurs in all the metal-bearing veins and also as disseminated cubic crystals in host rocks. It is generally euhedral idiomorphic crystals, between 5 and 20 mm on a side (Plate 9a), or it is subhedral grains and aggregates. Some pyrite grains have corroded edges. It is rarely colloform. The pyrite is simply S and Fe and has no minor elements (Table 7).

Pyrite is present in three principal textural relationships withother sulphide minerals: (1) anhedral pyrite grains are surrounded by euhedral to subhedral galena (Plate 9b); (2) remnant cores of pyrite occur in the middle of galena grains (Plate 9c,d,10);and (3) veinlets of chalcopyrite are on fractures in pyrite (Plate 9e). Pyrite with irregular internal fracturing veined by quartz and chlorite minerals is also common. Quite commonly small pyrite crystals, 2 mm, on a side occur within quartz but mostly pyrite is at the edges of quartz grains on both megascopic and microscopic scale (Plate 9f). Angular fragments of coarse grained pyrite cemented in fine grained pyrite is also present. This has

Plate 9

a. Polished section. Euhedral, some are six-sided pyrite crystal (PY) in quartz (black). Reflected light.

b. Polished section. Large idiomorphic pyrite crystal (PY) with smooth edges in quartz (black). Extremely fine-grained non identified material is contained within. Reflected light.

c. Polished section. Relect of pyrite grains (PY) in galena (GAL) in quartz (black). Reflected light.

d. Polished section. Large grain of galena (GAL) with triangular cleavages containing remnants of pyrite (PY) forming islands in galena. Reflected light.

e. Polished section. Fractured or shuttered pyrite crystal (PY) veined and surrouned by chalcopyrite (CPY). Reflected light.

f. Polished section. Pyrite crystal (PY) with irregular boundaries against quartz (black) and chalcopyrite (CPY). Reflected light.

PLATE 9

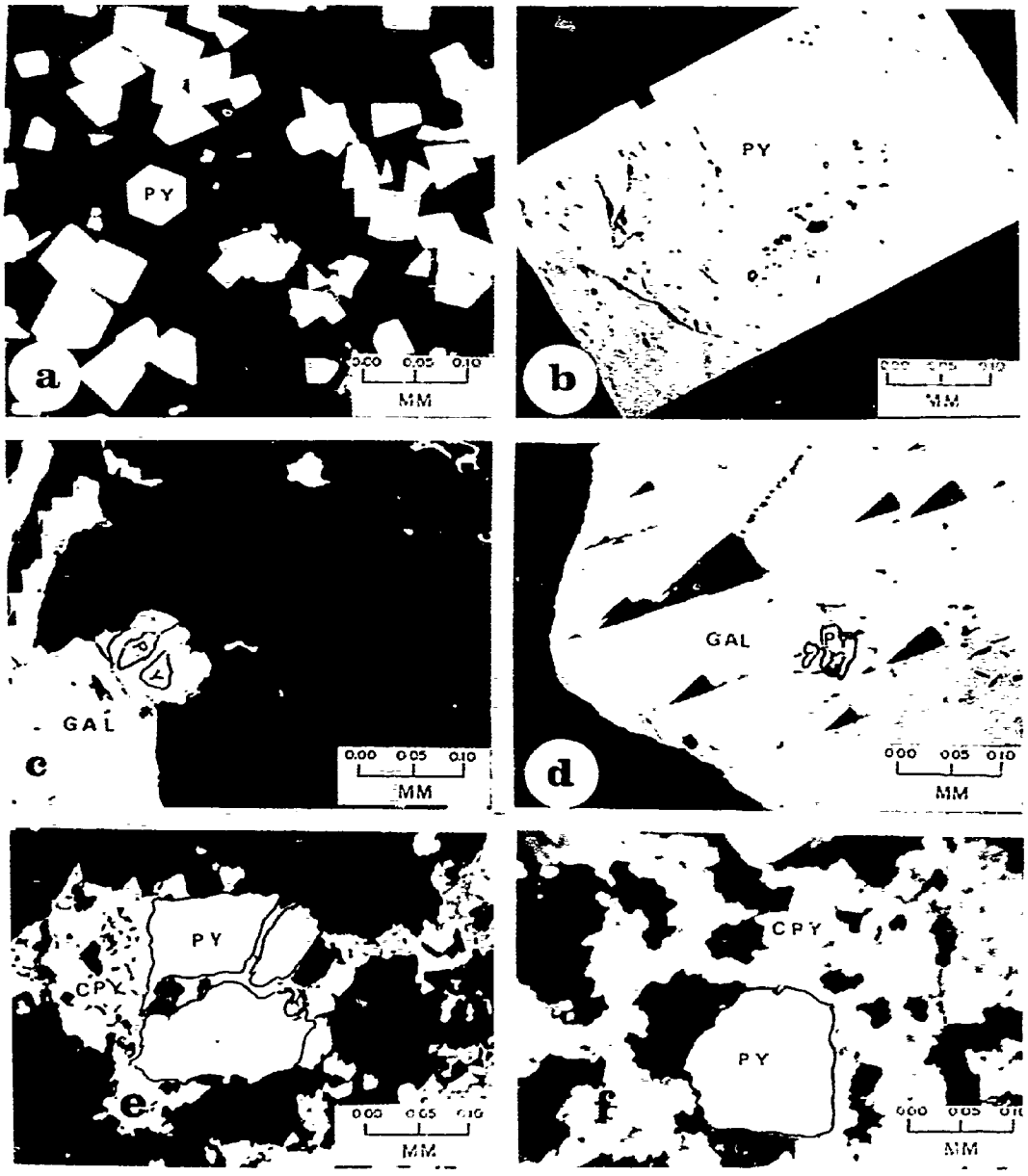
a
PY
0.00 0.05 0.10
MM
b
PY
0.00 0.05 0.10
MM
c
GAL
0.00 0.05 0.10
MM
d
GAL
PY
0.00 0.05 0.10
MM
e
PY
CPY
0.00 0.05 0.10
MM
f
CPY
PY
0.00 0.05 0.10
MM

Table 7. Analyses by electron microprobe of major and minor elements (wt.%) in pyrite from Mahd AD Dahab compared to pyrite from Undu Mine, Fiji, after Colley and Rice (1975).

	Mahd AD Dahab pyrite				Undu, Fiji pyrite	
Sample No.	Thin polished section H.H.1	Thin polished section 80B			No. 1 pit	
Au	.00	.00	.00	.00	-	-
S	54.05	55.69	54.79	53.94	52.65	52.92
Pb	-	.00	.00	.00	.04	.06
Ag	.00	.00	.00	.00	.03	nd
Te	.00	.00	.00	.00	-	-
Fe	45.30	47.47	47.33	46.47	48.20	47.88
Cu	.04	.00	.00	.00	.01	.05
Se	.00	-	-	-	-	-
Cd	-	-	-	-	.03	nd
Total	99.40	103.16	102.13	100.41	100.96	100.91

nd = not detected

- = not determined

Plate 10

a. Polished section. Triangular pyrite crystal (PY) being replaced by galena (GAL) internally and along its margins. Reflected light.

b. Polished section. Euhedral pyrite crystal (PY) partly replaced by galena (GAL). Reflected light.

PLATE 10

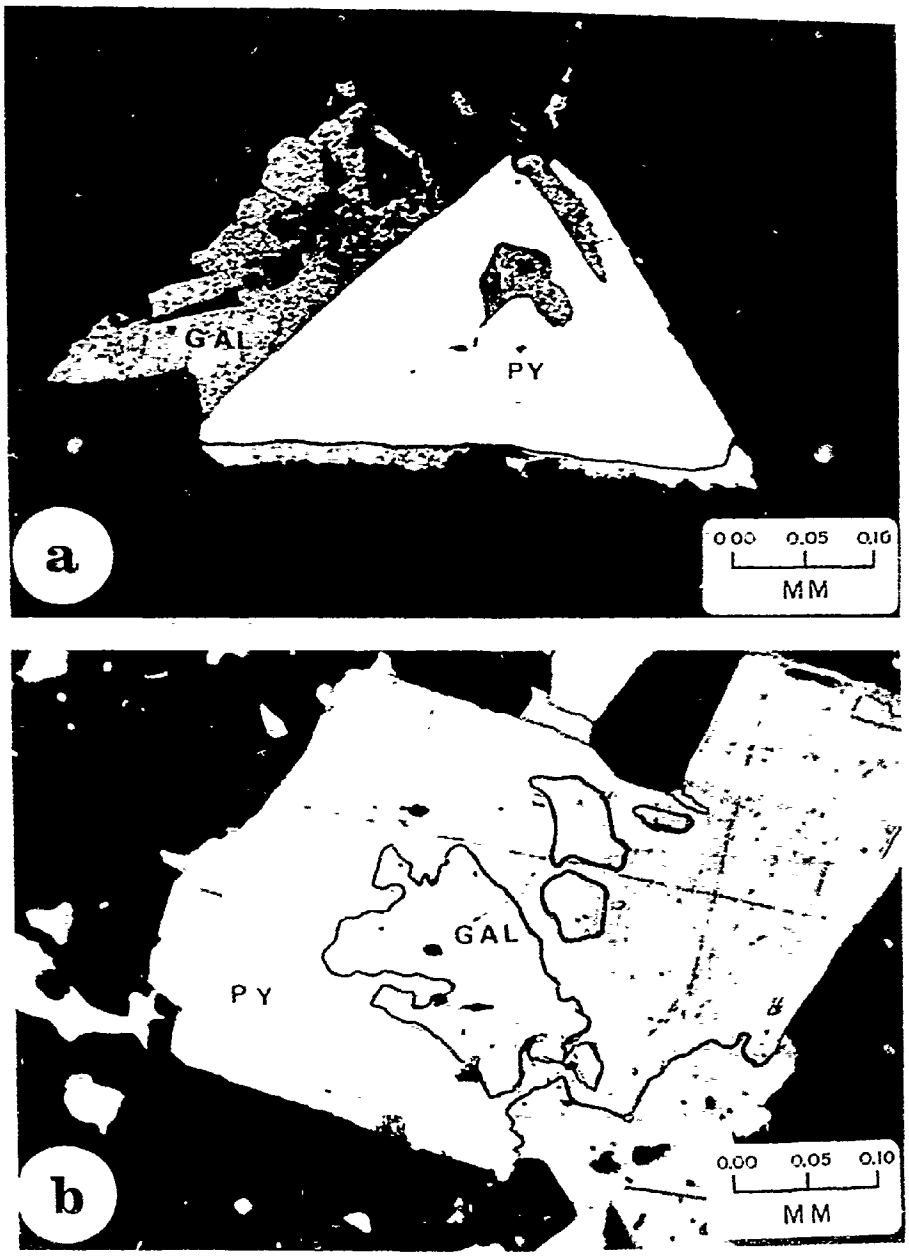

been explained by Kajiwara (1970) at the Shakanai mine in Japan as a post-depositional slumpage and brecciation of pyrite. The presence of minor pyrite and chalcopyrite veinlets within the quartz veins is suggestive of late movement or adjustment among the sulphide mineral. Also the occurrence of shapeless pyrite grains may be a result of chemical reaction that proceeded because of the addition of more sulphur to chalcopyrite

$$2CuFeS_2 + S \rightarrow FeS + 2CuS \text{ (covellite)}$$

This is a common phenomenon in subvolcanic deposits (Ramdohr, 1969).

4.3.2. Chalcopyrite, Bornite, Covellite, Chalcocite and Neodigenite

Chalcopyrite is the second most abundant sulphide mineral and the principal copper mineral present. It occurs as intergrown grains of varied size, as massive aggregates, along fractures forming irregular bodies or veinlets in pyrite grains and, as tiny exsolved bodies and as coarse unmixed grains in sphalerite (Plate lla). Three textures are noted: 1, An exsolution texture developed between chalcopyrite and sphalerite in the form of fine exsolved evenly distributed bodies. This is evidence of unmixing in solutions at high temperature. 2, Inclusion texture where some of the exsolved bodies are large because during slow cooling tiny particles can unite to form larger

Plate 11

a. Polished section. Sphalerite (SPH) contains very fine grains of exsolved chalcopyrite (white). Euhedral quartz crystal (black) enveloped by sphalerite with irregular crystal boundaries suggesting a reaction with sphalerite. Reflected light.

b. Polished section. Chalcopyrite (CPY) with thin marginal coating of chalcocite and neodigenite (light gray). The latter two sulphide minerals are replacing chalcopyrite along grain margins. The white crystals in quartz (black) are pyrite (PY). Reflected light.

c. Polished section. Chalcopyrite (CPY) with inclusions of gangue silicates (black). The light gray lamellae are bornite replacing chalcopyrite and developing between the gangue and chalcopyrite. Reflected light.

d. Polished section. Chalcopyrite (CPY) veined by covellite following thin microfractures. White spot is pyrite and the black is gangue. Reflected light.

e. Polished section. Chalcopyrite (CPY) randomly veined by neodigenite (gray) and covellite (black). Reflected light.

f. Polished section. Chalcopyrite (CPY) containing pyrite (PY) and gangue silicate (black). The chalcopyrite is replaced by chalcocite (CC).

PLATE 11

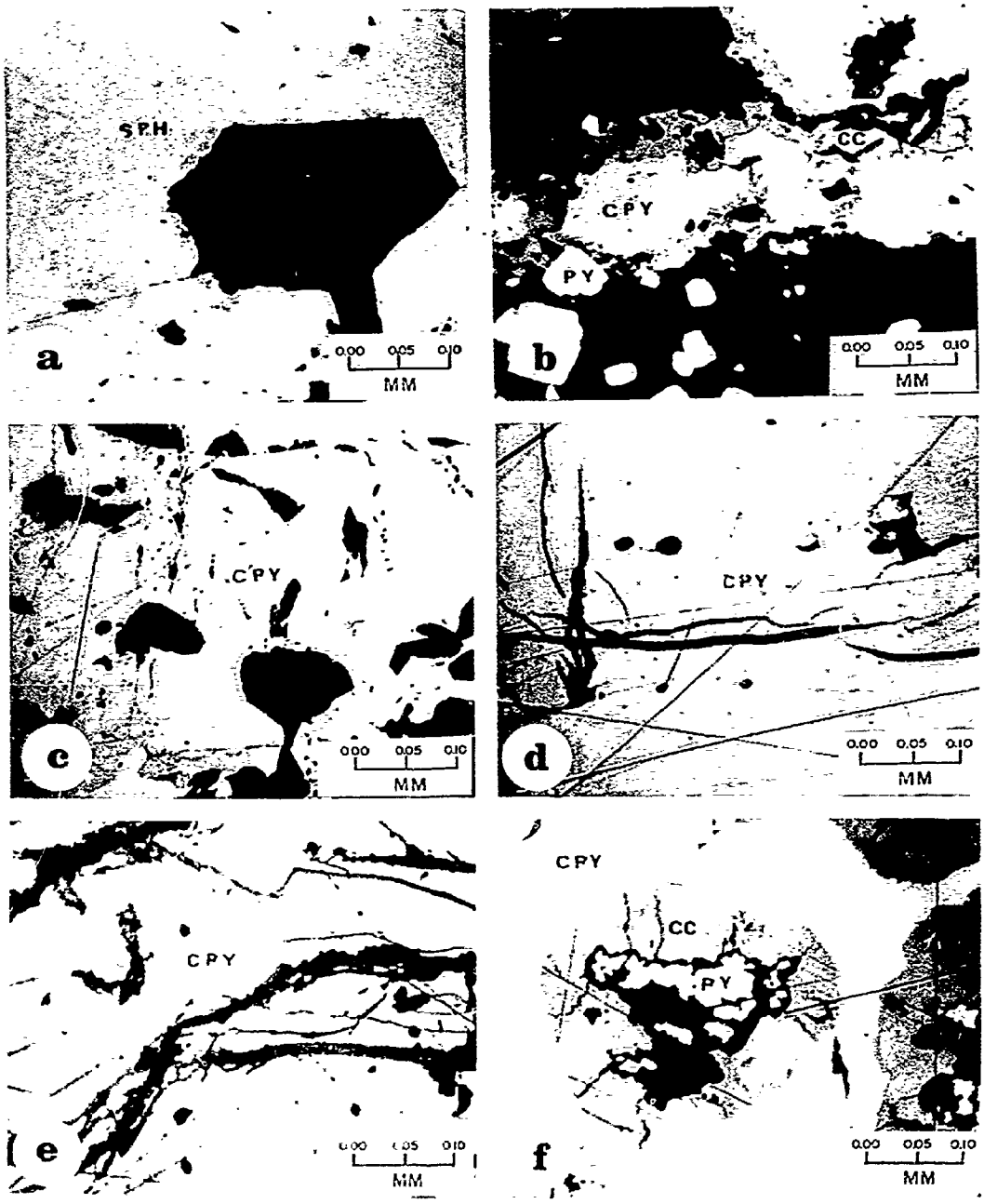
SPH
a
0.00 0.05 0.10
MM
CC
CPY
PY
b
0.00 0.05 0.10
MM
CPY
c
0.00 0.05 0.10
MM
CPY
d
0.00 0.05 0.10
MM
CPY
e
0.00 0.05 0.10
MM
CPY
CC
PY
f
0.00 0.05 0.10
MM

grains: 3, Open space filling texture, where chalcopyrite occurs along fractures or grain boundaries of pyrite. The chalcopyrite has three major elements, S, Cu and Fe (Table 8) and minor elements are either nil or trace and nearly identical to chalcopyrite from veins in similar host lithologies as at the Shakanai and Undu mines (Table 9). Au concentration in chalcopyrite grains from Mahd AD Dahab is minor compared to the amount of gold found in chalcopyrite from Undu mine, but slightly greater than from the Shakanai mine. Ag content in Mahd AD Dahab chalcopyrite is lesser than from both mines.

Bornite occurs as thin plates or lamellae radiating from grain boundaries toward the centre of chalcopyrite grains (Plate 11b, c). This is interpreted as a result of late chemical reaction between chalcopyrite and solutions rich in copper. Covellite is common as a thin film either partly or totally enveloping chalcopyrite or along fractures (Plate 11d, e). This covellite may be the product of sulphurization of chalcopyrite (Ramdohr, 1969).

Chalcocite was identified in two mineral phases, the blue, isotropic, pleochroic variety named neodigenite (Ramdohr, 1969) and bluish gray non-pleochroic chalcocite. Both phases developed after chalcopyrite along fractures and on grain boundaries (Plate 11d) and have pyrite as inclusions (Plate 11f). Most probably all the above mentioned copper sulphide minerals which have irregular shapes and rim or follow fractures in chalcopyrite are the result of breakdown

Table 8. Analyses by electron microprobe of major and minor elements (wt.%) in chalcopyrite from Mahd AD Dahab.

Sample No.	Thin Pol. Sect. H.H.1	Thin Pol. Sect. H.H.9	Thin Pol. Sect. H.H.7	Thick Pol. Sect. H.H.7	Thin Pol. Sect. H.H.10	Thick Pol. Sect. H.H.18	Thin Pol. Sect. H.H.20	Thin Pol. Sect. H.H.40
Au	.05	.00	.00	.03	.02	.02	.17	.03
S	35.29	34.80	35.32	34.73	34.58	34.17	34.77	34.65
Ag	.00	.00	.00	.03	.00	.03	.00	.01
Te	.00	.00	.00	.00	.00	.00	.00	.00
Fe	29.16	29.88	29.67	30.19	30.44	30.18	30.90	30.32
Cu	33.44	34.45	34.60	34.88	34.36	34.54		34.91
Se	.00	.07	.00	.00	.00	.00	.00	.00
Total	97.97	99.40	99.62	99.89	99.41	98.96	99.83	99.86
	Ave. of 4 Anal.	Ave. of 6 Anal.	Ave. of 8 Anal.	Ave. of 8 Anal.	Ave. of 7 Anal.	Ave. of 6 Anal.	Ave. of 6 Anal.	Ave. of 7 Anal.

Table 9. Analyses by atomic absorption spectrometry of minor elements (wt.%) in chalcopyrite from Shakanai mine, Japan after Nishshiyama (1974) and analyses by electron microprobe of major and minor elements in chalcopyrite (wt.%) from Undu mine, Fiji, after Colley and Rice (1975).

Sample No.	From Shakanai mine		From Undu deposit yellow ore No. 1 pit			
	1029	No. 1-9				
Au	.00	.00	.14	.05	nd	nd
S	nd	nd	35.12	34.64	34.84	35.66
Ag	.001	.00	.07	.16	.05	.03
Fe	nd	nd	30.83	30.70	30.70	31.31
Cu	nd	nd	33.47	34.13	33.89	33.67
Zu	nd	nd	.20	.06	.02	.10
Sb	.02	.04	nd	nd	nd	nd
As	.01	.05	.01	.02	.01	.01
Pb	nd	nd	.34	.18	nd	nd
Cd	.00	.00	.02	.02	nd	nd
Total	nd	nd	100.20	99.96	99.51	100.99

N.B. nd = not determined

of that chalcopyrite.

4.3.3. Galena

Generally galena occurs with all sulphide minerals but is most common with sphalerite. In some instances galena occurs alone. It is fine to medium irregular grains with irregular cleavage pits (Plate 12a, b). Rarely grain size exceeds 5 mm. It is mostly in irregular bands 5 to 10 mm wide alternating with bands of chlorite and cryptocrystalline quartz or as stringers and veinlets cutting through or filling tiny fractures in sphalerite, chalcopyrite, chlorite (Plate 12c) and other silicate minerals along grain boundaries, cleavages and fractures in pyrite, covellite, chalcocite and sphalerite. Euhedral quartz crystals are completely incorporated or included in galena (Plate 12d). Galena may also occur as subhedral crystals in sphalerite having smooth grain boundaries (Plate 12e) or as small islands with corroded edges in pyrite (Plate 12f) hence galena may be the main constituent with remnants of pyrite grains within the galena (Plate 9d). Both textures are interpreted as replacement of pyrite by galena. The galena has open and curved cleavages (Plate 13a, b) which is thought to be produced by distortion of the lattice during deformation (Salmon et al., 1974).

Galena has very little minor element content (Table 10) and is almost pure PbS. Compared to galena from Darwin, California which is generally considered a pure galena,

Plate 12

a. Polished section. Large grain of galena (GAL) with triangular cleavages. Grain boundaries are irregular and even toothed. This phenomenon is evidence of non recrystallization, because disappearance of toothing indicates recrystallization (Ramdahr, 1969). Reflected light.

b. Polished section. Galena grain (GAL) with non identified silicate inclusions embedded in quartz (QTZ). Reflected light.

c. Polished section. Galena (GAL) with triangular cleavage (black) filling fracture in chlorite (gray). Reflected light.

d. Polished section. Iodomorphic quartz crystal (QTZ) with smooth crystal boundaries enveloped by galena (GAL) that contains silicate inclusions (black). Reflected light.

e. Polished section. Galena (GAL) within sphalerite (SPH) with kink band of chlorite (black) on fracture. Reflected light.

f. Polished section. Galean (GAL) in pyrite (PY). Note the irregular grain boundaries of galena which indicate a reaction rim between galena and pyrite.

PLATE 12

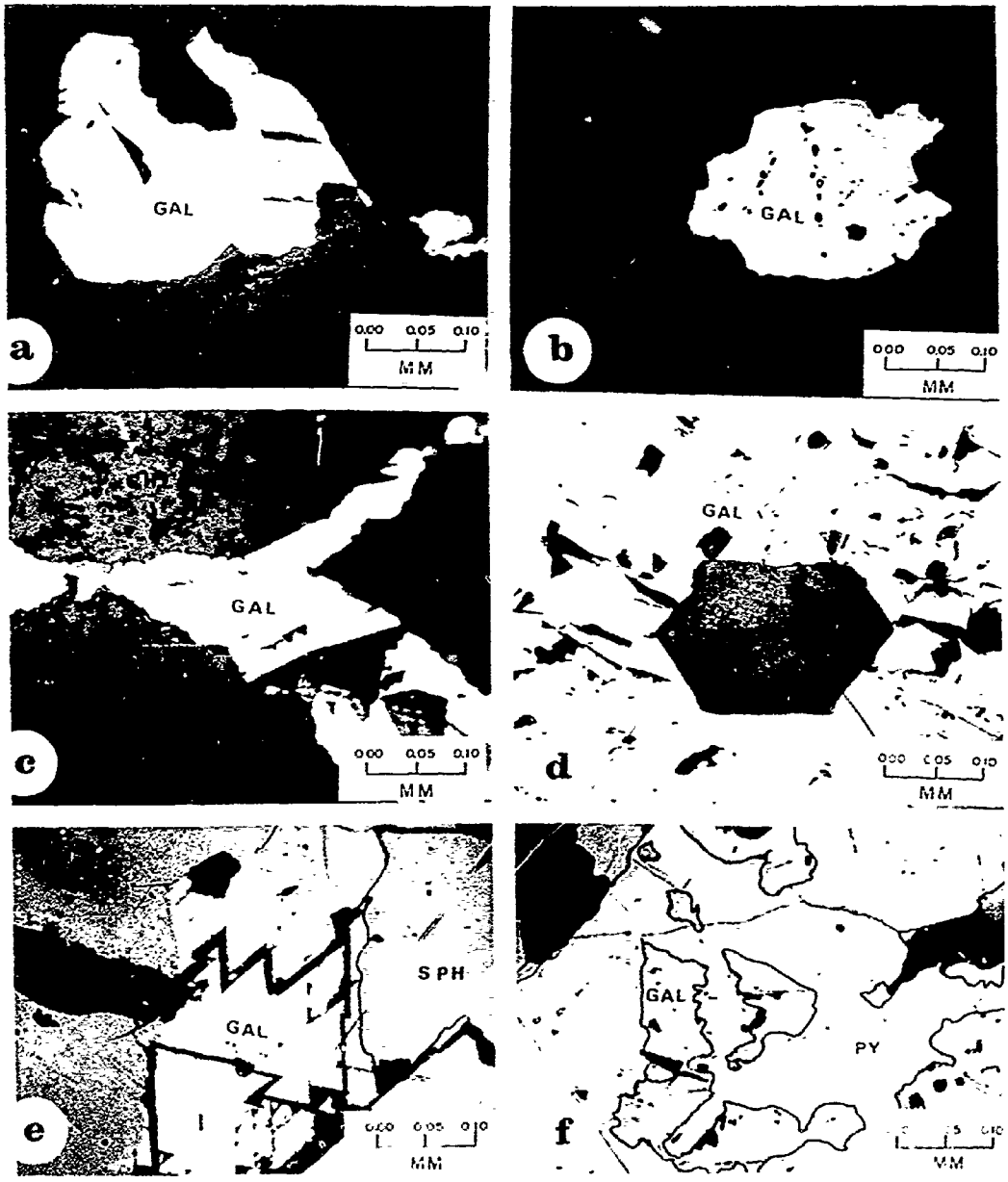
a
GAL
0.00 0.05 0.10
MM
b
GAL
0.00 0.05 0.10
MM
c
GAL
0.00 0.05 0.10
MM
d
GAL
0.00 0.05 0.10
MM
e
GAL
SPH
0.00 0.05 0.10
MM
f
GAL
PY
MM

Plate 13

a. Polished section. Bent lamellae in galena (GAL). A micro deformational feature. Reflected light.

b. Polished section. Enlarged part of previous photograph 13a. Reflected light.

c. Polished section. Sphalerite grain (SPH) with irregular grain boundaries totally enveloped by galena (GAL) and quartz (black). The white grain in the quartz is galena. The white inclusions in sphalerite are chalcopyrite blebs. Reflected light.

d. Polished section. Another grain of sphalerite grain (SPH) in quartz (QTZ) and in contact with galena (GAL). Reflected light.

e. Polished section. Sphalerite (SPH) with chalcopyrite exsolution blebs (CPY) in contact with galena (GAL). Reflected light.

f. Polished section. Sphalerite grain with irregular grain boundaries forming large inclusion in galena (GAL). Reflected ligth.

PLATE 13

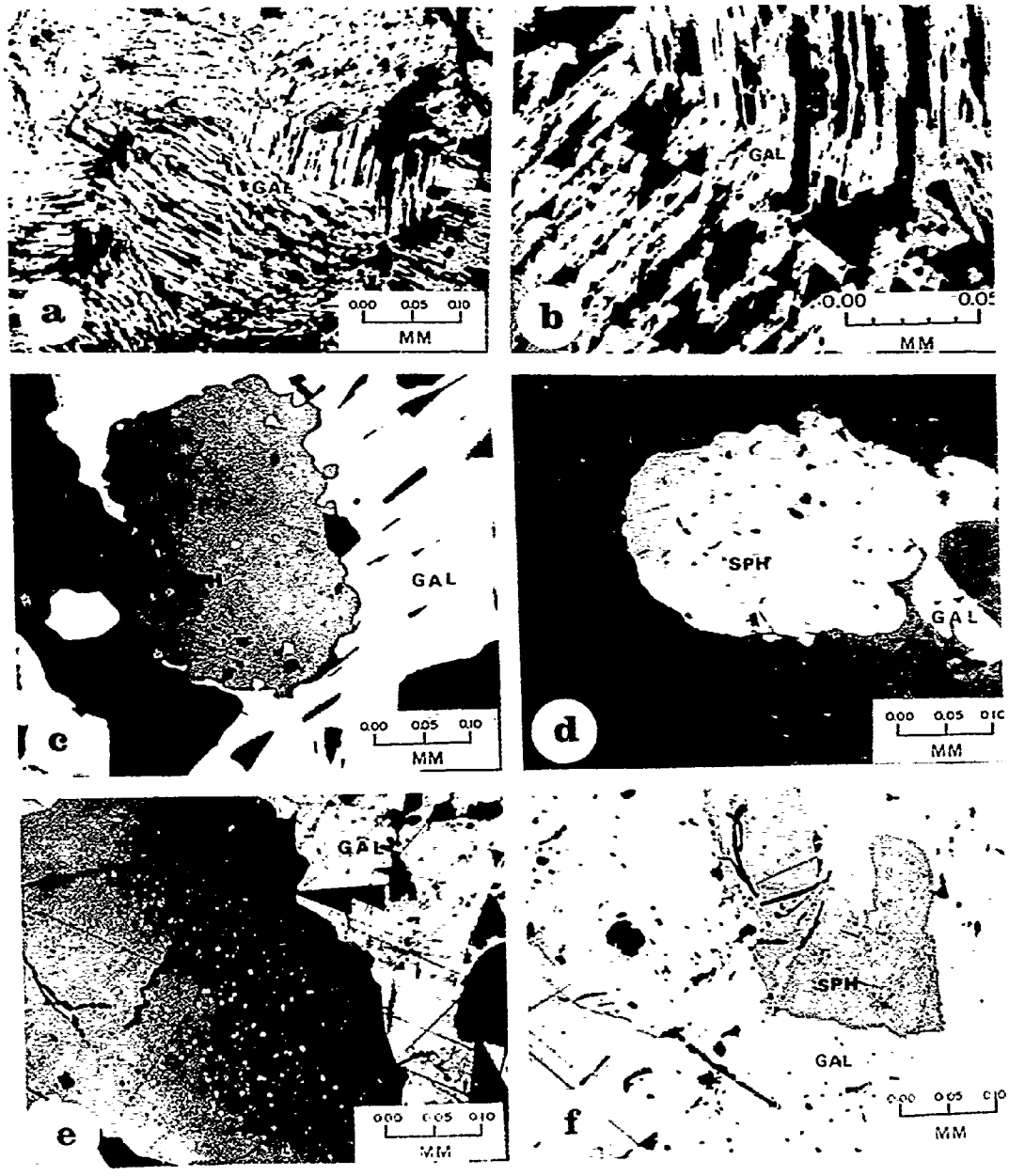
a
GAL
0.00 0.05 0.10
MM
b
GAL
0.00
MM
c
GAL
0.00 0.05 0.10
MM
d
SPH
GAL
0.00 0.05
MM
e
GAL
0.00 0.05 0.10
MM
f
SPH
GAL
0.00 0.05
MM

Table 10. Analyses by electron microprobe of major and minor element content (wt.%) in galena from Mahd AD Dahab.

Sample No.	Thin pol. sect. H.H.7	Thick pol. sect. H.H.7	Thick pol. sect. H.H.8	Thin pol. sect. H.H.10	Thin pol. sect. H.H.10A	Thin pol. sect. H.H.11	Thin pol. sect. H.H.40	Thin pol. sect. H.H.85
Au	.07	.00	.10	.00	.01	.00	.11	.13
S	13.28	13.22	13.35	13.16	13.10	13.06	13.26	13.19
Pb	86.35	86.84	85.35	85.96	86.00	85.31	86.66	86.11
Ag	.01	.00	.05	.00	.00	.00	.00	.00
Sb	.00	.00	-	-	.01	-	-	-
Fe	.00	.00	-	.00	-	.00	-	-
Te	-	-	.07	-	.02	.03	.06	.04
Cu	.00	.01	.00	.00	.00	.03	.00	.01
Bi	.00	.00	.00	.00	.05	.02	.01	.05
Zn	-	-	.03	-	.01	.03	.01	-
Se	-	-	.46	-	.64	.70	.26	.54
Total	99.84	100.23	99.45	99.13	99.86	99.32	100.05	100.02
	Ave. of 7 anal.	Ave. of 6 anal.	Ave. of 5 anal.	Ave. of 6 anal.	Ave. of 5 anal.	Ave. of 5 anal.	Ave. of 9 anal.	Ave. of 3 anal.

N.B. - = not determined

the Mahd AD Dahab specimens have ten times less Ag and Bi (Table 11) and have an Ag content comparable to that of the Shakanai mine (Table 12). Au content is up to .13% in the average of some analyses (Table 10) which may be because of some submicroscopic inclusions of Au.

Selenium content is relatively greater than in Darwin group 1 galena and less than in Darwin group 2 galena (Tables 10, 11). Compared to galena from the Mayflower mine, a vein deposit (Nash, 1975), Mahd AD Dahab galena contains more than 300 times as much Se. Compared to galena of a Kuroko-type deposits, the Undu mine, Fiji, (Table 12) Mahd AD Dahab galena has less Ag. The Cu content is less than that of galena from the Undu mine where enrichment is attributed to some submicroscopic chalcopyrite inclusions in galena.

4.3.4. Sphalerite

Sphalerite is as widely distributed as chalcopyrite and has a similar mode of occurrence. It is massive light gray, brownish to black in colour and occurs as thin bands alternating with cryptocrystalline quartz, pyrite, and chalcopyrite. Where it is massive, sphalerite occurs intergrown with chalcopyrite. It is mostly fine-grained but where grain size is larger than 0.1 mm (Plate 13c, d) grains and grain aggregates have corroded edges. Sphalerite contains chalcopyrite as fine exsolved bodies arranged along cleavage planes (Plate 13e), or as coarse subrounded to shapeless inclusion which may be interpreted also as fine exsolved

Table 11. Analyses by electron microprobe of major and minor elements in galena (wt.%) from Darwin lead-silver-zinc deposit S. California after Czamanske and Hall (1975).

	Group 1 galena			Group 2 galena		
Sample No.	18	A560	3506	5	H2	A561
Pb	86.6	86.1	86.3	80.5	73.7	75.00
Bi	.11	.33	.00	3.9	7.3	7.00
Ag	.14	.22	.18	1.7	3.3	3.2
Sb	.11	.04	.17	.02	-	-
S	13.5	13.4	13.3	13.5	12.2	12.6
Se	.04	.43	.01	.45	2.1	1.9
Te	.04	.01	.00	.13	.11	.11
Total	100.5	100.00	100.00	100.2	98.7	99.8

Table 12. Minor element content in galena (wt.%) through x-ray diffraction from Shakanai mine, Japan after Nishiyama (1974) and major and minor elements in galena from Undu mine, Fiji after Colley and Rice (1975).

	Shakanai mine			Undu mine			
Sample No.	1032	1005	1007	Yellow ore No. 1 pit		Black ore No. 2 pit	
Au	-	-		-	-	-	-
S	-	-		12.29	12.25	12.34	12.24
Pb	-	-	-	86.07	87.08	86.55	87.02
Ag	.01	.02	20	.10	.10	.02	nd
Sb	.02	-	-	-	-	-	-
Fe	-	-	-	.06	.09	.01	.07
Cu	-	-	-	.13	.06	.09	.07
Bi	.005	.008	.003	-	-	-	-
Zn	.01	-	-	.09	.01	.82	.11
Cd	-	-	-	.03	nd	.03	nd
Total	-	-	-	98.77	99.59	99.86	99.45

N.B. nd = not detected; - not determined.

bodies that joined each other to form coarse exsolution blebs. Small chalcopyrite veinlets are also observed in sphalerite.

Analyses of sphalerite by electron microprobe (Table 13) demonstrates that the sphalerite contains a relatively wide range of minor elements of which Fe is the most abundant with analyses averaging 0.69% and ranging from 0.00 to 2.65%. Low iron content is associated with the light coloured sphalerite. Cu is proportional to Fe and analysed spots averaged 0.85% Cu with a range between 0.01 and 3.03%. The latter analyses may result from tiny exsolved chalcopyrite blebs being struck by the electron microprobe beam. Cd, the third minor element after Fe and Cu, averaged 6.31% and it ranges from 0. to 0.42% Cd. In most sections, Ag was not detected and it does not exceed 0.02% where detected. Mn content is always less than Cd and where found it is not more than 0.04% and in many analyses Mn is not detected.

Sphalerite from Mahd AD Dahab is comparable to that from the Skakanai and Undu mines (Table 13) but has ten times less Mn than sphalerite from Kanizawa mine, a precious metal vein deposit (Hattori, 1975).

4.3.5. Electrum

Gold occurs principally as electrum at Mahd AD Dahab in fine, subhedral, dispersed grains within chalcopyrite, sphalerite galena and in the non-metallic gangue minerals.

Table 13. Analyses by electron microprobe of major and minor elements (wt.%) in sphalerite from Mahd AD Dahab compared to sphalerite from Shakanai mine, Japan after Nishiyama (1974), Undu mine, Fiji after Colley and Rice (1975) and Kanizawa Au-Ag vein, Japan after Hattori (1975).

	Sphalerite from Mahd AD Dahab						Sphalerite from Shakanai mine	Sphalerite from Undu mine	Spalerite from Kanizawa deposit		
Sample No.	Thin pol. sect. H.H.7	Thick pol. sect. H.H.7	Thin pol. sect. H.H.8	Thin pol. sect. H.H.10	Thin pol. sect. H.H.10A	Thin pol. sect. H.H.85			KN-772704		
S	33.10	32.82	33.17	33.48	33.24	32.91	-	35.53	33.2	33.2	32.9
Ag	.00	.00	.01	.00	.00	.00	.008	-	-	-	-
Cd	.21	.18	.16	.21	.34	.18	.26	.24	.2	.2	.1
Mn	.01	.03	.00	.00	.00	-	.06	-	.4	.8	.8
Fe	.90	.33	.65	.57	.58	1.02	.3	.00	1.1	1.0	1.0
Cu	.81	.21	.66	.59	.53	.74	-	.13	.3	.1	.1
Pb	-	-	-	-	-	-	-	.14	-	-	-
Zn	64.90	65.57	64.55	65.26	65.83	64.75	-	64.20	65.8	65.8	64.7
Total	100.14	99.17	99.19	99.97	100.42	99.94	-	101.22	101.0	100.8	99.5
									.7*	.9*	.9*
	Ave. of 6 anal.	Ave. of 7 anal.	Ave. of 9 anal.	Ave. of 7 anal.	Ave. of 8 anal.	Ave. of 3 anal.	Ave. of 3 anal.	Ave. of 3 anal.			

N.B.* Sphalerite from Shakanai mine was analysed by atomic absorption spectrometry.

* = Calibrated iron content.

It has serrate, irregular or smooth mutual boundaries with sulphide and gangue silicate minerals (Plate 14a). Grain size varies in diameter from 0.005 to 0.10 mm (Plates 14b, c). Electrum also occurs as thin stringers and veinlets more than 0.5 to 1.0 mm and less than .05 mm (Plates 14d, e and f). One inch of polished surface of sphalerite may contain more than 10 grains of electrum. It is identified in all types of metal-bearing veins but is more abundant in the crustified quartz veins.

The colour is generally light golden to deep yellow. In polished sections the colour and reflectivity are variable depending upon the amount of gold to silver. Ag content in electrum varies widely from 6.71% to 17.16% (Table 14). Cu and Fe were detected by microprobe analyses, but their amounts are not greater than 0.3% and 0.1% respectively.

Mahd AD Dahab electrum is not zoned and the analyses of large grains margins and centresindicates constant Au to Ag abundances. Electrum from the Koasaka and Shakanai mines (Table 14) is zoned with a greater amount of Ag in grain margins than centres. Generally Mahd AD Dahab electrum has more Au and less Ag than the other two mines. Sato (1974) reported that electrum from the Shakanai mine has Ag abundances from 3.4% to 12.6% with some Cu. This is comparable to that of Mahd AD Dahab. Chemical composition of the very thin electrum stringers was not determined, so their Au to Ag content is not known.

Plate 14

a. Polished section. Electrum grain (AU) between galena (GAL), sphalerite (SPH) and silicate gangue (black). Reflected light.

b. Polished section. Electrum grain with partly corroded boundaries between (GAL), sphalerite (SPH) and quartz (black). Electrum contains silicate inclusion. Fine white bodies in sphalerite are chalcopyrite exsolutions.

c. Polished section. Fine grains of electrum (AU) in quartz (QTZ). Reflected light).

d. Polished section. Stringers of native gold or electrum (AU), too thin for resolution by electron microprobe. Reflected light.

e. Polished section. Another example of native gold or electrum (AU) in sphalerite (SPH). The fine white bodies are exsolutions of chalcopyrite. Reflected light.

f. Polished section. Another example of native gold or electrum (AU) in sphalerite (SPH) together with galena (GAL). Reflected light.

PLATE 14

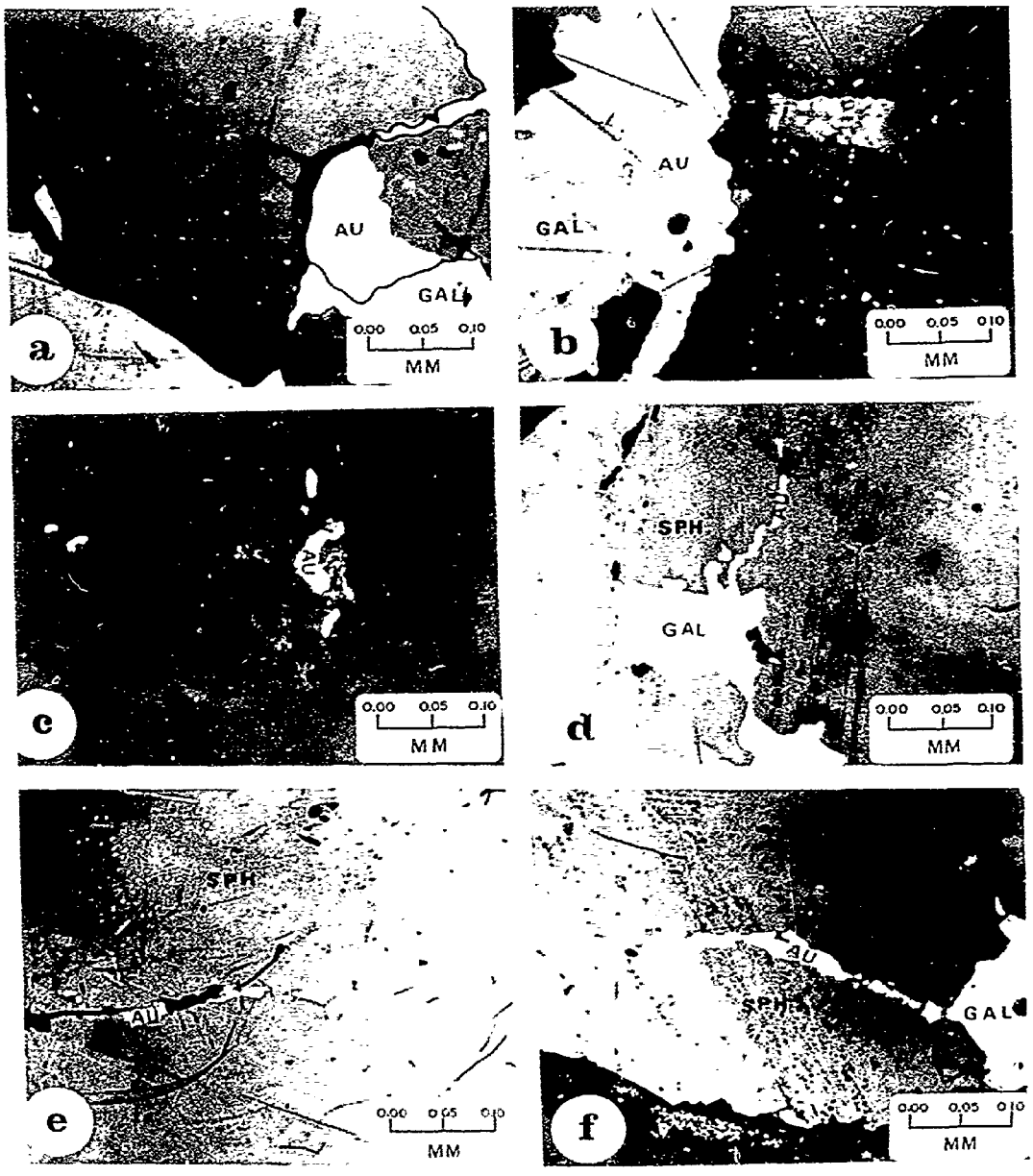
a
AU
GAL
0.00 0.05 0.10
MM
b
AU
GAL
0.00 0.05 0.10
MM
c
AU
0.00 0.05 0.10
MM
d
SPH
GAL
0.00 0.05 0.10
MM
e
SPH
AU
0.00 0.05 0.10
MM
f
AU
SPH
GAL
0.00 0.05 0.10
MM

Table 14. Analyses of electrum (wt.%) by electron microprobe from Mahd AD Dahab compared to electrum from Koasaka and Shakanai mines, Japan (after Shimazaki, 1974).

	From Mahd AD Dahab		From Kuroko ores, Koasaka mine	
			centre	margin
Ag	12.54	11.36	19.97	36.5
Au	87.06	88.57	77.4	59.3
Total	99.60	100.33	97.42	95.8
	Ave. of 5 anal.	Ave. of 5 anal.	Ave. of 4 anal.	Ave. of 4 anal.
Ag	11.98	11.68	23.15	39.76
Au	87.75	88.33	77.16	59.66
Total	99.77	99.99	100.3	99.43
	Ave. of 5 anal.	Ave. of 5 anal.	Ave. of 5 anal.	Ave. of 5 anal.
			From Shakanai Mine	
Ag	11.18	11.98	22.18	28.24
Au	88.12	87.55	78.12	71.26
Fe	-	.02	-	-
Cu	-	.22	-	-
Total	99.43	99.58	100.1	99.46
	Ave. of 5 anal.	Ave. of 7 anal.	Ave. of 5 anal.	Ave. of 5 anal.

Elemental gold has not been identified at Mahd AD Dahab, but it may occur within chalcopyrite where gold has been detected by the electron microprobe but not actually seen under the microscope.

4.3.6. Argentite

A few grains of argentite scattered as inclusions in galena and chalcopyrite do occur in some polished sections. Hence the principal source of the over 1 million ounces of Ag at Mahd AD Dahab must be electrum and hessite.

4.3.7. Tellurium Minerals

Tellurium is in the crystal structure of chalcopyrite and galena, but also forms hessite, joseite, altaite, and calaverite. These tellurium minerals occur more with chalcopyrite than sphalerite and galena.

4.3.7.1. Hessite, Ag_2Te

Hessite is the most common tellurium mineral found in Mahd AD Dahab. Microscopic grains are subrounded, light gray with lower reflectivity where compared to the bismith telluride joseite. It is mostly as inclusions in chalcopyrite but is also common in galena and sphalerite. Analyses of three hessite grains (Table 15) do not indicate any substitution of Ag by Au as compared to hessite from the Hidden Secret gold mine, Kalgoorlie, Australia (Table 15).

Table 15. Analyses by electron microprobe of major and minor elements (wt.%) in hessite* from Mahd AD Dahab

Sample No.	Thin pol. sect. H.H.20		Thin pol. sect. H.H.40	From Kalgoorlie Gold Mine after Markham 1960	after Markham 1960	after Simpson 1912
Au	.00	.00	.00		2	3
S	.05	.04	.11		.8	.1
Pb	.00	.00	.00		nd	nd
Bi	.00	.00	.01		nd	nd
Ag	61.91	61.05	61.56	62.86	61.0	61.7
Sb	.03	.00	.25		nd	nd
Te	37.83	37.14	39.57	37.14	nd	nd
Mn	.01	.00	.00		nd	nd
Fe	.06	.04	.04		nd	nd
Cu	.09	.14	.27		nd	nd
Zn	.05	.04	.00		nd	nd
Se	.00	.00	.00		nd	nd
Total	99.48	99.45	100.81			

NB *Hessite is a silver telluride of chemical composition Ag_2Te (Ramdohr, 1969).

4.3.7.2. Joseite, Bi_2TeS

Joseite comes after hessite in abundance in the tellurium minerals. It occurs as minute inclusions in chalcopyrite, sphalerite and galena closely associated with electrum and other tellurium minerals. It is white in colour with reflectivity higher than galena and has a relatively large content of minor elements as S, Ag, Sb, Fe, Cu and Se (Table 16) which suggests the existence of silver selenides and antimony silver minerals as submicroscopic inclusions. The S, Fe and Cu concentration may be attributed to the existence of small chalcopyrite inclusions.

4.3.7.3. Altaite PbTe

Altaite was recorded in two thick polished sections in lesser amounts than hessite and joseite. It occurs as fine microscopic grains forming inclusions in galena and chalcopyrite and the size of the grains is around .01 mm. Its chemical composition (Table 17) indicates that it has variable S and Pb content. In nearly all the analyses, the altaite from Mahd AD Dahab contains greater S and Pb content compared to altaite from Hidden Secret gold mine, Kalgoorlie (Table 17). This may be explained by the instability of altaite. Bi picks up Te to produce tetradymite, PbTeS (Scherbina, 1976):

$$2PbTe + Bi_2S_3 \rightarrow 2PbS + BiTeS$$

Table 16. Analyses by electron microprobe of major and minor elements (wt.%) in joseite* from Mahd AD Dahab.

Sample No.	Thin polished section H.H.80						
Au	.00	.00	.00	.00	.00	.63	.00
S	3.84	3.83	3.76	2.48	2.48	2.56	3.95
Pb	.00	.12	.13	.20	.00	.00	.00
Bi	53.13	58.05	58.34	56.60	57.39	59.66	58.11
Ag	.44	.46	.29	.00	.00	.00	.00
Sb	.38	.51	.55	.27	.30	.36	.34
Te	35.18	34.63	34.31	33.13	32.57	32.90	35.04
Mn	.00	.00	.00	-	-	-	-
Fe	.04	.24	.04	.57	.40	1.89	.00
Cu	.13	.62	.29	.71	.71	1.11	.04
Zn	.00	.11	.11	-	-	-	-
Se	1.60	2.69	2.74	4.61	4.40	4.27	.68
Total	100.42	101.25	100.55	98.57	98.27	100.38	98.19

N.B.*Joseite is a bismuth telluride of chemical composition Bi_2TeS (Ramdohr, 1969).

Table 17. Analyses by electron microprobe of major and minor elements (wt.%) in altaite* from Mahd AD Dahab.

Sample No.	Altaite from Mahd AD Dahab Thick polished section H.H.8				Altaite from Kalgoorlie gold mine after Markham (1960)	Altaite from Kalgoorlie gold mine after Simpson (1912)
Au	.14	.00	.00	.00		.02
S	.27	8.74	.89	2.75		-
Pb	61.79	70.41	68.89	64.64	61.91	61.33
Ag	.16	.00	.00	.00		.43
Bi	-	.00	.04	.00		nd
Te	26.46	13.53	31.04	27.48	38.09	38.43
Fe	.00	.00	.00	.00		.13
Cu	.00	.03	.00	.06		.01
Se	nd	nd	nd	nd		.08
Total	88.84	92.71	100.86	94.93	100.00	100.40

N.B.* Altaite is lead telluride of chemical composition PbTe (Ramdohr, 1969). Low totals in some samples are attributed to the tiny size of the grains.

- = not detected; nd = not determined

4.4. Distribution of Minor Elements in Metallic Minerals

Minor elements form their own minerals, occur as tiny inclusions in sulphide minerals or, enter into the crystal structure of these minerals. Concentration of minor elements in sulphide minerals at Mahd AD Dahab varies greatly from one mineral to the other as indicated by analytical data (Tables 7, 8, 10, 13). Minor elements are totally absent in pyrite and of low concentration in chalcopyrite.

Galena is the principal carrier of Se and has as much as seven times more Se than Te. This can be attributed to: 1, There are chemical and crystallographic similarities between S and Se hence Se substitute for S and enters the structure of sulphide minerals (Berzon et al., 1973). 2, Tellurium has a greater atomic weight, larger ionic and atomic radii, lower ionization potential and lower electronegativity compared to S and Se and hence does not enter into the sulphide mineral structures as easily as Se (Berzon et al., 1973). 3, Tellurium tends to form its own independent minerals, such as hessite, joseite and altaite, which are found as inclusions in some sulphide minerals at Mahd AD Dahb, rather than enters the structure of sulphide minerals.

Selenium and Te do not occur in galena in a constant ratio, but are always together suggesting that they have been formed from the same fluid. As there are no known mixed selenium-tellurium compounds known in nature, this can be explained by assuming simultaneous entrance of Se and Te

into the galena structure (Nechelyustov, et al., 1962). On the basis of this study it is interpreted here that the availability of Te in the mineralizing fluids reduced the chances for other minor elements such as Ag and Bi to enter into the crystal structure of galena and hence, Ag and Bi formed tellurium minerals.

Cadmium is among the minor elements that has a relatively large concentration in sphalerite from Mahd AD Dahab (Table 13). Average Cd content in sphalerite is 0.21% which is very close to its content in sphalerite from other localities (Table 13). Despite its relative concentration in Mahd AD Dahab, Cd content is minor compared to sphalerite deposits in carbonate rocks, such as in Selisian and Alpine lead-zinc deposits.

Under equilibrium conditions Cd is strongly fractionated toward sphalerite relative to galena (Bethke and Barton, 1971). Zinc deposits formed in alkaline environments contain more Cd than sphalerite crystallized from acid fluids and as alkalinity of the metal-bearing fluids increases a greater amount of Cd is precipitated from them (Ivanov, 1964). Badalov and Enikeev (1959) found that Cd content in sphalerites of the Middle Asian deposits increases regularly as temperature of deposition decreases. Also it was found that the Cd content in sphalerite crystallizing from low temperature hydrothermal fluids depends to a considerable degree on the concentration of chlorine ion in solution (Mookherjee, 1961).

It is suggested that the Cd content in sphalerite from Mahd AD Dahab is a function of the pH of the metal-bearing fluids and, the temperature at time of deposition. It is also suggested that the metal-bearing fluids were carrying the dispersed elements as chloride complexes where the pH of the solution is low near the end of sulphide mineral deposition, fluids become more alkaline and Cd starts to accumulate in aphalerite.

Both Ag and Bi tellurides occur as microscopic inclusions and also in the crystal structure of sulphide minerals as indicated by the microprobe analyses (Tables 8, 10, 13). Concentration of Bi in galena depends upon its initial concentration in the fluids from which galena is deposited (Panfilov, 1972). It is suggested that the concentration of Ag is greater than Bi at the beginning of sulphur and precious metal precipitation, and at the later stages Bi combines with Te to from BiTe, joesite. When the mineralizing solutions become depleted in Bi which is an important factor for Ag fixation in galena, chances are restricted for Ag to enter into the crystal structure of galena.

4.4. Non-Metallic Minerals

4.4.1. Quartz

Quartz is the most abundant vein mineral at Mahd AD Dahab and occurs as cryptocrystalline bands at vein margins, fine grains between coarse crystals especially at the vein centers and, as coarse euhedral crystals. The first

variety, alternating bands of cryptocrystalline quartz with chlorite, and sulphide minerals particularly galena and chalcopyrite is distinctive to the margins of some metal-bearing veins (Plate 15a, b). The bands are less than 1 mm to 5 mm thick and they pinch and swell, are in small folds, and are locally colloform (Plate 15c, d). Bands are internally layered on both megascopic and microscopic scales and are reminiscent of banded chert as described by Beukes (1973), and where hematite-bearing they look like cherty iron formation as described by Garrels et al. (1973). The cryptocrystalline quartz is white to light grey to green in colour where chlorite is included (Plate 15e), and reddish where hematite is included.

The second variety, fine grained quartz, is a white dense filling between euhedral quartz crystals especially at vein centers where it is intergrown with calcite and ankerite (Plate 7c, d), surrounded by chlorite (Plate 16a, b) or along veinlets of pyrite or totally surrounding pyrite grains (Plate 16c, d).

The third variety of quartz, the coarse euhedral crystals, are up to 2 cm long and arranged with their long axis perpendicular to both vein walls making a comb texture of terminating crystal faces at the vein center where they are rimmed with chlorite and infilled with fine grained quartz, calcite and ankerite (Plate 7d, d, 8a, 16e). These coarse crystals are white to yellow brown in colour or a light red.

The varieties of quartz in both metal-bearing and barren quartz veins at Mahd AD Dahab suggests changing

Plate 15

a. General view of 15 cm long polished slab consisting of, from top to bottom, massive galena (light gray) with chalcopyrite inclusions (white), cryptocrystalline quartz (white), rock fragment, alternating bands of cryptocrystalline quartz (white) and chlorite (black) and massive galena to the left hand side of the bottom of the picture.

b. The upper part of plate 15a enlarged to show the development of fine recrystallized quartz crystals along the margins of the rock fragment. Crystal oriented from the edges of the fragment. The white dispersed grains in the rock fragment are pink orthoclase. A small fracture 2 cm long, at the left end of the fragment is a slump feature rather than the result of tectonism.

c. The middle part of plate 15a is enlarged. Fine banding of alternating cryptocrystalline quartz (white) and chlorite (black). Very fine band of chalcopyrite (white) within chlorite. At the lower of the picture cryptocrystalline quartz (chert) has a colloform texture.

d. The lower part of plate 15a is enlarged. Colloform texture developed between cryptocrystalline quartz (white) and chlorite (black). The light gray spots are disseminated pyrite and chalcopyrite grains. The thin banding is disturbed by very local movements before total consolidation of these layers. At the lower left corner there is massive galena containing chalcopyrite and cryptocrystalline quartz.

e. Polished slab. Banded cryptocrystalline quartz (white) with chlorite (black) in galena (GAL). At the lower right corner ankerite (white) is in cryptocrystalline (white).

PLATE 15

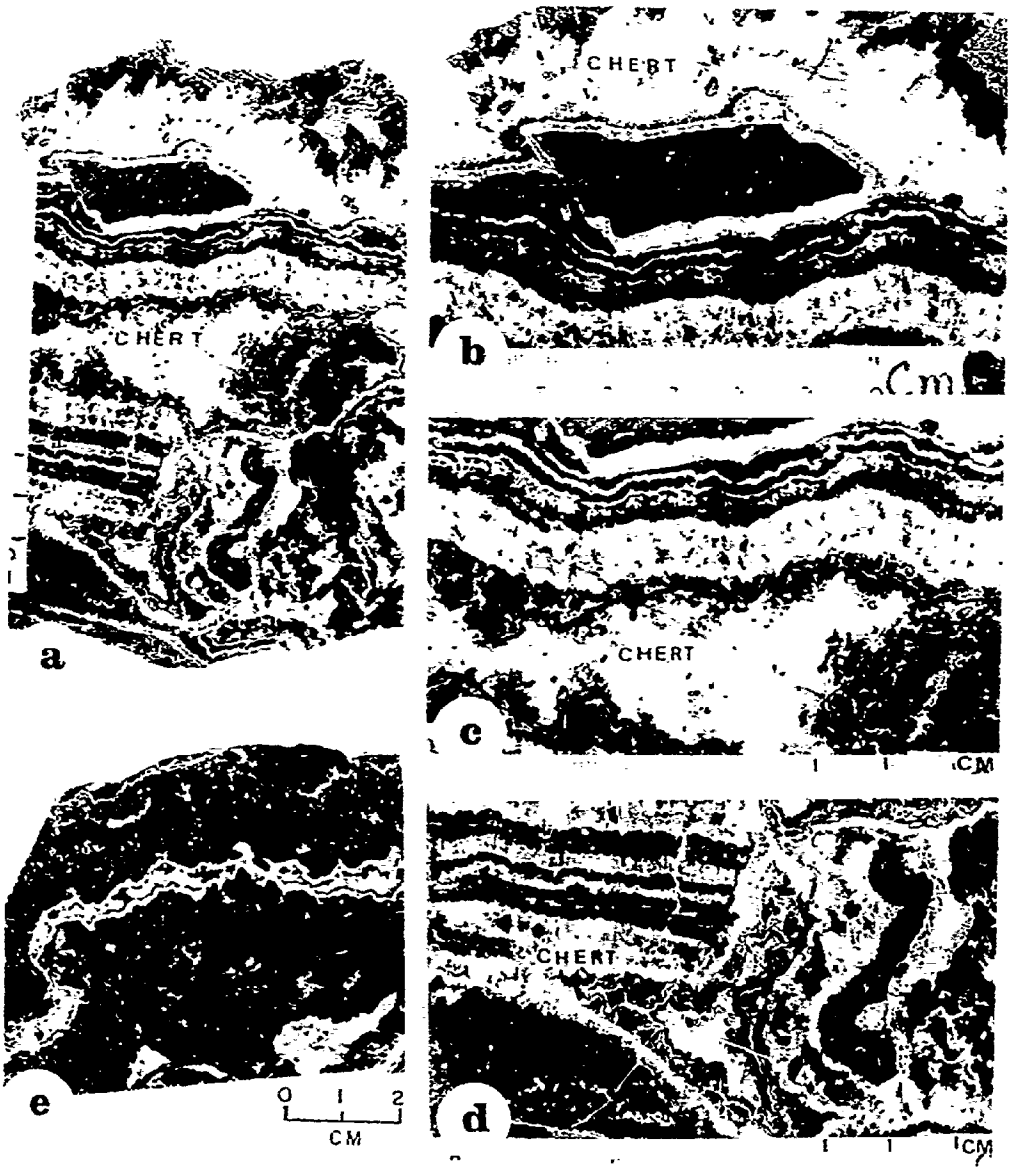

Plate 16

a. Thin section. Radiating grains of chlorite (black) surrounding quartz grains (dark gray). Crossed nicols.

b. Thin section. Radiating chlorite (black) surrounding quartz grains (gray and white).

c. Thin section. Quartz (white) on veinlets of sulphide minerals, pyrite (black) the light gray is radiating chlorite.

d. Thin section. Triangular pyrite grain (black) surrounded by alternating bands of quartz (gray and white) and chlorite (black). Crossed nicols.

e. Thin section. Quartz crystals (QTZ) oriented from the edges of fracture toward the centre. The black thin layer of zig zag shape in the centre of the fracture is chlorite.

PLATE 16

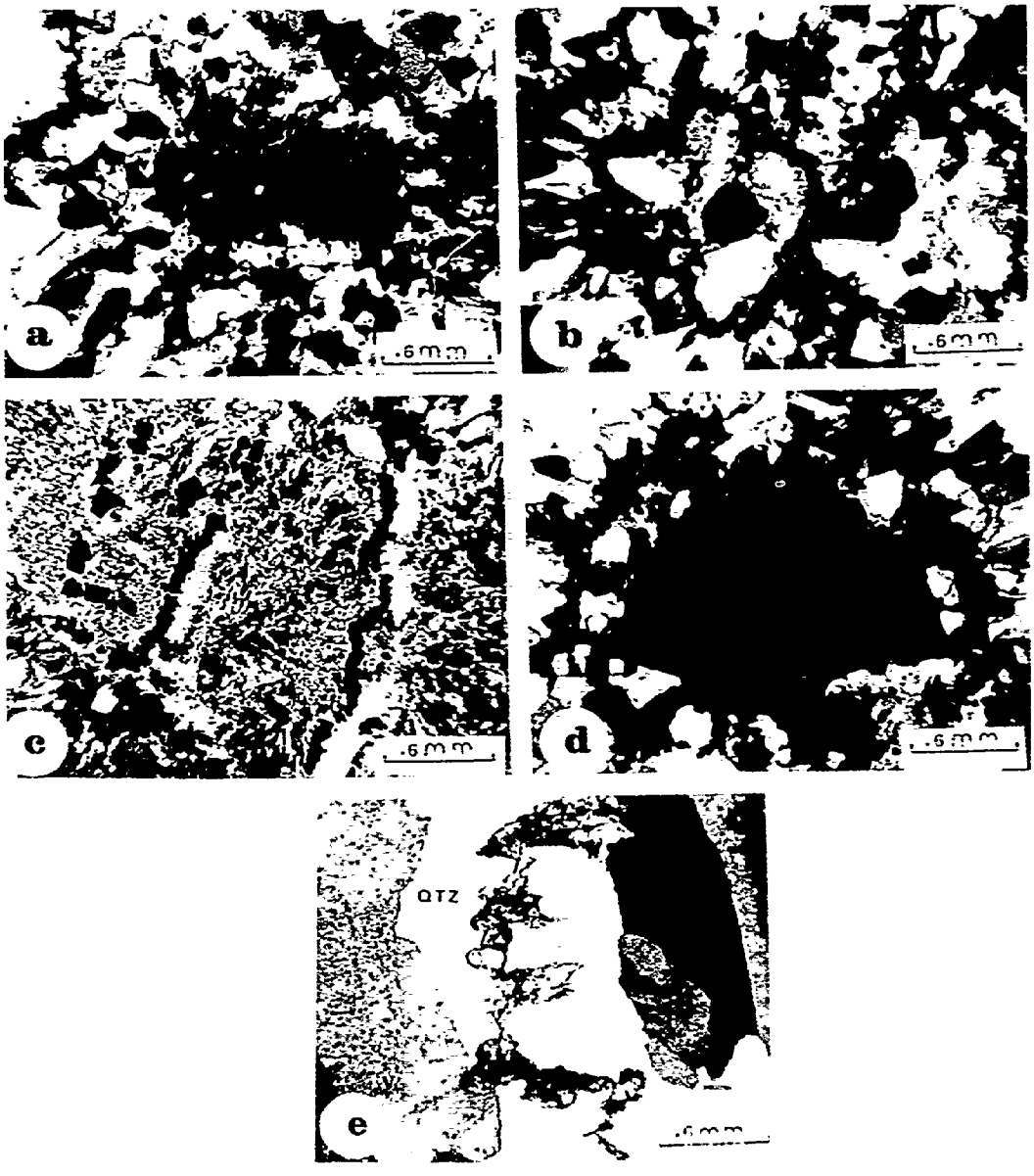

physical and chemical conditions during deposition of silica from a fluid filling open spaces. Initially it appears as if silica was deposited alernatively with chlorite and sulphide minerals along the edges of some fractures to be succeeded by relatively slow quartz crystal growth inward toward the center of the fracture and, followed by rapid deposition of fine grained quartz, calcite and ankerite to complete the fracture filling.

4.4.2. Chlorite

Chlorite occurs in bands alternating with crystocrystalline quartz and sulphide minerals along the margins of veins (Plate 15), as thin seams against terminating faces of coarse quartz crystals at vein centers (Plate 16e), and as radiating acicular grains surrounding sulphide minerals or at the cores of 3 mm round blebs of chalcopyrite (Plate 8b). Both a dark green pleochroic iron-rich chamosite and the magnesium-rich penninite, with its anomalous blue interference colours, are present and have been identified by probe analyses (Table 18).

The presence of chlorite alternating with quartz and sulphide mineral bands, and occurring both about and within sulphide minerals suggest simultaneous precipitation of all of these minerals from a fluid of complex composition emplaced into an open space where chemical and physical conditions differed considerably from those where the fluid was generated.

Table 18. Analyses by electron microprobe of chlorite (wt.%) from Mahd AD Dahab.

Sample No.	HH10	HH10	HH17A 07	HH17A 07	HH45B	HH80	HH80
Mg	23.75	23.88	16.37	15.80	14.64	14.31	14.62
Al	16.95	17.11	16.80	17.18	19.28	20.11	19.27
Si	29.26	29.67	27.35	27.22	26.42	26.04	25.78
Ca	.08	.05	.15	.09	.07	.05	.06
Ti	.01	.00	.05	.03	.05	.06	.06
Mn	.81	.82	.55	.56	.70	1.15	1.25
Fe	15.59	15.66	25.88	26.34	25.47	26.68	27.32
Total	86.49	87.20	87.91	86.40	86.82	88.34	88.37
	Ave. of 5 Anal.	Ave. of 6 Anal.	Ave. of 6 Anal.	Ave. of 5 Anal.	Ave. of 5 Anal.	Ave. of 5 Anal.	Ave. of 5 Anal.

4.4.3. Orthoclase

Orthoclase occurs as thin bands from 2 to 4 mm thick in some barren quartz veins. It is pink, fine grained and mixed with fine grained quartz along thin quartz stringers particularly within the porphyritic rhyolite (Plate 8f).

4.4.4. Calcite and Ankerite

Both calcite and ankerite occur with fine grain quartz filling intertices between other mineral grains in the quartz veins. They appear to be late in the crystallization sequence and would suggest increasing alkalinity of the fracture-filling fluid as it crystallized.

4.5. Barren Quartz Veins

The three-fold classification of metal-bearing quartz vein on the basis of texture also applies to barren quartz veins. There is however a fourth variety which is barren. This latter variety is essentially a variation on the crustified milky quartz veins as it has thin colloform bands of chlorite and in some instances hematite. Such veins are very local to the north central part of the mountain and are confined to the lower rhyolite tuff and lithic crystal tuff over an area 100 m in diameter.

Rock fragments are rare within barren veins and minerals other than quartz are simply chlorite, orthoclase in 2 to 4 mm thick bands at vein margins, minor hematite and

relatively minor calcite in vein centers. Quartz accounts for an average of 93% of the barren veins (Table 19) and the only noticeable variation in composition is in Al_2O_3 and Fe_2O_3 mainly present as hematite content as the nature of the wall rock changes. For example, the Al_2O_3 content of a vein is greater where that vein traverses lithic crystal tuff than where it traverses lower rhyolite. Iron has the same trend in its abundance. Five chip samples across two barren quartz veins of the massive milky quartz variety H4, H8, H9, H14, and H19 (Appendix 5) bear minor gold and silver.

4.6. Wallrock Alteration

The volcanic rock succession at Mahd AD Dahab has essentially three late mineral assemblages which, because of their proximity to quartz veins, similarity to other pseudomorphing phenomena described from many localities and reproduced experimentally (Meyer and Hemley, 1967), are considered alterations of original constituent minerals of wall rock during vein emplacement. The most abundant and pervasive of these mineral assemblages is chlorite, calcite and epidote occupying the site of primary ferromagnesium minerals in the andesite at the base of the exposed volcanic rock section, and in andesite fragments in the lithic crystal tuff. There is an obvious difficulty distinguishing an assemblage of these minerals as an alteration phenomenon accompanying vein emplacement in rocks which regionally have mineralogy attributable to greenschist facies metamorphism. However, the chlorite,

Table 19. Chemical analyses (major oxide wt.%) of barren quartz veins from Mahd AD Dahab.

Sample No.	3	4	8	9	14	15
SiO_2	94.44	95.46	96.55	93.28	99.41	98.64
TiO_2	.00	.00	.00	.03	.00	.00
Al_2O_3	2.00	1.34	.83	2.78	.24	.19
Fe_2O_3	1.44	.82	1.79	1.26	.11	.01
MnO	.01	.05	.00	.00	.00	.00
MgO	.00	.12	.00	.00	.00	.00
CaO	.04	.23	.07	.37	.00	.01
Na_2O	.00	.07	.00	.08	.08	.00
K_2O	.35	.31	.09	.76	.00	.00
P_2O_5	.02	.00	.05	.03	.05	.02
Total	98.34	98.47	99.41	98.64	99.91	98.90

calcite, epidote assemblage is most extensive and intensive at the edges of quartz veins to support the contention that it is an alteration product.

The second most abundant late mineral assemblage is quartz, and sericite after primary orthoclase and plagioclase and quartz of the more felsic volcanic rocks in the upper part of the volcanic succession. This assemblage is particularly apparent in those areas where quartz veins and veinlets are most frequent and where concentrations of quartz veins and stringers form stockworks described in the mapping as silicified areas (Fig. 6, 6a). In this latter instance silica content of the rocks is considerably greater than in areas of less abundant quartz veining.

The third late mineral assemblage is orthoclase, quartz and sericite particularly in the upper part of the lithic crystal tuff and in the porphyritic rhyolite where pink orthoclase occurs as dispersed grains after plagioclase and with quartz in 2 to 4 mm thick bands at the edges of quartz veinlets (Plate 8f).

These three late mineral assemblages are comparable respectively to the propylitic, phyllic, and potassic alteration assemblages described from porphyry copper deposits in general (Meyer and Hemley, 1967, Lowell and Guilbert, 1970, Rose, 1970) and specifically by Camus (1975) for El Teniente and by Sales and Meyer (1948) for Butte. They are also described from stockworks beneath the

massive sulphide deposits and from the walls at several vein deposits (Meyer and Hemley, 1967). Generally propylitic alteration is most widespread, the phyllic is dominant where quartz veining and sulphide mineral content is greatest and, the potassic is localized and internal to a veined and metal-bearing area interpreted as a hydrothermal system. This holds generally for Mahd AD Dahab where the propylitic assemblage is the most widespread as an alteration of primary ferromagnesium inerals in the rock. The phyllic assemblage of quartz and sericite is most common after primary feldspars and as additive quartz in areas of greatest vein density in the upper part of the section. The greatest sulphide mineral content also occurs in this part of the section as dispersed pyrite in the upper rhyolite tuff and associated chert, and in the stockwork vein areas within the porphyritic rhyolite. The phyllic assemblage, but generally without sericite, is also commonly internal to chlorite in individual veins. The potassic assemblage is local within wall rocks to veins, at some vein margins, and is not notably associated with sulphide minerals.

Alteration of this nature is commonly ascribed by hydrogen metasomatism (Hemley and Jones, 1964) controlled by variations in the ratio of common metal cations to hydrogen in the altering fluid. Such altering fluids have cation H^+ below the limits of stability for feldspar and other minerals and hence alteration of the wall rocks takes place

by consumption of H^+ from the fluid and release of metal cations to the fluid raising the ratio toward equilibrium. The extent of the hydrogen metasomatism or hydolysis, is expressed in the alteration mineral assemblages from an incipient hydolysis in the propylitic assemblage, to a moderate hydolysis in the phyllic assemblage, to an extreme hydolysis in the potassic assemblage which can be expressed as

$$3NaAlSi_3O_8 + 2H^+ + K^+ \rightarrow KAl_3Si_3O_{10}(OH)_2 + 6SiO_2 + 3Na^+$$

This stage of hydrogen metasomatism is well illustrated at Mahd AD Dahab by the presence of potassium and the virtual exclusion of sodium in analyses of the porphyritic rhyolite in areas of stockwork fractures.

In brief, observed alteration is compelling evidence that aqueous fluids have coursed through fractures at Mahd AD Dahab and have reacted with wall rocks. This reaction of fluid and wallrock contributed to change in composition of the fluid and precipitation of minerals in the fractures. Precipitation was undoubtedly aided by falling temperature, changing fluid density, and probably mixing of dissimilar fluids such as discussed in the following section.

4.7. Summation

There are four textural varieties of quartz veins at Mahd AD Dahab. All four exist as barren quartz veins but only three of the four varieties carry metals. Pyrite is

the most abundant metallic mineral and it appears to be without minor element content. Chalcopyrite is next most abundant and it and pyrite are generally enveloped by sphalerite, galena, bornite, chalcocite, and neodigenite. Chalcopyrite veins pyrite and in turn is veined by covellite. Gold and silver occur as electrum and tellurium minerals within chalcopyrite, sphalerite and galena, or between sphalerite and galena. There is also very fine elemental gold within chalcopyrite. There are also lead and bismuth telluride minerals. Concentration of minor elements in sulphide minerals and tellurium minerals at Mahd AD Dahab varies greatly from one mineral to the other in that Se and Te are totally absent in pyrite and either absent or minor in chalcopyrite. Galena is the main carrier of Se where it probably substitutes for S. Tellurium tends to form tellurides instead of substituting for S in sulphide minerals. Cadmium is concentrated in sphalerite relative to other sulphide minerals which is perhaps another sign of the alkalinity of the mineralizing fluid.

The intergrowth of metallic minerals and the silicate and carbonate gangue minerals suggest that they all crystallized from the same fluid and that that fluid was alkaline otherwise the CO_2 pressure could not have been contained (Barton, 1959). The alteration accompanying fracture filling is a progressive hydolysis indicating that the fluid was aqueous and hot. The banded nature of some veins could

result from multiple pulses of fluid flow along fractures and the quartz cemented breccia veins suggest a rapid large volume fluid flow which could tear fragments from fracture walls (Durney and Ramsy, 1973).

CHAPTER 5

FERROUS/FERRIC IRON IN QUARTZ VEINS AND WALL ROCKS

5.1. General Statement

The FeO/Fe_2O_3 in primary igneous rocks is a rather consistent 0.7. This ratio changes only in response to pervassive interaction between water and rock where water acts either as an oxidant or a reductant depending on chemical conditions and path of fluid flow. The general conditions of oxidation and reduction reactions in rocks have been discussed by Eugster (1959) and Eugster and Wones (1962) and, the usefulness of FeO/Fe_2O_3 in determining the nature and source of mineralizing fluids has been described by Kerrich et al. (1977) in a consideration of the gold-bearing quartz veins of the Yellowknife District, N.W.T., Canada.

In samples from Mahd AD Dahab total iron was determined by x-ray fluorescence spectrometry and FeO was analyzed volumetrically by the method of Wilson (1955) described in Appendix 7.

5.2. Ferrous/Ferric Iron

Abundances of FeO and Fe_2O_3 were determined in 17 samples of metal-bearing veins, barren veins, and wall rocks to veins (Table 20). Five of these samples are from the body of porphyritic rhyolite, 5 are from the underlying

Table 20. Abundances of total iron, ferrous iron in lithologies and vein systems at Mahd Ad Dahab.

Sample No.	Sample Description	Total Iron (Fe_2O_3)	FeO	FeO/Fe_2O_3
22	Sulphide-bearing veins	25.76	.70	.02
24	" " "	25.64	3.87	.15
29	" " "	9.18	.18	.02
30	" " "	4.31	1.02	.23
41	" " "	2.96	.25	.08
2	Barren vein	5.08	.63	.12
1	Lithic crystal tuff	3.85	.46	.12
10	" " "	3.52	1.89	.53
11	" " "	3.31	1.36	.41
21	" " "	11.91	.07	.005
28	" " "	4.43	.32	.07
12	Lower rhyolite tuff	2.99	1.89	.60
20	Porphyritic rhyolite	4.61	.28	.06
25	" "	7.02	.57	.08
35	" "	4.95	.07	.01
39	" "	5.49	3.49	.63
40	" "	3.18	.09	.02

lithic crystal tuff and 1 is from the lower rhyolite tuff. Another 5 samples are from metal-bearing veins, and 1 sample is from a barren quartz vein. Each sample contained in excess of 3% total Fe by weight.

In metal-bearing veins FeO/Fe_2O_3 averages 0.10 and, the ratio in the barren vein sample is 0.12. The porphyritic rhyolite has an average FeO/Fe_2O_3 of 0.16 except for sample 39 which has a ratio of 0.6. In the lithic crystal tuff the average is 0.21 and, the single sample of lower rhyolite tuff has a ratio of 0.6. Hence, on the basis of this limited sampling there appears to be an increase in ferric iron relative to ferrous iron down stratigraphic section and, the vein material has the greatest relative amount of oxidized iron.

5.3. Discussion

At Yellowknife Kerrich et al. (1977) describe gold-bearing quartz veins and wall rocks with iron predominately in the reduced state and attribute mineralization to fluids derived from within the rocks during metamorphism. At Mahd AD Dahab, however metal-bearing quartz veins and wall rocks are characterized by iron predominately in the oxidized state and hence an appeal must be made to a mineralizing fluid with abundant oxygen, or to mixing of a metal-bearing fluid with an oxygen-bearing fluid resulting in oxidation of the former and precipitation of vein material. The most available oxygen-bearing fluid is surface water, either sea water

or meteoric water. There are essentially 3 ways oxygen can be taken from these surface waters:

1. Thermal dissociation of water

$$2H_2O \rightarrow 2H_2 + O_2$$

The amount of oxygen produced through dissociation of water is not great, on the order of 10^{-27} moles of oxygen per liter of water, and is probably only geologically significant at temperatures in excess of 500°C. The oxidation of iron is simply $2FeO + H_2O \rightarrow Fe_2O_3 + H_2$.

2. Free oxygen dissolved in either sea water or meteoric water. Each liter of sea water contains about 10^{-4} moles of dissolved oxygen (Spooner et al., 1977), and each liter of normal surface water contains nearly the same number of moles of dissolved oxygen as in sea water (Fyfe, personal communication).

3. Reduction of sulphate in water.

$$2S_4 + 11\ Fe_2SiO_4 + 4H^+ \rightarrow FeS_2 + 7Fe_3O_4 + 11SiO_2 + 2H_2O$$

Sulphate can be as abundant as 2,688 ppm (Pytkwicz and Kester, 1971) in sea water and hence the source of about 6×10^{-2} moles of oxygen per liter of sea water. Sulphate content in normal surface water is 11.2 ppm (Fyfe, 1974) or about 1.1×10^{-3} moles of oxygen per liter of water. Sulphate reduction could also contribute sulphur for pyrite and other sulphide minerals. Drawing the required sulphur from water during the mixing of fluids also avoids the problem of transporting both metals and sulphur together in the same fluid, a problem that has

long plagued proponents of a single fluid rising from a crystallizing magma and source to all materials filling fractures.

Besides the requirement of oxygen in the system as indicated by the FeO/Fe_2O_3, there are the constraints of temperature, pH, solubility of gold and silica, and volumetric considerations. There is a distinct absence of usable fluid inclusions at Mahd AD Dahab and no attempt has been made to determine temperature of formation by this method. However, Batchelder determined temperatures of between 155 and 278°C from secondary and psuedo-secondary fluid inclusions in veins at this site (Robert et al., 1974). From comparative data drawn from other vein systems temperatures under 300°C appear reasonable for precipitation and indeed Henley (1973) reports gold solubility decreases from about 1000 ppm at 480°C to 200 ppm at 450°C, to 6 ppm at 300°C.

The presence of calcite and ankerite with sulphide minerals in the veins suggest the mineralizing fluids were alkaline at least in their late stages (Barton, 1959). This is in keeping with the conclusions of Smith (1944) and Weissberg (1970). Krauskopf (1951) however concludes that gold, in addition to being soluble and transportable in alkaline solutions, can also be transported as chloride complexes in acid solutions. Helgeson and Garrels (1968) believe gold is transported only in acid solutions as chloride complexes. Most recently Seward (1973) has suggested that the solubility

of gold decreases with increasing alkalinity and that at 300°C with pH 9.6, 15 ppm gold are in solution but at the same temperature and pH 7.4, 60 ppm gold are in solution. At 180°C and pH 7.6 only 5 ppm gold are in solution. Seward also concluded gold can be carried as thio and chloride complexes. Without fluid inclusion there is no definite conclusions as to the pH of mineralizing fluids at Mahd AD Dahab.

On the matter of silica, there are at least 50 quartz veins at Mahd AD Dahab approximately 500m long and 1m wide. These veins are known through a vertical extent of 200m. In addition there are several quartz-rich, or silicified zones, and many quartz veinlest within an area of lower rhyolite tuff which in plan is 100 by 30m and which probably extends to a depth of 200m. Hence, the probable total of additive silica at Mahd AD Dahab is

$$50 \times (500 \times 200 \times 1) + (100 \times 30 \times 200)$$

or 6×10^6 m^3, which is 15.6×10^{12} gm or 2.6×10^6 gm/m3

If one assumes a temperature of 400°C at 500 bars to simulate a depth of 2 km, water can have in solution 0.1 wt.% SiO_2 (Fyfe, 1974). Therefore, 15.6×10^{15} gm or 15 km^3 of water would be required to carry the 6×10^6 m^3 of silica present at Mahd AD Dahab. An approximately similar volume of meteoric water containing about 11 ppm sulphate could provide enough sulphur for the 1% sulphide mineral content of the veins. Sea water could provide much more sulphur. Finally, to heat 15 km^3 of fluid to 400°C would require about 4×10^{18}

calories assuming constant Cp of water at about 1, The porphyritic rhyolite body has a surface area of about 400 m^2 and a possible volume of 1 km^3 which could release upon cooling, from above 400°C, on the order of 3 x 10^{17} calories (Fyfe, personal communication) plus some latent heat of crystallization. Therefore heat from the rhyolite body is not sufficient by itself to raise fluids above 400°C and to achieve the required solubilities. Indeed a rhyolite body on the order of 10 km^3, not 1 km^3, would be required. As there is no field evidence to suggest other rhyolite bodies in the immediate area some appeal for additional heat must be made to a large magma chamber at depth which perhaps ultimately feeds succeeding flows and fragmental rocks, or to heat dissipating from the thick pile of volcanic rocks which are intruded by the local body of porphyritic rhyolite and which is cut by the quartz veins of Mahd AD Dahab.

In brief, it appears fluids responsible for vein fillings at Mahd AD Dahab may have been ascending, voluminous, aqueous, reduced metal-bearing, silica-rich and above 400°C and mixed with descending, voluminous, aqueous, oxygenated, cold surface water with a sulphate content. The mixing of the ascending and descending fluids resulted in cooling, oxidation of wall rocks and ascending fluid, and precipitation of a disequilibrium assemblage as fracture fillings.

CHAPTER 6

A GENETIC MODEL FOR VEINS AT MAHD AD DAHAB

6.1. General Statement

The Mahd AD Dahab area has volcanic rocks of the Proterozoic Halaban Group of differentiated flows and pyroclastic rocks metamorphosed to the greenschist facies. They are underlain by more volcanic rocks of varied composition and a schistose and gneissic basement. They are overlain by clastic sedimentary rocks and rhyolite. The Halaban Group is comparable to an island arc or continental margin type of volcanic succession and is probably a product of compressive tectonics and perhaps subduction. Most of the metal occurrences in this part of the Arabian Shield, including Mahd AD Dahab are in the middle to upper part of the Halaban Group and are considered herein to have developed as part of that sequence, not as the result of some later unrelated igneous or metamorphic event.

Metal-bearing and barren quartz veins at Mahd AD Dahab traverse volcanic rocks of intermediate to felsic composition and a small body of porphyritic rhyolite which intrudes the layered rocks. A rhyolite tuff with interlayered and hanging wall chert tops the layered section, the porphyritic rhyolite body and the quartz veins. Wall rocks to the

veins have been oxidized, subjected to hydrogen, potassium, and silica metasomatism, and silica has been essentially removed. All of these features are cut by andesite dikes which feed overlying flows. Mineralizing fluids appear to have been an ascending hot reduced aqueous and metal-bearing one which mixed with a descending cold oxygenated and sulphate-bearing one resulting in precipitation of the vein material near surface.

6.2. A Sequence of Events in Vein Development at Mahd AD Dahab

1. Differentiated volcanic rocks and derived sedimentary rocks were deposited over a large, probably submarine, area, upon older volcanic rocks and were subsequently intruded by plutons of similar composition during early stages of the compressive Hijaz Tectonic Cycle. This formed the base, or platform, for the progressively centralized volcanism of the Halaban Group.

2. Intermediate to felsic volcanic products were deposited locally, probably in sea water, upon the aforementioned platform during middle and late stages of the Hijaz Tectonic Cycle. These layered rocks were accompanied by intrusive bodies of similar composition, This produced the middle part of the Halaban Group.

3. At Mahd AD Dahab, during a hiatus in this volcansim of middle Halaban Group the rocks cooled by convecting water, either sea water or meteoric water, which percolated

downward over a broad recharge area and returned to surface in focused flow about a point heat source, the body of porphyritic rhyolite (Fig. 17), (Ohmoto and Rye, 1974).

Water in descending lost its oxygen to the volcanic rocks and was modified to a hot reduced brine-like fluid capable of leaching and transporting metals and silica. This fluid returned toward surface along fractures virtually chemically in tact in the most focused and hotest part of the area, about the body of porphyritic rhyolite. Upon meeting descending cold, oxygenated and sulphate-bearing water near surface metallic sulphide minerals and silicate minerals were deposited in fractures and at surface. The most complex mineralogy in fracutres and the most metalliferous chert deposited on surface are within and closest to the porphyritic rhyolite, the local heat source which kept fluids focused and intact until in contact with descending oxygenated and sulphate-bearing water. Farther away from the hot porphyritic rhyolite where temperature and water/rock was less, only quartz was precipitated in the fractures as most metals came out of solution along the course of the fracture during progressive cooling. That is, the fluid dissipated its metal content at depth along the vertical extent of the fracture leaving only barren quartz for the upper reaches and the surface. Banding and wall rock brecciation on vein margins attests to the forceful and voluminous flow of the fluid in pulses.

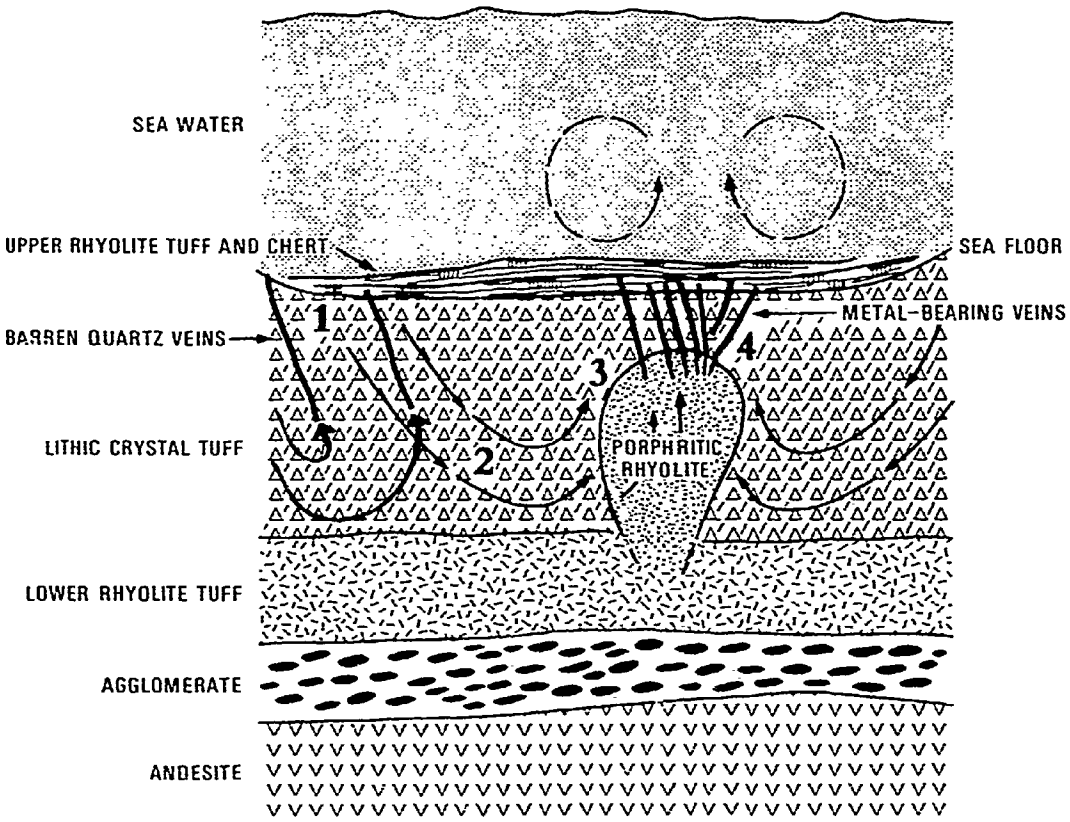

1 Percolation of cold oxygenated sea water

2 Oxygen in sea water consumed; modified fluid is reduced, heated; leaches metals and silica

3 Hot metal – bearing fluid ascends through fractures

4 Ascending fluid meets descending cold oxygenated sea water and precipitates fracture fillings

Figure 17. Convective Movement of Sea Water through the Volcanic Section at Jabal Al–Mahd.

4. Convection of water continued until the rocks cooled. Locally derived clastic rocks subsequently covered the immediate area and were eventually followed by the next cycle of flows and pyroclastic rocks.

5. The area was folded and metamorphosed in the late stages of the Hijaz Tectonic Cycle, eventually broken by tension fractures of the Najd Fault System and, overlain by rhyolite.

6.3. Discussion

There are some distinct similarities between the veins of Mahd AD Dahab, the stringer zones beneath massive sulphide bodies of Kuroko type and, also the precious metal veins of bonanza type (Table 21). The similarity appears to be most striking between Mahd AD Dahab and the Kuroko stringer zones, particularly because of likeness of strata-bound setting in differentiated volcanic and sedimentary rocks of an island arc environment and because of the base metal mineralogy. The obvious difference between Mahd AD Dahab veins and a massive sulphide situation is of course that Mahd AD Dahab is virtually all fracture filling and has very little strataform material in the form of pyritic chert. This difference could be attributed to a number of variables in the fluid system which resulted in precipitation mostly in the fractures rather than at surface. Perhaps one of those variables could have been that meteoric water and not sea water was the main fluid component of the system resulting

Table 21. A Comparison of Mahd AD Dahab to Kuroko deposits in Japan and Fiji (Colley and Rice, 1975) and Bonanza type deposits in Western North America (Silltoe 1977).

	Mahd AD Dahab	Kuroko	Bonanza
Nature of metal concentration and the section	Base and precious metals in stratabound walled quartz veins and some calcite and ankerite cutting flows and fragmental rocks of intermediate to felsic composition within and about an intrusive rhyolite body, and terminating in chert.	Base and precious metals in massive sulphide stratabound within flows and pyroclastic rocks intermediate to felsic in composition and underlain by stockwork fractures bearing sulphide minerals. Massive sulphide is commonly overlain by and laterly equivalent to chert. Both massive sulphide and stockwork fractures are commonly near a clacitic to rhyolitic intrusive body.	Base and precious metals in sharpe walled quartz-calcite veins cutting flows and fragmental rocks of mafic to felsic composition in some instances near latitic to rhyolitic intrusions and ring and radial fractures within and about Calderas. Intrusive rocks are not always evident.
		Example	Example
	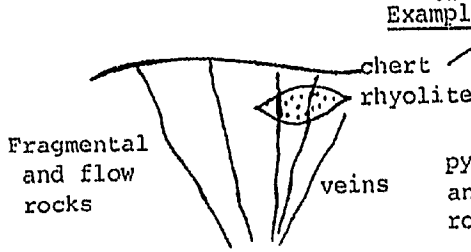	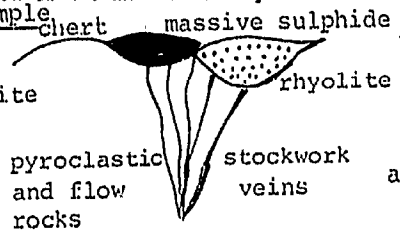	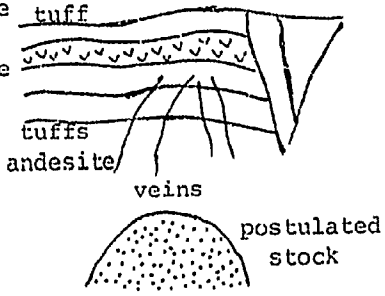
	Mahd AD Dahab-by Hakim (1978) Section may be submarine or subaerial no definite evidence it is part of Halaban Group.	Shakanai (after Kajiwara 1970) Section is submarine (Green-tuff island arc).	Creede (after Steven and Eaton 1975). Section is subaerial a continental volcanic setting.
Veinform	Sharp walled, massive to mineralogically banded, comb structure, cemented breccia, though going to stockwork, crustification and colloform. Veins have restricted vertical extent at 1.5 km.	Stockwork, massive to banded. Stockworks have vertical extent at several hundreds of feet.	Sharp walled, massive to banded, breccia zones. Comb structure, colloform and crustifiform, though going to stockwork. Veins rarely have more than 600 m vertical extent.

Table 21 Cont'd.

Vein Mineralogy	Pyrite, chalcopyrite, bornite, covellite, neodigenite, galena, sphalerite, electrum, pyrargerite, tellurides. Gangue is quartz, calcite, ankerite, chlorite, K spar, hematite. Vein assemblage is not an equilibrium assemblage i.e. pyrite and hematite.	Massive ore is pyrite, sphalerite, galena. Stockwork veins are mostly pyrite, chalcopyrite plus gold generally as fine inclusions in chalcopyrite. Gangue is minor quartz, chlorite. Sulphate is common at base of massive sulphide body and gnerally cut by stockwerd zone. Stockwork veinlet assemblage can have pyrite, pyrhotite and magnetite, hence not an equilibrium assemblage.	Enargite, sphalertie, galena, As, Sb, sulphosalts, native Au, electrum, tellurides, stibnite, cinnabar and pyrite. Gangue, quartz, calcite dolomite, barite, adularia, rodochrosite, rhodomite, fluorite, sulphate present but generally subordinate to silicates and carbonates.
Alteration	Propylitic - peripheral regional phyllic - predominant and intermediate in position, potassic. K-metasomatism is a predominant feature in the wall rock. Na is totally leached from the areas closer to metal-bearing veins.	Prophylitic predominates in the stockwork area, albitization or Na metasomatism particularly of rocks above massive sulphide is recorded. K-metasomatism is prominent in chlorite-sericite and transitional zones as in Hokuroku district and Na leaching is also evident in all zones (Iijima 1974).	Prophylitic, argillic, phyllic, potassic. Prophylitic is regional. Advanced argillic accompanied by wide spread silicification is common.
	Ferrous-ferric ratios are small.	No data available.	No data available.
Ore genesis	Convecting surface water, either sea water or meteoric water leaches metals at depth, deposit them in fractures where mixing with surface water which takes place in focused discharge site about porphyritic rhyolite.	Convecting sea water leaches metal at depth, deposits them on the sea floor and in stockwork fractures where mixing of fluids takes place in focused discharge even near felsic intrusions.	Convecting meteoric water leaches metal at depth returns to near surface along fractures resulting from Caldera development or regional tectonism and deposit upon mixing with near surface fluids.
Critical points	1. Veins and stockwork are open space fillings.	1. Massive sulphide is deposited on the sea floor where fluids discharge, stockworks are open space fillings.	1. veins are barren zones are open system fillings.
	2. Fluids on the bases of vein mineralogy and alteration were columinous, aqueous, base and precious metal-bearing perhaps alkaline and deposited during forceful pulsations. System was probably relatively low in sulphur, low temperature 200 to 300°C, low pressure.	2. Fluids are voluminous, aqueous, base and precious metal-bearing, system is sulphur-rich, moderate temperature low pressure, fluid is believed to be sea water dominated.	2. Fluids are voluminous, aqueous, alkaline, system is low sulphur, low salinity, low temperature, low pressure, fluids dominated by meteoric water but several districts have O isotopes suggesting a magnetic component.

in greater oxygenation, less sulphur, and so forth than encountered in sea water. Although there is no conclusive evidence at this time as to sea water or meteoric water dominance of the system it is the preferred contention from this study that sea water did dominate and did provide the main ascending fluid but that perhaps the system was sub-aerial in its late stages, a system of volcanic rocks and convection which began submarine and which eventually broke surface. Had it remained submarine throughout its life it might have debouched most of its products on the sea floor to make a massive sulphide deposit of base metals with a precious metal content.

CHAPTER 7

CONCLUSIONS AND RECOMMENDATIONS FOR FURTHER WORK

Both metal-bearing and barren quartz veins at Mahd AD Dahab are stratabound products of sea water circulation through a cooling accumulation of flows and pyroclastic rocks, which leached metals from those volcanic rocks, and deposits them upon mixing with cold oxygenated surface water in fractures in and about a small sub-volcanic intrusion which focused discharge. This took place at a hiatus in extrusion of volcanic rocks of the middle part of the Halaban Group during the late stage of the Hijaz Tectonic Cycle. Previous explanations of the veins as isolated filling of fractures related to the Najd Fault System are untenable in the light of present work.

The current study has basically documented the nature of the veins and proposed a genesis. This is the basis for continuing work as recommended below.

1. A study of relative abundances of oxygen isotopes in vein material and the chert within the upper rhyolite tuff to establish contributions to mineralizing fluids of sea water, meteoric water and igneous water. This will be of inestimable help in elaborating upon genesis of the veins and in explaining nature and distribution of other sulphide-bearing occurrences in rocks of the Halaban Group in this area.

2. Local and regional mapping should be extended in search for areas of albitization which might be sites of deposition for sodium leached from the volcanic rocks. The rocks at Mahd AD Dahab are virtually lacking in sodium and if leached by coursing fluids it should have been deposited somewhere nearby. One should begin carefully examining the upper rhyolite tuff and chert and hence progress laterally and up section from the vein area. An examination of the granodiorite at the base of the section would also be warranted as it appears more sodic than an average granodiorite. This would contribute to the understanding of the fluid composition and the convective process.

3. The area to the west, in which veins of somewhat similar aspect are known, should be mapped and the occurrences compared to Mahd AD Dahab in the interest of developing a regional scheme of metal distribution. Similarly the comparison to massive sulphide and bonanza deposits should be expanded. This would help in the evaluation of specific occurrences in this part of the Arabian Shield and also in developing an appreciation for overall potential of the Shield area.

APPENDICES

APPENDIX 1: Analysis by x-Ray Fluorescence Technique

X-Ray Fluorescence

Selected samples representing different rock units were crushed and ground in a Bleuler apparatus to less than 200 mesh. Pressed powder pellets and fused discs were made from the powder of each sample according to the method of Norrish and Chappel (1967) and Norrish and Hutton (1969).

All the analyses were done in a Phillips PW1450 AHP automated x-ray fluorescence. The standards used were: FS72 (for all major elements except for Na), GA (for Na). The chemical compositions, in wt.%, were determined from the absorption values using a computer programme obtained from Dr. H. Hunter, University of Western Ontario. The calculated chemical composition was punched on cards and they were run through a second programme which calculated the CIPW molecular norms.

The analyses are accurate to within 1% of the amount present for the major elements except Na and to within 10% for Na.

Totals in most samples are a bit low because no loss on ignition for determining the total of volatiles was done.

APPENDIX 2: Chemical analyses (major oxides wt.%) of the porphyritic rhyolite at Mahd AD Dahab.

Sample No.	32	34	35	36	38	39	40	42
SiO_2	74.68	74.91	74.05	75.90	77.00	71.06	74.04	74.46
TiO_2	.18	.17	.18	.18	.18	.26	.18	.19
Al_2O_3	12.70	11.26	12.42	11.21	11.09	8.42	12.14	12.73
Fe_2O_3	1.09	3.15	4.95	2.13	1.07	5.49	3.18	1.68
MnO	0.00	.27	.00	.00	.00	.35	.00	.00
MgO	1.21	1.31	1.42	1.13	1 02	2.19	1.21	1.33
CaO	.18	.12	.08	.13	.05	.13	.07	.07
Na_2O	.00	.00	.00	.00	.00	.00	.00	.00
K_2O	8.29	6.42	8.50	8.12	8.04	3.19	8.34	7.23
P_2O_5	.00	.00	.00	.00	.00	.00	.00	.00
Total	98.35	97.66	101.64	98.82	98.48	91.13	99.21	97.74
			Norms (CIPW)					
Q	40.80	48.57	38.62	43.35	44.65	58.31	40.51	45.71
or	49.82	38.87	49.45	48.54	48.26	20.78	49.72	43.74
an	.91	.61	.39	.65	.25	.71	.35	.36
co	3.46	4.19	3.03	2.21	2.33	5.22	3.01	4.89
hy	4.50	4.97	3.48	2.85	4.00	11.86	3.04	3.39
mt	.16	2.47	.00	1.53	.15	2.57	.00	.00
il	.35	.33	.15	.35	.35	.54	.19	.37
hm	.00	.00	4.79	.54	.00	.00	3.10	1.55

Appendix 2 Chemical analyses (major oxides wt.%) of the porphyritic rhyolite at Mahd AD Dahab.

Sample No.	804	805	809	830	832	834	28	31
SiO_2	84.46	77.62	72.98	75.83	76.22	69.63	81.26	73.90
TiO_2	.13	.20	1.21	.43	.44	.20	.20	.18
Al_2O_3	8.08	11.23	8.23	10.29	10.34	11.51	6.97	12.36
Fe_2O_3	1.47	.95	6.47	2.84	1.63	3.91	4.43	1.64
MnO	.07	.01	.27	.07	.07	.12	.03	.00
MgO	.56	.06	3.82	1.32	1.27	2.41	2.11	1.27
CaO	.28	.09	.61	.14	.12	.07	.20	.07
Na_2O	2.58	1.51	.58	.	0.09	.00	.00	.00
K_2O	2.10	6.21	1.69	6.73	6.27	7.12	1.10	8.49
P_2O_5	.57	.03	.24	.64	.04	.05	.00	.00
Total	100.42	98.05	96.15	97.73	98.25	95.06	96.33	97.95
			Norms (CIPW)					
Q	60.35	48.70	56.71	48.92	48.67	39.64	76.33	40.20
or	12.35	19.35	10.39	40.71	40.45	44.28	6.75	51.24
ab	21.73	14.90	5.11	.00	.78	.00	1.03	.35
an	2.39	-	1.53	.45	.34	.03	1.03	0.35
co	2.39	3.90	5.11	2.91	2.85	3.99	5.63	3.11
hy	3.45	9.04	15.17	3.64	3.36	8.88	5.46	3.23
mt	.20	2.63	3.00	2.43	2.41	2.65	.57	.00
il	.42	.88	2.39	.84	.85	.40	.39	.30
hm	-	-	-	-	-	-	3.83	1.54
ap	1.34	.39	.59	.10	.10	.12		

Appendix 3 Whole rock analyses (in wt.%) of the lithic crystal tuff.

Sample No.	1	2	5	6	7	10
SiO_2	85.08	76.28	78.62	85.06	87.32	81.77
TiO_2	.15	.09	.30	.09	.10	.18
Al_2O_3	5.89	6.81	9.58	5.90	6.17	8.04
Fe_2O_3	3.85	5.08	2.61	2.27	1.29	3.52
MnO	.00	.01	.08	.02	.01	.02
MgO	.22	4.67	.56	.41	.33	.68
CaO	.32	.12	.22	.12	.13	.07
Na_2O	.00	.00	.00	.00	.00	.00
K_2O	2.61	1.71	4.85	1.78	2.08	3.43
P_2O_5	.10	.05	.15	.08	.07	.07
Total	98.27	94.86	97.01	95.76	97.55	97.83
			Norms (CIPW)			
Q	75.97	66.13	60.94	81.08	80.63	
or	15.63	10.67	29.55	10.99	12.65	
an	.95	.29	.13	.08	.20	
co	2.76	5.13	4.42	4.12	3.96	
hy	.56	12.27	1.60	1.07	2.01	
mt	1.36	1.66	2.41	2.08	.19	
il	.10	.18	.59	.18	.20	
he	2.44	3.55	.00	.20	.00	
ap	.24	.12	.37	.20	.17	

Appendix 3 (cont...)

Sample No.	11	17	20	21	23	28
SiO_2	77.23	80.74	83.27	81.16	73.90	81.26
TiO_2	.36	.23	.15	.01	.17	.12
Al_2O_3	10.17	7.46	6.52	1.46	12.01	3.68
Fe_2O_3	3.31	3.12	4.61	11.91	2.31	3.10
MnO	.04	.14	.02	.10	.00	.02
MgO	.64	4.58	1.61	.92	1.25	1.27
CaO	.67	.14	.12	.61	.42	.14
Na_2O	.00	.00	.00	.00	.00	.00
K_2O	5.90	1.32	1.27	.13	7.93	1.10
P_2O_5	.15	.00	.00	.00	.00	.00
Total	98.53	97.77	97.59	96.34	98.02	96.33
			Norms (CIPW)			
Q	53.35	69.60	77.68	80.99	41.63	76.33
or	35.46	7.98	7.70	.80	47.83	6.75
an	2.39	.71	.61	3.14	2.13	1.03
co	2.97	5.91	5.05	.22	2.72	5.63
hy	2.12	12.89	4.11	2.38	3.18	5.46
mt	2.65	2.46	.55	.54	1.87	.57
il	.70	.45	.29	.02	.33	.39
he	.00	.00	4.01	11.91	.33	3.83
ap	.36	.00	.00	.00	.00	.00

Appendix 3 (cont....)

Sample No.	203	2010	7010	1102	6010	1908
SiO_2	62.73	77.72	71.31	66.10	66.75	63.37
TiO_2	.68	.32	.20	.84	.92	.79
Al_2O_3	12.02	7.77	9.16	12.33	11.74	13.17
Fe_2O_3	8.54	3.48	5.54	5.94	6.09	7.71
MnO	.24	.14	.29	.25	.24	.43
MgO	6.37	3.92	7.86	3.91	3.95	4.12
CaO	.44	.10	.04	1.14	1.51	1.28
Na_2O	2.42	.00	.00	2.16	.12	2.20
K_2O	1.38	3.43	2.00	3.55	2.22	3.42
P_2O_5	.12	.05	.00	.32	.25	.16
Total	95.09	97.09	96.53	96.83	93.97	97.02
			Norms (CIPW)			
Q	30.66	59.78	51.29	31.90	50.00	26.30
or	8.59	20.91	12.26	21.82	13.99	20.91
ab	21.57	.00	.00	19.01	1.08	19.26
an	1.48	.18	.21	3.73	6.26	5.50
co	6.36	4.12	7.18	3.77	7.45	4.0r
hy	26.32	11.72	25.81	14.47	15.70	18.86
mt	3.36	2.54	2.86	2.87	3.03	3.18
il	1.36	.63	.39	1.66	1.86	1.55
ap	.30	.12	.00	.79	.63	.39

APPENDIX 4: Determination of Au and Ag by the atomic absorption procedure

1. Ten gm. of the sample is ground to 300 mesh, transferred to a 400 ml teflon beaker, dissolved in 75 ml. of aqua regia and digested on a hotplate overnight or until complete dryness.
2. The digested material is attacked by 40 to 50 ml. aqua regia three times to assure the complete solubility of precious metals present.
3. The sample is then treated in the centrifugal separator and solid material is rejected.
4. Twenty ml. of HF acid is added to the solution and left on a hotplate to evaporate. HF acid is added to dissolve any remaining silica and forms SiF_2 (gas).
5. Twenty five ml. aqua regia is added to the dried material and is left for 6 minutes on a hotplate so that all the solid comes to solution.
6. The solution is transferred to 200 ml. flasks. Distilled water is added to make the measurement accurate.
7. The sample is taken for analyses by the Atomic Absorption Spectroscopy.

NOTE: Detection limit for 10 gm. sample the useful working range is 0.6 to 60 ppb Au.

APPENDIX 5

Sample No.	Sample Description	Au in ppm	Ag in ppm	Au/Ag ratio
	White massive milky quartz veins			
H.H.1	A grab sample collected from the dump material, represents the white massive milky quartz vein. The sulphide minerals are along the vein selvages.	170.9	95.00	1.79
H.H.1A	This sample represents the same type of the above mentioned vein.	0.98	10.59	0.09
H.H.24	Massive milky quartz vein rich in pyrite. Other sulphide minerals are either minor, chalcopyrite or absent as galena and sphalerite.	1.48	14.65	0.10
H.H.26	Whitish to red massive milky quartz vein with hematite filling along the joints parallel to the wall rock. The quartz has pore spaces, some are filled with iron oxides. Dissiminated sulphide minerals are rare.	0.24	1.38	0.17

Sample No.	Sample Description	Au in ppm	Ag in ppm	Au/Ag ratio
H.H.27	White milky quartz vein sample with some dissiminated pyrite grains. Chalcopyrite is very minor.	40.79	190.80	0.21
H.H.33	Sample from 1 m wide massive white milky quartz vein. Malachite is quite common. No sulphide minerals.	0.00	3.58	0.00
H.H.10H6	A drill core sample taken from white massive milky quartz vein 242 feet below surface. Sulphide mineral such as pyrite and chalcopyrite are abundant.	0.00	10.36	0.00
	Crustified milky quartz veins			
H.H.10	Crustified milky quartz vein, contains mainly galena. Dissiminated 2 mm long pyrite crystals are common. Banded green chlorite is common.	26.34	179.00	0.15
H.H.30	Crustified milky quartz vein sample. The most common sulphide mineral present is galena followed by some pyrite.	24.03	292.56	.002

Sample No.	Sample Description	Au in ppm	Ag in ppm	Au/Ag ratio
H.H.40	Chalcopyrite is the most abundant sulphide mineral present in this crustified quartz vein bounded by black chlorite. Two mm pyrite crystals are present.	136.77	46.76	2.75
H.H.45	Grab sample taken from dump material. The crustified vein sample contains dissiminated pyrite and chalcopyrite. The sample also contains dissiminated potash feldspar grains and banded chlorite.	4.36	15.44	0.28
H.H.46	Crustified quartz vein sample contains chalcopyrite as the most abundant sulphide mineral with some galena and sphalerite	288.29	39.60	7.40
H.H.3V	Crustified milky quartz vein sample collected from dump material. Galena is the most abundant sulphide mineral present followed by chalcopyrite and sphalerite. Pyrite occurs as 2 to 3 mm dissiminated pyrite crystals. Bornite is also present.	2.66	41.52	0.06

Sample No.	Sample Description	Au in ppm	Ag in ppm	Au/Ag ratio
	Quartz-cemented breccia veins			
H.H.BV	Quartz-cemented breccia vein sample with chalcopyrite and galena as the two dominant sulphide minerals present. Potash feldspar crystals are common. Chlorite occurs as thin bands around galena.	0.98	6.92	0.14
H.H.29H7	A drill core sample taken from 266 feet below surface and it represents the cemented breccia vein-type. Minor chalcopyrite and galena are present.	0.00	3.58	0.00
	Barren quartz veins			
H.H.4	Massive, pure, white with hematite along the contact with the wall rock. The sample is taken from the north end of 200 m long 1 to 1.20 wide.	4.96	1.06	4.68
H.H.8	Massive, white quartz vein cut by numerous hematite veinlets. It is taken from the central part of the above mentioned vein.	0.00	1.15	0.00

Sample No.	Sample Description	Au in ppm	Ag in ppm	Au/Ag ratio
H.H.9	Massive, white quartz vein, taken from the same location as sample H.H.8. The sample has traces of secondary copper minerals.	1.77	4.42	0.40
H.H.14	Massive, white quartz vein, from the same above mentioned vein at its south end. The sample has limonite tarnishes.	0.00	0.00	0.00
H.H.19	Chip sample from ½ m wide white barren quartz vein. The sample has malachite staining. Primary sulphide minerals are rare. There are however dissiminated particles of chalcopyrite. The quartz is vuggy. Vugs are filled with hematite.	0.46	2.56	0.18

TABLE 1-6

CHALCOPYRITE

Sample No.	Thick polished section H.H.1			
Au	.00	.09	.14	.00
S	35.75	35.39	34.92	35.12
Ag	.00	.03	.00	.00
Te	.00	.00	.00	.00
Fe	29.34	29.66	29.21	28.46
Cu	34.55	34.73	30.90	33.61
Se	.00	.00	.00	.00
Total	99.65	99.91	95.17	97.18

Thick polished section H.H.9

Au	.00	.00	.00	.00	.00	.11
S	34.51	34.64	35.03	35.09	34.83	34.72
Ag	.00	.02	.00	.02	.00	.00
Te	.00	.00	.00	.00	.00	.00
Fe	29.81	30.02	29.64	27.43	30.12	30.27
Cu	34.34	34.07	34.57	34.05	34.89	34.23
Se	.05	.11	.26	.00	.00	.00
Total	98.70	99.47	99.50	99.59	99.84	99.34

TABLE 2-6

CHALCOPYRITE

Sample No. Thin polished section H.H.7

Au	.00	.00	.00	.00	.00	.03	.00	.00
S	35.69	35.27	34.98	35.32	35.35	36.02	35.09	34.90
Ag	.00	.00	.05	.04	.04	.02	.00	.00
Te	.00	.00	.00	.00	.00	.00	.00	.00
Fe	29.81	29.67	29.66	29.50	29.62	29.10	30.09	29.93
Cu	35.28	34.32	34.42	34.32	35.32	34.95	34.37	33.83
Se	.00	.00	.00	.00	.00	.00	.00	.00
Total	100.78	99.26	99.11	99.18	100.33	100.11	99.55	98.66

Thick polished section H.H.7

Au	.05	.12	.06	.13	.22	.00	.00	.07
S	34.81	34.71	34.58	34.28	35.48	35.30	33.66	35.09
Ag	.04	.09	.04	.02	.11	.00	.00	.00
Te	.00	.00	.00	.00	.00	.00	.00	.00
Fe	30.31	30.31	30.00	29.92	30.40	30.61	30.27	29.73
Cu	34.96	34.55	24.34	35.08	34.64	34.62	35.31	35.50
Se	.00	.00	.00	.00	.00	.20	.00	.00
Total	100.16	99.35	99.01	99.43	100.86	100.73	99.24	100.39

TABLE 3-6

CHALCOPYRITE

Sample No.	Thin polished section H.H.10						
Au	.00	.00	.00	.00	.01	.12	.04
S	34.37	34.50	34.75	34.56	35.45	34.27	34.16
Ag	.00	.00	.00	.00	.00	.03	.00
Te	.00	.00	.00	.00	.00	.00	.00
Fe	30.63	29.76	30.68	30.71	30.04	30.41	30.87
Cu	34.24	34.33	34.39	34.52	34.40	34.04	34.60
Se	.00	.00	.00	.00	.00	.00	.00
Total	99.24	98.59	99.83	99.80	99.89	98.86	99.67

	Thick polished section H.H.18					
Au	.00	.00	.00	.06	.07	.00
S	34.04	33.73	34.57	34.86	34.30	33.57
Ag	.01	.04	.04	.00	.00	.14
Te	.00	.00	.00	.00	.00	.00
Fe	29.87	30.16	31.01	30.17	29.52	30.36
Cu	35.02	34.86	34.74	33.94	34.50	34.19
Se	.00	.00	.00	.00	.00	.00
Total	98.94	98.79	100.37	99.05	98.39	98.26

TABLE 4-6

CHALCOPYRITE

Sample No.	Thin polished section H.H.20						
Au	.00	.32	.14	.00	.21	.36	
S	36.21	34.41	34.59	33.86	35.12	34.46	
Ag	.00	.00	.00	.00	.00	.00	
Te	.00	.00	.00	.00	.00	.00	
Fe	28.41	30.31	30.61	30.57	30.56	30.97	
Cu	34.98	34.68	34.95	35.20	34.56	33.97	
Se	.00	.00	.00	.00	.00	.00	
Total	100.32	99.72	100.29	99.63	100.68	98.36	
	Thin polished section H.H.40						
Au	.08	.03	.11	.00	.00	.00	.00
S	34.87	34.45	34.14	34.47	34.29	34.56	35.77
Ag	.03	.00	.05	.00	.00	.00	.04
Te	.00	.00	.00	.00	.00	.00	.00
Fe	30.31	30.84	30.29	30.31	30.21	30.29	30.02
Cu	34.29	35.23	35.27	35.04	34.97	35.16	34.42
Se	.00	.00	.00	.00	.00	.00	.00
Total	99.57	100.56	99.84	99.83	99.48	100.02	100.02

TABLE 5-6

GALENA

Sample No.	Thin polished section H.H.7						
Au	.00	.00	.00	.54	.00	.00	.00
S	13.39	13.27	13.34	13.22	13.20	13.24	13.34
Pb	85.70	86.38	86.63	86.61	86.71	86.56	85.89
Ag	.00	.00	.00	.00	.00	.05	.02
Sb	.00	.00	.00	.00	.00	.00	.04
Fe	.00	.00	.00	.00	.00	.00	.00
Cu	.00	.00	.00	.00	.00	.00	.00
Total	99.17	99.65	100.09	100.93	99.92	99.85	99.27

Thick polished section H.H.7

Au	.03	.00	.00	.00	.00	.01
S	13.23	13.13	13.30	13.40	13.39	13.50
Pb	87.29	86.25	87.07	86.70	87.18	86.60
Ag	.00	.00	.00	.00	.00	.00
Sb	.04	.00	.00	.00	.00	.00
Fe	.00	.00	.00	.00	.00	.00
Cu	.00	.00	.00	.00	.11	.00
Bi	.00	.00	.00	.00	.00	.00
Total	100.59	99.38	100.37	100.29	100.69	100.11

TABLE 6-6

GALENA

Sample No.	Thick polished section H.H.8				
Au	.04	.05	.20	.04	.20
S	13.30	13.29	13.36	13.34	13.47
Pb	85.11	84.79	85.76	85.34	85.79
Ag	.09	.05	.01	.08	.04
Te	.04	.08	.11	.03	.08
Cu	.02	.00	.03	.05	.01
Bi	.00	.04	.00	.00	.00
Zn	.16	.00	.00	.00	.00
Se	.63	.41	.29	.54	.45
Total	99.38	98.71	99.76	99.41	100.03

Thin polished section H.H.10

Au	.00	.00	.00	.00	.00	.00
S	12.96	12.99	13.08	13.11	13.41	13.45
Pb	85.65	86.91	86.02	85.62	85.63	85.96
Sb	.00	.00	.00	.00	.01	.00
Fe	.00	.00	.00	.00	.00	.01
Cu	.00	.00	.00	.00	.00	.00
Bi	.00	.00	.00	.00	-	-
Total	98.61	99.90	99.10	98.73	99.05	99.42

TABLE 7-6

GALENA

Sample No.	Thin polished section H.H.10A				
Au	.04	.00	.00	.00	.04
S	13.26	13.03	13.18	13.05	13.02
Pb	85.32	85.89	86.21	86.20	86.41
Ag	.00	.00	.00	.00	.00
Sb	.00	.00	.05	.00	.00
Te	.00	.02	.04	.04	.02
Cu	.02	.00	.02	.00	.00
Bi	.09	.09	.07	.00	.00
Zn	.00	.01	.02	.02	.00
Se	.73	.52	.60	.54	.83
	Thin polished section H.H.11				
Au	.00	.00	.02	.00	.00
S	13.22	13.18	12.96	13.01	12.95
Pb	85.20	85.33	85.01	85.54	85.48
Ag	.00	.00	.00	.00	.00
Fe	.00	.00	.00	.00	.00
Te	.04	.03	.00	.04	.04
Cu	.06	.00	.02	.00	.07
Bi	.00	.09	.00	.00	.01
Zn	.04	.09	.03	.01	.01
Se	.76	.68	.66	.67	.73
Total	99.92	99.40	98.72	99.27	99.29

TABLE 8-6

GALENA

Sample No. Thin polished section H.H.40

Au	.43	.13	.05	.02	.05	.00	.13	.17
S	13.25	13.18	13.29	13.17	13.30	13.35	13.17	13.30
Pb	26.52	86.50	86.88	86.93	86.42	85.96	86.93	86.64
Ag	.00	.00	.00	.00	.00	.00	.00	.00
Te	.03	.05	.07	.04	.02	.06	.02	.02
Cu	.00	.00	.00	.00	.00	.01	.01	.00
Bi	.00	.00	.05	.06	.06	.00	.00	.00
Zn	.02	.02	.00	.00	.00	.07	.02	.00
Se	.38	.24	.19	.21	.13	.36	.25	.30
Total	100.96	100.11	100.52	99.38	99.97	99.80	100.53	100.44

Thin polished section H.H.85

Au	.06	.09	.26
S	13.08	13.16	13.33
Pb	85.71	85.26	87.36
Ag	.00	.04	.00
Te	.04	.00	.02
Cu	.01	.02	.00
Bi	.05	.09	.02
Se	.65	.76	.23
Total	99.60	99.41	101.07

TABLE 9-6

SPHALERITE

Sample No.	Thin polished section H.H.7						
S	33.83	32.94	33.46	33.98	33.19	33.00	
Ag	.00	.00	.02	.00	.00	.00	
Cd	.30	.15	.15	.16	.25	.28	
Mn	.00	.00	.00	.03	.02	.01	
Fe	1.33	.70	1.09	.60	.14	1.54	
Cu	1.13	.70	.97	.33	.00	1.73	
Zn	64.05	65.55	64.56	65.56	66.00	63.73	
Total	100.19	100.05	100.03	100.66	99.59	100.32	
	Thick polished section H.H.7						
S	32.69	32.63	32.80	32.65	32.66	32.95	33.37
Ag	.02	.02	.00	.00	.00	.00	.00
Cd	.12	.19	.20	.21	.27	.13	.16
Mn	.04	.03	.02	.03	.04	.04	.03
Fe	.19	.25	1.19	.14	.17	.12	.31
Cu	.08	.24	.87	.03	.01	.00	.30
Zn	66.55	65.47	63.23	65.47	65.33	66.57	65.39
Total	99.69	98.84	98.32	98.54	98.48	99.80	100.52

TABLE 10-6

SPHALERITE

Sample No. Thick polished section H.H.8

S	33.14	33.27	33.02	32.90	32.88	32.94	33.37	33.57	33.20
Ag	.00	.15	.00	.02	.00	.00	.00	.02	.00
Cd	.28	.17	.15	.20	.26	.15	.22	.13	.13
Mn	.00	.00	.00	.00	.00	.00	.01	.00	.02
Fe	.49	.25	1.15	.10	.51	.70	.53	2.65	.14
Cu	.53	.36	1.01	.02	.46	.70	.48	3.03	.07
Zn	64.46	65.24	63.03	65.43	65.39	65.55	64.54	59.09	65.89
Total	98.90	99.43	98.36	98.72	99.39	100.05	99.14	98.69	99.45

Thin polished section H.H.10

S	33.80	33.69	33.56	33.64	33.75	32.89	33.05
Ag	.00	.00	.00	.00	.00	.00	.00
Cd	.18	.27	.27	.26	.00	.21	.29
Mn	.00	.00	.00	.00	.00	.00	.00
Fe	.39	.76	.83	.61	.00	.96	.44
Cu	.31	.89	.83	.59	.00	1.05	.46
Zn	65.36	64.61	63.79	65.76	67.19	64.30	65.85
Total	100.04	100.23	99.30	100.86	100.94	99.42	99.64

TABLE 11-6

SPHALERITE

Sample No. Thin polished section H.H.10A

S	32.84	33.02	33.12	33.56	33.66	33.12	33.16	33.46
Ag	.00	.00	.00	.00	.00	.00	.00	.00
Cd	.37	.34	.36	.37	.27	.36	.26	.42
Mn	.00	.00	.00	.01	.02	.00	.02	.00
Fe	.70	.71	.88	.68	.14	.09	.48	.96
Cu	.82	.75	.83	.63	.02	.01	.25	1.00
Zn	65.44	65.39	65.69	65.10	66.49	66.35	66.57	65.62
Total	100.17	100.20	100.80	100.35	100.58	98.93	100.93	101.46

Thin polished section H.H.8

S	32.21	33.20	33.33
Ag	.00	.00	.00
Cd	.11	.27	.17
Fe	1.14	1.14	.79
Cu	1.02	.78	.44
Zn	64.21	64.84	65.22
Total	99.68	100.21	99.95

TABLE 12-6

ELECTRUM

Sample No.	Thick polished section H.H.7				
Ag	12.33	13.38	11.58	13.25	12.16
Au	86.52	87.66	87.73	86.36	87.04
Total	98.84	101.04	99.25	99.62	99.26
Ag	11.25	11.66	11.27	11.21	11.41
Au	89.37	87.99	86.79	89.87	88.85
Total	100.62	99.66	100.06	101.06	100.27
Ag	11.02	11.61	12.08	12.45	12.77
Au	87.94	88.62	88.35	85.75	88.13
Total	98.96	99.93	100.85	98.20	100.91
Ag	11.49	11.94	11.46	11.77	11.74
Au	87.19	27.08	89.09	89.73	88.57
Total	98.63	99.02	100.49	101.51	100.31
	Thin polished section H.H.7				
Ag	11.50	11.77	11.25	11.11	10.31
Au	88.61	87.27	88.83	87.58	88.35
Total	100.11	99.04	100.65	98.69	98.66

	Thin polished section H.H.40					Thin polished section H.H.80	
Au	86.73	91.63	91.36	87.09	81.31	87.67	87.01
Ag	11.89	6.71	7.06	13.21	17.91	11.84	12.49
Fe	.07	.00	.00	.01	.01	.05	.00
Cu	.36	.06	.02	.29	.25	.30	.27
Total	99.04	98.39	99.89	100.59	99.48	99.87	99.83

TABLE 13-6

CHLORITE

Sample No.	Thin polished section H.H.10					
Mg	22.02	24.58	24.10	24.08	24.33	24.20
Al	17.91	17.98	17.34	16.61	16.36	16.48
Si	29.94	28.56	30.13	29.67	29.88	29.77
Ca	.06	.06	.06	.03	.05	.04
Ti	.00	.01	.00	.00	.01	.00
Mn	.56	.71	.70	1.02	.98	1.00
Fe	15.82	15.88	15.64	15.59	15.52	15.56
Total	86.32	87.78	87.98	87.00	87.12	87.04

	Thin polished section H.H.10				
Mg	23.45	23.70	23.23	24.09	24.32
Al	17.09	15.75	17.62	17.43	16.88
Si	29.68	30.16	28.58	28.59	29.38
Ca	.05	.06	.16	.04	.09
Ti	.00	.01	.01	.00	.03
Mn	.75	.90	.66	.78	.97
Fe	15.74	15.47	15.60	15.34	15.83
Total	86.77	86.05	85.86	86.28	87.50

TABLE 14-6

CHLORITE

Sample No.	Thin Section H.H.17A07					
Mg	15.88	16.66	16.37	16.23	16.06	17.07
Al	17.07	17.01	16.99	15.98	16.43	17.31
Si	28.04	27.66	26.91	26.81	26.60	28.09
Ca	.16	.12	.20	.15	.14	.14
Ti	.04	.04	.06	.04	.04	.13
Mn	.42	.47	.48	.54	.57	.48
Fe	25.72	25.74	25.93	25.68	26.52	25.70
Total	87.34	87.70	86.95	85.41	86.38	88.91
Remarks:	small chlorite area	small chlo. area	small chlo. area	small chlo. area	small chlo. area	small chlo. area
	Thin Section H.H. 1707					
Mg	15.70	15.45	15.77	16.23	15.88	
Al	17.12	17.24	17.50	17.50	16.58	
Si	26.63	26.65	26.86	28.64	27.32	
Ca	.08	.08	.11	.14	.08	
Ti	.02	.03	.01	.05	.05	
Mn	.52	.58	.57	.51	.65	
Fe	27.05	26.71	26.08	25.71	26.17	
Total	87.18	86.74	86.90	85.71	85.51	
Remarks	large chlorite patch, centre	some chlo. patch, edge	small chlo. area	small chlo. area	small chlo. area	

(cont...)

TABLE 14-6 (Cont.)

CHLORITE

Sample No.	Thin section H.H.17A07					
Mg	15.88	16.66	16.37	16.23	16.06	17.07
Al	17.07	17.01	16.99	15.98	16.43	17.31
Si	28.04	27.66	26.91	26.81	26.60	28.09
Ca	.16	.12	.20	.15	.14	.14
Ti	.04	.04	.06	.04	.04	.13
Mn	.42	.47	.48	.54	.57	.48
Fe	25.72	25.74	25.93	25.68	26.52	25.70
Total	87.34	87.70	86.95	85.41	86.38	88.91
Remarks:	small chlorite area	small chlo. area	small chlo. area	small chlo. area	small chlo. area	small chlo. area
	Thin section H.H.1707					
Mg	15.70	15.45	15.77	16.23	15.88	
Al	17.12	17.24	17.50	17.50	16.58	
Si	26.63	26.65	26.86	28.64	27.32	
Ca	.08	.08	.11	.14	.08	
Ti	.02	.03	.01	.05	.05	
Mn	.52	.58	.57	.51	.65	
Fe	27.05	26.71	26.08	25.71	26.17	
Total	87.18	86.74	86.90	85.71	85.51	
Remarks:	large chlorite patch, centre	some chlo. patch, edge	small chlo. area	small chlo. area	small chlo. area	

(cont...)

TABLE 14-6 (cont.)

CHLORITE

Sample No.	Thin section H.H.1707				
Mg	16.30	14.94	15.83	15.13	16.02
Al	17.70	17.49	17.01	18.24	16.93
Si	27.64	27.00	27.63	26.28	27.54
Ca	.07	.08	.15	.07	.09
Ti	.03	.03	.02	.05	.08
Mn	.50	.68	.48	.51	.55
Fe	26.39	26.82	25.29	27.14	26.11
Total	88.84	86.99	86.42	87.41	87.24
Remarks	chlorite spot in chlorite patch	another chlo. spot in the same chlo. patch	small area of chlo. in country rock	large chlo. patch, edge	some chlo. patch, centre

TABLE 15-6

CHLORITE

Sample No.	Thin polished section H.H.45B					
Mg	14.83	14.79	14.38	15.42	15.02	13.40
Al	19.11	18.75	19.78	19.68	19.24	19.15
Si	26.31	26.08	27.05	26.27	26.38	26.45
Ca	.03	.11	.08	.05	.11	.08
Ti	.04	.02	.05	.04	.04	.07
Mn	.68	.57	.62	.61	.72	1.04
Fe	25.27	25.02	24.52	25.14	25.99	27.92
Total	86.31	85.32	86.50	87.20	87.49	88.11

APPENDIX 7: Determination of FeO in the Fe_2O_3

The total iron content, determined by the X-ray fluorescence is in the form of (Fe_2O_3). Determination of FeO was done volumetrically by Wilson's method (1955). The analyses was done in duplicate for all the samples and three times for some of them.

Choice of samples:

The analysed 18 samples were chosen among 42 geochemical samples collected across ore-bearing and barren quartz veins and the adjacent rocks where the total iron is above 3.5%. The anlysed samples were carefully selected so that the obtained data became helpful in determining the type of process that was going on during ore-formation.

Procedure:

A certain amount of the rock powder, 0.25 gm when the iron content in the rock is high, and it gives up to 1.00 gm when the total iron is low, is digested in HF in the presence of ammonium metavanadate (AMV), which is an oxidizing agent. The solution is titrated against standardised ferrous ammonium sulphate (FAS).

NOTE: Some of the samples contain sulphide minerals, pyrite in particular, but it is resistant to cold HF digestion and hence it does not give rise to errors in FeO determination. For the same reason the sample should not be digested in HF more than 24 hours or an overnight to avoid any decomposition of sulphide minerals.

REFERENCES

Aguttes, J. and Duhamel, M. 1971. Geology and mineral exploration of the Jabal Sayid quadrangle. Directorate General of Mineral Resources, Bureau de Recherches Geologiques et Miners. Report 71 JED 4, 49 p.

Alabouvette, B. 1973. Geology and prospecting at Jabal Sayid. Directorate General of Mineral Resources, Bureau de Recherches Geologiques et Miners. Report 74 JED 2, 63 p.

Andrews, A.J. and Fyfe, W.S. 1976. Metamorphism and massive sulphide generation in oceanic crust. Geoscience Canada, 3, pp. 84-94.

Badalov, S.T. and Enikeev, M.P. 1959. Geochemistry of cadmium in the Almalyk and Altyn-Tobkan mineralized areas of the Karamazar region. Translated from Geokhimiya. Geochemistry, 4, pp. 406-415.

Barton, Jr. P.B. 1959. The chemical environment of ore deposition and the problem of low temperature ore transport. In Researches in Geochemistry, Edited by P.H. Abelson. John Wiley and Sons, Inc., New York, pp. 279-300.

Berzon, R.O. and Karyashev, Yu. M. 1973. Selenium and tellurium in the gold deposits of the Urals. Translated from Geokhimiya, 11, pp. 1615-1619. Geochemistry International, pp. 1188.

Bethke, P.M. and Barton, Jr. B. 1971. Distribution of some minor elements between coexisting sulphide minerals. Economic Geology, 66, pp. 140-163.

Beukes, N.J. 1973. Precambrian iron formation of South Africa. Economic Geology, 68, pp. 960-1004.

Brown, G.F., Jackson, R.O., Bogue, R.G. and MacLean, W.H. 1962. Geology of the Southern Hijaz Quadrangle, Kingdom of Saudi Arabia. United States Geological Survey, Miscellaneous Investigation Map I-210A.

_____ 1972. Tectonic map of the Arabian Peninsula. Map Ap-2. Directorate General of Mineral Resources, Jiddah, Saudi Arabia.

_____ 1973. List of age determinations. Directorate General of Mineral Resources. United States Geological Survey open file, 3 p.

Camus, F. 1975. Geology of El Teniente orebody with emphasis on wall-rock alteration. Economic Geology, 70, pp. 1341-1373.

Carmichael, S.E., Turner, F.J. and Verhoogen, J. 1974. Igneous Petrology. McGraw-Hill, New York, 739 p.

Colley, H. and Rice, C.M. 1975. A Kuruko-type deposit in Fiji. Economic Geology, 70, pp. 1373-1386.

Czamanske, G.K. and Hall, W.E. 1975. The Ag-Bi-Pb-Sb-S-Se-Ti mineralogy of the Darwin lead-silver-zinc deposits, Southern California. Economic Geology, 70, pp. 1092-1111.

Davis, W.E., Allen, R.V. and Akhrass, M.N. 1965. Geophysical exploration in the Mahd Adh Dhahab district, Saudi Arabia. United States Geological Survey Saudia Arabian Project Report 14, 4 p.

Dickinson, W.R. 1970. Relation of andesite, granites and derivative sandstones to arc-trench tectonics. Review geophysic, 8, pp. 813-860.

Dirom, G.A. 1946. Geological examination, Mahd adh Dhahab mine. Progress Summary, Saudi Arabian Directorate General of Mineral Resources open-file Report, 24, 8 p.

_____ 1947. Mahd adh Dhahab mine and vicinity. Surface geologic plan and cross sections. Saudi Arabian Minin Syndicate, Ltd., unpublished maps in files of Saudi Arabian Directorate General of Mineral Resources, Jiddah.

Durney, D.W. and Ramsay, J.G. 1973. Incrimental strains measured by syntectonic crystal growths. In Gravity and Tectonics, Edited by K.A. De Jong and R. Scholten, John Wiley and Sons, Inc. New York, pp. 67-96.

Eugster, H.P. 1959. Reduction and oxidation in metamorphism. In Researches in Geochemistry, Edited by P.H. Abelson John Wiley and Sons, Inc. New York, pp. 397-426.

_____ and Wones, D.R. 1962. Stability relations of the ferrogenous biotite, annite. Journal of Petrology, 3, pp. 82-115.

Fyfe, W.S. 1974. Geochemistry - Oxford chemistry series. Edited by P.W. Atkins, J.S.E. Halkerand A.K. Holliday Clarendon Press. Oxford, 107 p.

Garrels, R.M., Perry, Jr., E.A. and MacKenzie, F.T. 1973. Genesis of Precambrian iron-formations and the development of atmospheric oxygen. Economic Geology, 68, pp. 1173-1179.

Garson, M.S. and Shalaby, I.M. 1974. Precambrian-Lower Paleozoic plate tecontics and metallogenesis in the Red Sea region. In Symposium on metallogy and plate tectonics, GAC/MAC meeting 1974, St. John's, Newfoundland.

Goldsmith, R. 1971. Mineral resources of the Southern Hijaz Quadrangle, Kingdom of Saudi Arabia, Directorate General of Mineral Resources, Jiddah, Saudi Arabia Bulletin, 5, 62 p.

_____ and Kouther, J.H. 1971. Geology of the Mahd Adh Dahab - Umm AD Damar area, Kingdom of Saudi Arabia. Directorate General of Mineral Resources, Jiddah, Saudi Arabia Bulletin, 6, 20 p.

Goodwin, A.M. and Ridler, R.H. 1970. The Abitibi orogenic belt. In Symposium on basins and geosynclines of the Canadian Shield. Edited by A.J. Baer. Geological Survey of Canada, paper 70-40, pp. 1-30.

Greenwood, W.R. and Brown, G.F. 1973. Petrology and chemical analysis of selected plutonic rocks from the Arabian Shield. Kingdom of Saudi Arabia, Directorate General of Mineral Resources Bulletin, 9, 9 p.

_____, Hadley, D.G., Anderson, R.E., Fleck, R.J. and Schmidt, D.C. 1976. Late proterozoic cratonization in southwestern Saudi Arabia. Philosophical Transactions of the Royal Society of London, Series A, 280, pp. 517-527.

Gustafson, L.B. and Hunt, J.P. 1975. The porphyry copper deposit at El Salvador, Chile. Economic Geology, 70, pp. 857-912.

Hans van Daalhoff 1974. Mineral locality map of the Arabian Shield Metalliferous minerals. Directorate General of Mineral Resources, Jiddha, Saudi Arabia.

_____ 1974. Mineral locality map of the Arabian Shield. Industrial minerals and dimension stone marble and others. Directorate General of Mineral Resources, Jiddah, Saudi Arabia.

Hattori, K. 1975. Geochemistry of ore deposition at the Yatani lead-zinc and gold-silver deposit, Japan. Economic Geology, 70, pp. 677-694.

Helgenson, H.C. and Garrels, R.M. 1968. Hydrothermal transport and deposition of gold. Economic Geology, 63, pp. 622-635.

Hemley, J.J. and Jones, W.R. 1964. Chemical aspects of hydrothermal alteration with emphasis on hydrogen metasomatism. Economic Geology, 59, pp. 538-569.

Henley, R.W. 1973. Solubility of gold in hydrothermal chloride solutions. Chemical Geology, 11, pp. 73-87.

Iijima, A. 1974. Clay and zeolite alteration zones surrounding Kuroko deposits in the Hokuroku district, Northern Akita, as submarine hydrothermal-diagenetic alteration product. Mining Geology Special Issue, 6, pp. 267-289.

Ivanov, V.V. 1964. Distribution of Cadmium in ore deposits. Translated from Geokhimiya, 8, pp. 766-779. Geochemistry International pp. 757-768.

Kajiwara, Y. 1970. Syngenetic features of the Kuroko ore from the Shakanai mine. Volcanism and ore genesis. Edited by T. Tatsumi. University of Tokyo Press, pp. 197-206.

Kerrich, R., Fyfe, W.S. and Allison, I. 1977. Iron reduction around gold-quartz veins, Yellowknife District NW Territories, Canada. Economic Geology, 72, pp. 657-663.

Krauskopf, K.B. 1951. The solubility of gold. Economic Geology, 48, pp. 858-870.

Lowell, J.D. and Guilbert, J.M. 1970. Lateral and vertical alteration-mineralization zoning in porphyry ore deposits. Economic Geology, 65, pp. 373-408.

MacLean, W.H. 1961. Preliminary notes on the Umm Ad Damar mine. Saudi Arabian Directorate General of Mineral Resources open-file Report 128, 6 p.

Markham, N.L. 1960. Synthetic and natural phases in system Au-Ag-Te. Economic Geology, 55, pp. 1143-1178.

Marzouki, F. and Fyfe, W.S. 1977. Pan-African plates: Additional evidence from igneous events in Saudi Arabia. Contribution to Mineralogy and Petrology, 60, pp. 219-224.

_____ 1977. Petrogenesis of Al Hadah plutonic rocks, Kingdom of Saudi Arabia. Unpublished Ph.D. thesis, University of Western Ontario, Canada, 267 p.

Meyer, C. and Hemley, J.J. 1967. Wall rock alteration. In Geochemistry and hydrothermal ore deposits. Edited by H.L. Barnes, Holt, Rineheart and Winston, Inc. pp. 166-235.

Mookherjee, A. 1962. Certain aspects of the geochemistry of cadmium. Geochimica et Cosmochimica Acta, 26, pp. 351-360.

Moorehouse, W.W. 1959. The study of rocks in thin sections. Published by Harper and Row, New York, 514 p.

Nash, J.T. 1975. Geological studies in the Park City District: II. Sulphide mineralogy and minor element chemistry, Mayflower mine. Economic Geology, 70, pp. 1038-1049.

Nechelyustov, N.V., Popova, N.N. and Minister, E.F. 1962. On the isomorphism of selenium and tellurium in galena. Translated from Geokhimiya, 11, pp. 993-999. Geochemistry International, pp. 1129-1135.

Nebert, K. 1965a. Geology of Jabal Farasan region. Saudi Arabian Directorate General of Mineral Resources open-file Report 260, 45 p.

_____ 1965b. Regional geology of Jabal Samran area. Saudi Arabian Directorate General of Mineral Resources open-file Report 261, 33 p.

Nishiyama, T. 1974. Minor elements in some sulphide minerals from the Kuroko deposits of Shakanai mine. Mining Geology Special Issue, 6, pp. 371-376.

Nockolds, S.R. 1954. Average chemical composition of some igneous rocks. Geological Society of America, Bulletin, 65, pp. 1007-1032.

Norrish, K. and Chappell, B.W. 1967. X-ray fluorescence spectrography, In Zussman, J. Edited by physical press, London, pp. 161-214.

_____ and Hutton, J.T. 1969. An accurate x-ray spectrographic method for the analysis of a wide range of geological samples. Geochimca et Cosmochimca Acta, 33, pp. 431-453.

Ohmoto, H. and Rye, R.O. 1974. Hydrogen and oxygen isotope compositions of fluid inclusions in the Kuroko deposits Japan. Economic Geology, 96, 6, pp. 947-953.

Playter, R.F. 1953. Mahad AD Dahab mine. Saudi Arabian Directorate General of Mineral Resources open-file Report 29, 12 p.

Panfilov, R.V. 1972. Bi/Sb ratio in galena from east Transbaykaliya sulphide deposits. Translated from Geokhimiya, 7, pp. 810-816. Geochemistry International pp. 545-551.

Pytkamiez, R.M. and Kester, D.R. 1971. The physical chemistry of sea water. Oceanography and Marine Biology Annual Review, 9, pp. 11-60.

Ramdohr, P. 1969. The ore minerals and their intergrowths. Perganon Press, Berlin, 1089 p.

Robert, W., Luce, Baghdady, A. and Roberts, R. 1975. Geology and ore deposits of the Mahd ADH Dhahab District. Directorate General of Mineral Resources, Jiddah, Saudi Arabia. United States Geological Survey, Saudi Arabian Project Report 195, 29 p.

Rose, A.W. 1970. Zonal relation of wall-rock alteration and sulphide distribution at porphyry copper deposits. Economic Geology, 65, no. 8, pp. 920-936.

Routhier, P. and Delfour, J. 1975. Gitology of massive sulphide deposits associated with acidic volcanism and its application for such deposits in the Precambrian of Saudi Arabia. Directorate General of Mineral Reources, Bereau de Recherches Geologiques et Miners. Report 75 JED 10, 210 p.

Sales, R.H. and Meyer, C. 1948. Wall rock alteration at Butte, Montana. American Institute of Mining and Engineering Transactions 178, pp. 9-35.

Salmon, B.C., Clark, B.R. and Kelly, W.C. 1974. Sulphide deformation studies: II. Experimental deformation of galena to 2,000 bars and 400°C. Economic Geology, 69, pp. 1-17.

Sato, J. 1974. Ores and ore minerals from the Shakanai mine, Akita prefecture, Japan. Mining Geology Special Issue, 6, pp. 323-335.

Schmidt, D.L., Hadly, D.G., Greenwood, W.R., Coleman, R.G., Gonzalies, L. and Brown, G.F. 1972. Stratigraphy and tectonism of the Southern part of the Precambrian Shield of Saudi Arabia. Saudi Arabian Directorate General of Mineral Resources Bulletin 8, 13 p.

Seward, T.M. 1973. Thio complexes of gold and transporting of gold in hydrothermal ore solutions. Geochimica et Cosmochimica Acta, 37, pp. 379-399.

Shcherbina, V.V. 1976. Sulphide minerals as geochemical indicators. Translated from Geokhimiya, 10, pp. 1451-1461. Geochemistry International pp. 92-100.

Shimazaki, Y. 1974. Ore minerals of the Kuroko-type deposits. Geological Survey of Japan, 8 Kawada-Cho, Shinjuku, Tokyo 162 Mining Geology Special Issue, 6, 311-322 pp.

Sillitoe, R.H. 1977. Metallic mineralization affiliated to subaerial volcanism: A Review. In: volcanic process in ore genesis. The institution of Mining and Metallurgy The Geological Society of London. Special publication 7, of the Geological Society of London, pp. 99-116.

Simpson, E.S. 1912. Detailed mineralogy of Kalgoorlie and Boulder with special reference to ore deposits. Geological Survey Western Australia Bulletin, 42, pp. 77-152.

Smith, F.G. 1944. The alkali sulphide theory of gold deposition. Economic Geology, 38, pp. 561-590.

Spooner, E.T.C., Beckinsale, R.D., England, P.C. and Senior, A. 1977. Hydration, O^{18} enrichment and oxidation during ocean floor hydrothermal metamorphism of ophiolitic metabasic rocks from E. Liguria, Italy. Geochimica et Cosmochimica Acta, 41, pp. 857-871.

Steven, T.A. and Eaton, G.P. 1975. Environment of ore deposition in the Creede Mining District, San Juan Mountains, Colorado: I. Geologic, hydrologic and geophysical setting. Economic Geology, 70, pp. 1023-1037.

Strecheisen, A.L. 1967. Classification and nomenclature of igneous rocks (final report of inquiry). News Jahrb Mineral Abhandl, 107, pp. 144-244.

Theobald, Jr. P.K. 1965a. Geologic status report, April 1965, Mahd adh Dahab area, Saudi Arabia: United States Geological Survey Saudi Arabian project. Technical Letter 15, open-file Report, 11 p.

Tilling, R.I., Gottfried, D. and Rowe, J.J. 1973. Gold abundance in igneous rocks: Bearing on gold mineralization. Economic Geology, 68, pp. 168-186.

United States Geological Survey and Arabian American Oil Company 1963. Geological map of the Arabian peninsula United States Geological Survey Miscellaneous Investigation Map I-270A.

Weissberg, B.G. 1970. Solubility of gold in hydrothermal alkaline sulphide solutions. Economic Geology, 65, pp. 551-556.

Wilson, A.D. 1955. A new method for the determination of ferrous iron in rocks and minerals. Great Britain Geological Survey Bulletin, 9, pp. 56-58.